Numerical and Experimental Investigations of Vibration-based Assessment of Timber Beams Rehabilitated by Fibre-Reinforced Polymer

By

Runhua Xiao

A thesis submitted for the degree of
Master of Engineering (Research)

Faculty of Engineering and Information Technology (FEIT)
University of Technology, Sydney (UTS)

February, 2014

CERTIFICATE OF ORIGINAL AUTHORSHIP

I certify that the work in this thesis has not previously been submitted for a degree nor has it been submitted as part of requirements for a degree except as fully acknowledged within the text.

I also certify that the thesis has been written by me. Any help that I have received in my research work and the preparation of the thesis itself has been acknowledged. In addition, I certify that all information sources and literature used are indicated in the thesis.

Signature of Student:

Date:

ABSTRACT

Timber has been traditionally used all over the world as a construction material. Built timber structures may require repair and/or strengthening because of a number of factors such as age-related deterioration, fungus or termite attacks and damage caused by overloading. In recent years, a great deal of research and development has been focused on utilizing vibration based methods to detect structural damage and use of fibre reinforce polymer (FRP) on timber for strengthening or repair damaged timber structural members in various types of structures. Although the application of FRP for repair and/or strengthening of structures has been researched for a decade, anon-destructive evaluation of the effectiveness and reliability of the FRP repaired or strengthened structure are yet to be investigated.

In this study, the damage index method, i.e. a robust vibration-based damage detection method, is proposed to localize and quantify damage in timber beams and to evaluate the effectiveness of repair for the damaged timber beams, in which the damaged timber beams are repaired by applying carbon fibre reinforced polymer (CFRP).

In addition to numerical investigation using Finite Element (FE) analysis, an experimental program comprising of static and dynamic testing was carried out on five laminated veneer lumber (LVL) beams. Different damage cases (severe, moderate, minor) are introduced on these beams. The experimental results indicate that the use of CFRP was effective in repairing the damaged timber beams. Both numerical and experimental investigations have also shown that the proposed damage index method is able to accurately detect damage location and severity, and evaluate the repair effectiveness for damaged timber beam after repairing with CFRP.

ACKNOWLEDGEMENT

This Master research could not have been possible without the assistance, understanding and guidance rendered by numerous people throughout the project. The author would very much like to express his appreciation and gratitude to his supervisors, Associate Professor Jianchun Li, and Docter Rijun Shrestha, for their support and guidance throughout this work and for their patience with proof-reading this thesis. The author would also like to thank Yunlong Luo, who had given the author invaluable advice and assistance in writing this thesis. Utmost gratitude is also due to Xiang Luo and Nin Yan who helped the author for familiar with the ANSYS and MATLAB.

Furthermore, the author would like to thank staff of the UTS Structures Laboratory for their help in the experimental work. Special thanks must also go to David Dicker and Peter for helping the author in setting up static test system and the acquisition system. I wish to sincerely thank Muhammad for helping author applying CFRP on damaged beams. The author also feels a deep sense of gratitude to all the academic and non-academic staff in the Faculty of Engineering and Information Technology for the help rendered.

Finally, the author wishes to thank for my family. For my parents, it is their altruistic and unimaginable support through my master research period. Thank to my aunt, Dr Linda Xiao for giving me a lot of support and guidance on my study and daily life.

LISTOFPUBLICATIONS BASED ON THIS RESEARCH

Refereed Journal Articles

1. Xiao, R., Li, J. & Shrestha, R. (2014), 'Investigations of Vibration Based Condition Assessment of Timber Beams Strengthened with Fibre Reinforced Polymer', *Advanced Materials Research Vol.831 (2014) pp 53-57.*
2. Xiao, R., Li, J. & Shrestha, R. (2014), 'A Novel Vibration Based Assessment Approach for Repair Effectiveness of Damaged Timber Beam Rehabilitated by Fibre Reinforced Polymer', *In Preparation.*

Refereed Conference Papers

1. Xiao, R., Li, J. & Shrestha, R. (2014), 'Investigations of Vibration Based Condition Assessment of Timber Beams Strengthened with Fibre Reinforced Polymer', *3rd International Conference on Civil Engineering and Building Materials, 2013.*
2. Xiao, R., Li, J. & Shrestha, R. (2014), 'A Novel Vibration Based Assessment Approach for Repair Effectiveness of Damaged Timber Beam Rehabilitated by Fibre Reinforced Polymer', *In Preparation.*

TABLE OF CONTENTS

LIST OF FIGURES

LIST OF TABLES

LIST OF NOTATIONS

Δ	change in the flexibility
φ_i	eigenvector of mode I of undamaged model
φ_j	eigenvector of mode I of damaged model
$\emptyset$	mode shape vector
$\emptyset_i$	mode shape of mode i
$\emptyset_{ij}$	mode shape vector of the i^{th} mode and j^{th}element of undamaged beam
$\emptyset_{ij}^*$	mode shape vector of the i^{th} mode and j^{th}element of damaged beam
δ	deflection of the LVL beam
β	damage indicator
β_j	damage indicator of j^{th}member
α	severity estimator
α_j	severity estimator of j^{th}member
α_{cj}	calibrated severity estimator of j^{th}member
η	calibration factor
$\Delta\alpha_d$	indicator of effectiveness of the repair calculated from dynamic test results
$\Delta\alpha_s$	indicator of effectiveness of the repair calculated from static test results
α_s	severity estimation of damage
α_r	severity estimation of the repair
3-D	three-dimensional
9-nodes	9 measuring points taken from the VEMA
CFRP	carbon fibre reinforced polymer
COMAC	coordinate modal assurance criterion
DD	damage detection
Denom	denominator
DOF	degree of freedom
E	modulus of elasticity
E_j	j^{th}equivalent elemental modulus of elasticity of undamaged beam
E_j^*	j^{th}equivalent elemental modulus of elasticity of damaged beam
EI	flexural stiffness
EMA	experimental modal analysis
F	system force vector
FE	finite element
FEA	finite element analysis
FEM	finite element model

FFT	fast Fourier transform
FRF	frequency response function
I	moment of inertia
K	system stiffness matrix
L	light damage
LVDT	linear variable differential transformer
LVL	laminated veneer lumber
M	medium damage
MAC	modal assurance criterion
MSE	modal strain energy
NFerror	natural frequency difference between FE and experimental models
Num	numerator
VEMA	Virtual Experimental Modal Analysis
Z	system displacement vector
Z_j	damage location index

CHAPTER 1INTRODUCTION

1.1Background

Timber has been traditionally used all over the world in structural applications ranging from residential framing to more complex timber system such as timber bridges and wharf deck, as shown in Figure 1.1(a). There are more than 2900 timber bridges still in service in Australia (Department of Transport and Regional Services 2003). The extensive use of timber as a construction material is because of its cost efficiency and environmentally sustainable characteristics. However, being a naturally produced material with hydroscopic properties and strength reducing characteristics such as knots or splits, timber is susceptible to deterioration and damage. Therefore, assessment of existing condition of timber structures and suitable strengthening or repair techniques are essential.

(a) Timber bridge

(b) Repairing Timber structure

Figure 1. 1 Timber structures

In order to strengthen or rehabilitate damaged timber structures, selections of the most efficient solution for identification of the damaged timber structures are crucial. In the recent two decades, a large amount of damage detection methods, termed as "global damage detection methods" have been rapidly developed to overcome the limitations of local damage detection methods such as most of Non-destructive Testing (NDT) approaches. For example, most of local damage detection methods require that the vicinity of the damage is known a priori and that the portion of the structure being inspected is readily accessible (Doebling et al., 1996). Among global damage detection methods, the vibration-based methods are the most popular non-destructive damage detection methods. The fundamental principle behind these methods is that dynamic

characteristics such as frequencies, mode shapes, modal damping and frequency response functions are functions of the physical properties of the structure (mass, damping, and stiffness). Among the vibration-based methods, modal-based damage detection methods have received a significant amount attention in civil engineering applications. To date, a large number of research publications have confirmed that, derivatives or combination of derivatives (such as modal strain energy) of mode shapes are more sensitive to detect structural damage than the other parameters such as natural frequency and mode shape itself. Utilising modal strain energy based on mode shape curvature to locate structural damage and evaluate damage severity has demonstrated certain degree of success in field applications.

After identification of extent of damage in a timber structure, repairing the damaged timber structure is necessary. There are a number of different materials to repair the damaged beam components. This study will focus on utilizing Carbon Fibre Reinforced Plastic (CFRP) to repair damaged timber beams.

Fibre reinforced polymer (FRP) has been widely used in civil engineering applications since 90's shown in Figure 1.1 (b). According to Nanni (2000), the market growth of using FRP is reflect to the increased needs for repaired or strengthening of deficient structures and for new infrastructure systems that last longer and cost less to maintain. Furthermore, applications of FRP composites in civil or infrastructure engineering include different methods such as internal reinforcement and externally bonded reinforcement (Nanni, 2000). This popularity of utilizing FRP has arisen due to the well-known advantages of FRP composites, such as good corrosion resistance and ease for site handling due to their light weight. Minimum increases in structural size and weight as a result of FRP strengthening or repair also contribute to their popularity(Smith and Teng, 2002).

It should be noted that, although the applications of FRP have been researched for a long time and has made a lot of contributions on the improvement of FRP architecture and the methods to utilize FRP to repair or reinforce structures, an assessment on the effectiveness and reliability after repairing or strengthening with FRP is not yet reported in the open literatures. In this thesis, it is proposed to evaluate effectiveness and reliability of repaired or strengthened damage beam utilising damage index method

developed from modal strain energy based damage detection method. The modal strain energy based damage detection methods were initially proposed for damage identification by Kim and Stubbs (1995).This method will be discussed in Chapter 2 in more detail.

Furthermore, many practical problems relate to the poor performance of damage detection in real field applications including processing error, environmental influences, and limited number of sensors, operational influences and measurement noise. Specifically, modal parameters of modal based damage detection methods require Experimental Modal Analysis (EMA) to produce modal parameters for damage detection. The results estimation is heavily affected by imperfections or errors, and environmental and operational conditions during process. For instance, the influence of environmental conditions results in changes in modal properties which can be more than the changes in these properties due to damage. Moreover, the reconstruction of mode shapes is necessary for conducting damage detection because of the limitation of the number of measurement points, the reconstruction method has detailed in Chapter 5. The mode shapes reconstruction may cause errors particularly under noise influence. It is also necessary to indicate that most sensitive damage indicator, such as mode shape curvatures, is also sensitive to these influences. This is part of the reason that most damage detection methods perform poorly in field applications. It is, therefore, important to select a reliable and robust damage detection method that is potentially suitable for field application.

In this study, a non-destructive modal based damage detection methods, namely Damage Index method is selected to locate and to estimate severity of damage and more importantly, it will be modified to evaluate the effectiveness and capacity of repair of damaged timber beam repaired by CFRP.

1.2 Objective of the Study

Due to lack of knowledge on utilizing non-destructive method to evaluate the effectiveness of repair for repaired damaged timber beam, this study sets its aims to investigate a vibration based damage detection method to accurately detect the location and severity of damage as well as utilizing the method to evaluate the effectiveness of

CFRP repairing for damaged timber beams. Specifically, the main objectives of this study are comprised of the following aspects:

- Develop numerical models of timber beams with different type of damage and damaged timber beams repaired with CFRP;
- Perform static loading tests and dynamic tests on timber beams in order to validate the finite element modelling of the timber beams;
- Numerically evaluate and verify the performance of the damage detection method for detecting location and estimating severity of damage in timber beams, using finite element models inflicted with single and multiple damage scenarios, including refining the damage detection method;
- Validate the reliability of the proposed damage detection method on timber beams, using experimental data obtained from experimental modal analysis on pin-pin supported timber beams inflicted with single and multiple damage scenarios.
- Experimentally apply CFRP to repair damaged timber beam;
- Application of a damage detection method to investigate the effectiveness of CFRP in repairing damaged timber beam ;

1.3 Scope of the Work

The research work presented in this thesis is concerned detecting damage in timber structures and evaluating repair effectiveness for repaired timber structures. The damage considered here is localised defects, such as artificially inflicted notches.

In the light of complexity of timber structures, the research started with a pin-pin supported LVL timber beam, which is a basic but an important element in many types of timber structures, such as a timber bridge. An analytical model of a timber beam was numerically developed using a commercial finite element analysis package (ANSYS 14). For the FE modelling, the material properties input were obtained from manufacturer supplied data. Localised damage was simulated in the numerical model by local stiffness reduction method. The finite element (FE) model is then validated by experimental results obtained from the experimental static loading and dynamic test.

Two modal strain energy based damage detection methods were investigated in the research. The methods are based on a reasonable assumption that most damage will result in an equivalent stiffness change, other than the geometric property changes. After obtaining modal parameters (mode shape) calculated from the finite element model, the proposed damage detection method was employed to predict damage location, to estimate damage severities for single and multiple damage scenarios and to investigate the effectiveness of CFRP rehabilitation.

For the experimental work, experimental modal analysis (EMA) is performed on five reinforced timber beams before and after the beams was inflicted with various damage scenarios. In the experimental work, damage is simulated by cutting small notch from the soffit of the timber beams. The EMA is adopted to obtain modal parameter data from both the undamaged and damaged beams.

For CFRP rehabilitation and repair, a small timber block which has same size with damaged parts was glued on the damaged timber beam to let CFRP sheets fully bond onto the tension face. Then, the LVL beams were repaired using Sikadur330epoxy and MBrace Carbon Fibre.

1.4 Significance of the Research Work

In this research, two modal strain energy based method were investigate to detect damaged timber beam, and comparison between these two methods were made to evaluate which one is more sensitive to detect damage. One of the methods will be utilized to evaluate the effectiveness of damaged timber beam rehabilitation. The proposed damage detection methods are numerically investigated using experimentally validated finite element timber beam. Data for verification of the proposed damage detection method were obtained from five LVL timber beams tested in the laboratory. From the numerical and experimental study, the capability of detecting damage and evaluating effectiveness of rehabilitation based upon the measured mode shapes from undamaged and damaged beams of the proposed method has been proved.

The main contribution of this study is to propose modal strain energy based damage detection method to evaluate the effectiveness of rehabilitation/repair of damaged timber beams repaired by CFRP, and the repaired timber beams numerically and

experimentally created for evaluation and verification of the capability of the proposed method.

1.5 Organisation of the Thesis

In Chapter 1, a general overview of the work, the objective of the study, the scope of the work and the contribution of the research are reported.

In Chapter 2, presents a literature review of the damage detection methods mainly focusing on modal based damage detection methods. Subsequently, the literatures of using fibre reinforced polymer to repair timber structure are reviewed. Moreover, the finite element modelling of timber structure and repaired timber structure is also reviewed in this chapter.

In Chapter 3, a general description of tested specimens is presented. Then material property obtained from manufacturer provided data is reported. The set-up of four point bending test is also described.

In Chapter 4, the procedure of developing a reasonable and reliable finite element (FE) model of laboratory timber beams is first described. The simulation of the damage in timber beam and mesh density comparison are also introduced in this chapter. Furthermore, the method of simulating repaired timber beams is also presented. The four point bending test validation using results from the experimental results is briefly discussed in the chapter.

In Chapter 5, damage detection results from the finite element model of a timber beam using different damage detection methods are presented, and an over view of the tests using experimental modal analysis on timber beams is given. Different damage scenarios are discussed and the proposed damage detection methods are used to identify the evaluate damage.

In Chapter 6, conclusions and recommendations are summarised in this Chapter.

CHAPTER 2 LITERATURE REVIEW

2.1 Vibration Based Damage Detection

2.1.1 Methods Based on Natural Frequency

Natural frequency is an essential property of vibration system. It is mainly related to the modulus of elasticity or stiffness of an intact or damaged beam. Due to this theory, shift in natural frequencies can be considered as damage indicators. This method has been widely used in civil engineering. The popularity of this method is due to the fact that natural frequencies are easy to determine and only a single sensor is sufficient in many applications. However, the disadvantage of this method is that environmental changes such as temperature and humidity can easily influence the natural frequencies. Furthermore, the location and severity of damage is difficult to be identified by natural frequencies only in many structures

A large number of literatures can be found on the use natural frequencies in detecting damage. Most of the early research on natural frequencies was grounded on simple structures and structural elements. Cawley and Adams (1979)published a paper which is one of the most commonly referenced work using natural frequencies in damage detection. This paper proves analytically and experimentally that damage can be detected, located and quantified by using a single point in the structure. Utilizing the ratio of frequencies in two modes as a function of the damage location is the concept of the method. The theoretically calculated ratio equals the experimentally measured value which is used to determined possible damage positions. Superimposing the loci of several pairs of modes and the intersection of the curves is used to predict the actual damage location. This method was successfully applied to free-free carbon fibre reinforced polymer (CFRP) plates. The further study of this paper was to filter out the affection of temperature from the measured natural frequencies.

A method utilising a frequency based damage detection (FBDD) to locate damage and assess the damage quantity was presented by Kim et al. (2003). The main idea of FBDD method is the ratio of fractional changes in Eigenvalue because of damage and modal energy. Utilizing a localization error norm to define a single damage index that would

determine location of damage was introduced in the two fractional ratios. The single damage indicator approaches its maximum point represents the damage location. According to Euler-Bernoulli beam theory, a damage-sizing algorithm was improved using the correlation between fractional changes in modal strain energy and fractional changes in frequency. Furthermore, because of crack, the shift in modal strain energy could be rated to the energy loss rate. Therefore, this reason will result in a relationship between crack depth and fractional change in Eigen value. For single damage cases, the FBDD method can determine the damage location of the inflicted crack but not exactly. Moreover, it presents a symmetrical false positive for damage inflicted at quarter span. However, the FBDD method aims at single damage while it did not solve multiple damage cases.

2.1.2 Mode Shape Method

The modal assurance criterion (MAC) was firstpresented in 1983(Allemang and Brown, 1983) This method uses mode shapes data to identify the location and quantity of damage of a structural. MAC is defined as:

$$MAC(\varphi_i, \varphi_j) = \frac{\left|\varphi_i^T \varphi_j\right|^2}{\varphi_i^T \varphi_i \varphi_j^T \varphi_j}$$

φ_i = eigenvector of mode I of undamaged model;

φ_j = eigenvector of mode I of damaged model;

MAC is a correlation coefficient; it varies between 0 and 1. The value evaluates the related degree between damaged and undamaged mode shapes vectors. A value of 1 indicates that two mode shapes vectors are perfect related, which is an undamaged model. A value of 0 indicates that these are no relation at all between both vectors, which means damaged model. The main advantage of MAC is that it quantifies the degree of proportion with on number. However, the MAC method cannot localise the damage.

A further development of MAC method is the coordinate modal assurance criterion (COMAC) (Lieven and Ewins, 1988). COMAC compares two sets of modes to identify the location of damage. COMAC is defined as

$$COMAC(i) = \frac{\left[\sum_{j=1}^{N} \left|\varphi_{ij}^{A} \varphi_{ij}^{B}\right|\right]}{\sum_{j=1}^{N} (\varphi_{ij}^{A})^2 \sum_{j=1}^{N} (\varphi_{ij}^{B})^2}$$

A, B= damaged and undamaged model;

$\varphi_{ij}^{A}, \varphi_{ij}^{B}$ = Modal coefficient of damaged and undamaged model for degree-of-freedom I, mode j.

The change of COMAC is not obvious when the damage is not significant. Moreover, if using COMAC method to accurately localize damage, it will detect a large amount of mode shapes. Therefore, it is not cost-efficient.

Abdo and Hori (2002)reported a damage indicator utilizing shifts in the rotations or slop of mode shapes to detect presence of structural damage. To demonstrate the robustness of the method a finite element model of steel plated was developed. It was noted that using the rotations of mode shapes to identify damage are better than the changes in the displacement mode shapes. The numerical results presented that higher modes are not essential for indicating light damage (5% reduction in the modulus of elasticity). A good selection of mode shapes is necessary in the method in order to get accurate results and this can be completed using sensitivity of natural frequency to damage.

Pandey et al. (1991)found a method of using mode shape curvature in damage detection. A finite element model of a cantilever beam and a simply supported beam was created, and using central difference approximation acquired mode shape curvatures for intact and damaged beams. The results showed that for a damaged simply supported beam with 50% decline in modulus of elasticity and pertaining to a single damage scenario, mode shape curvature is much more accurate than modal assurance criterion (MAC) and coordinate modal assurance criterion (COMAC) values.

2.1.3 Dynamic Flexibility Based Method

Another damage detection method has been presented by Pandey and Biswas (1994). In their research, they used flexibility to detect damage. The flexibility matrix F was defined as

$$\mathrm{F} = \Phi\Omega^{-1}\Phi^{T} = \sum_{i-1}^{n} \frac{1}{\omega_i^2}\Phi_i\Phi_i^T$$

where $\Phi = [\Phi_1\Phi_2 \ldots \Phi_n]$ is the mode shape matrix, Φ_i is the *i*th mode shape, $\Omega = \mathrm{diag}(\omega_i^2)$ is the mode eigen vector, ω_i is the *i*th modal frequency, Based on the flexibility matrices, change in the flexibility matrix Δ can be obtained as

$$\Delta = F_i - F_d$$

where F_i and F_d are the flexibility matrices for the intact and damage cases, respectively. For each degree of freedom *j*, $\overline{\delta_j}$ is the maximum absolute value of the elements in the corresponding column of Δ, i.e.,

$$\overline{\delta_j} = max_i|\delta_{ij}|$$

where δ_{ij} are elements ofΔ. Thus, in the research, $\overline{\delta_j}$ was used as measure of change of flexibility for each measurement location, in order to be able to detect and locate damage in a structure. The measured flexibility of the structure was tested with numerical examples and then with experimental data collected on a wide range of steel beams. The result of single damage testing of both numerical and experimental examples demonstrated that the location of damage could be identified from just the first two measured modes of the structure.

Bernal and Gunes (2002) develop a method that using extension of flexibility based method to detect the localization of damage. His basic concept was as follows: lack of deterministic information on the input can be partially compensated for, by know ledge of the structure of the mass matrix. A damage location vector (DLV) was proposed to locate the damage by inspecting stress fields created by vectors that are contained in the null space of the change in flexibility. The method was applied on a numerical example

of a cantilevered spring-mass system. The results indicated showed that the DLV method only identified small sets containing the damaged elements. The author suggested that a final assessment on robustness, therefore, awaits experimental validation.

Kim et al. (2002)developed a new method based on modal flexibility to identify location and severity of damage in a structure using limited modal data. An assumption was made that a small damage event will have an insignificant effect on the internal forces in a structure under certain loading conditions. In the case of coarse sensor intervals, cubic spline interpolation technique was adopted to create a diner grid. Using the Modal flexibility and its relationship with slope deflection formulae, the flexural damage index equation (FDIE) was formulated. The Z24 Bridge was tested with the FDIE. The example of a single damage case showed that using the first three modes the damage was detected.

2.1.4 Modal Strain Energy Based Method

2.1.4.1 General Modal Strain Energy Method

Zhu and Xu (2005) presented that mode shape is an typical feature of any structure, and it is considered as an indicator in damage detection, whereas a large amount of research works has noted that derivatives of mode shapes are more sensitive to detect damage than mode shapes themselves such as mode shape curvatures which is twice differentiation of mode shape, modal strain energy which is a function of mode shape curvature. Therefore, using modal strain energy method has been very popular in damage detection.

A non-destructive damage detection method to identify and assess damage from a few mode shapes of structures was presented by Kim and Stubbs (1995). This method developed from an original conception that the fraction of modal strain energy is same for both damaged and undamaged structures. A damage index β_{ji} of i^{th} mode and j^{th} member was acquired:

$$\beta_{ji} = \frac{E_j}{E_j^*} = \frac{\emptyset_i^{*T} C_{jo} \emptyset_i^*}{\emptyset_i^T C_{jo} \emptyset_i} = \frac{NUM}{DEN}$$

E_j and E_j^* are parameters of the material stiffness properties associated with undamaged and damaged states, respectively; $\emptyset_i$ and $\emptyset_i^*$ are the i^{th} modal shapes associated with undamaged and damaged states, respectively; C_{jo} represented geometric quantities; and superscript 'T' denotes transpose of a vector.

For NM vibrational modes, a damage index β_i of j^{th} member was obtained:

$$\beta_j = \frac{\sum_{i=1}^{NM} NUM}{\sum_{i=1}^{NM} DEN}$$

where $\beta_j \geq 0$ and damage is indicated at the j^{th} member if $\beta_j \geq 1$.

Moreover, the predicted location j was defined as follows:

$$Z_j = \frac{(\beta_j - \bar{\beta})}{\sigma_\beta}$$

β_j was the mean of the collection of β_j values and σ_β was the standard deviation of the collection of β_j values respectively. Finally, the severity of damage in the j^{th} member was estimated in the research work as follows:

$$\alpha_j = \frac{1}{\beta_j} - 1; \alpha_j \geq -1$$

This research study verified this damage detection method. The experimental result indicated that a single damage can be confidently located with relatively small localisation error and relatively small false negative (missing detection of true damage locations) error but a relatively large false positive (prediction of locations that are not damaged) error. Severity estimation error was generated in this method and also generated in quantifying the severity of damage.

In another research work,Stubbs et al. (1995) demonstrated a similar damage index method while the partial modal energy is combined with a unity in the numerator and denominator. This step was used to derive a consistent indicator of damage localisation and to avoid division-by-zero simply by shifting the axis of reference. Employing the first three modes in the numerical and experimental models of a steel plate girder,

damage localisation for single damage cases were accurate but with some false positives.

Another study upgraded the 1-D strain energy method to a 2-D strain energy method for application to plate-like structures (Cornwell et al., 1999). It is noteworthy that, through decomposing the 2-D and 3-D structures into beam-like elements, the 1-D strain energy method has been properly applied to detecting damage. It was presumed that the decomposition technique using the 1-D algorithm would not outperform the 2-D algorithm as it did not preserve the torsional stiffness between slices. Both 1-D and 2-D options were analysed using numerical simulations and experimental methods. During the numerical simulation, a pinned-pinned plate with several elements with reduced 10% stiffness using the first for modes, the 2-D method displayed the general location of damage, which is, however, not detected in the 1-D decomposition method. For the experimental test using an aluminium plate with two saw cuts, both methods provided similar outcomes. At low degrees of damage, both methods had the potential to generate spurious damage locations.

2.1.4.2 Damage Index Method

Choi et al. (2008) presented a modified damage index (MDI) method, based on modal strain energy, for detecting damage to a timber beam. The sawn timber beam was of treated radiate pine measuring 45mm × 90mm in cross section, with a span length of 4500 mm. In the damage detection process, cubic spline data interpolation function was used to perform mode shapes reconstruction of the experimental data. The reconstructed mode shapes were then differentiated to obtain mode shape curvatures which were then normalised for damage index calculation. The proposed MDI method was capable of detecting the damage location from the experimental data with false positive error. However, using a combination of high and low modes proved to be more favourable for detecting multiple damage locations. Regarding the estimation of severity of damage, the authors claimed that it will be possible to further explore the MEI method, especially in regard to multiple damage scenarios.

In 2002, Kim and Stubbs (2002)improved their original damage detection method. In their new research, a new damage detection algorithm was formulated to overcome

limitations of the previous method (Kim & Stubbs 1995), and to thereby improve the accuracy of damage localization and severity estimation. Three damage indices (Damage Index A, Damage Index B and Damage Index C) were presented in their new algorithm.

For Damage Index A:

$$\beta_j = \frac{E_j}{E_j^*} = \frac{\sum_{i=1}^{nm} \gamma_{ij}^* K_i}{\sum_{i=1}^{nm} \gamma_{ij} K_i^*}$$

$$\alpha_j = \frac{\sum_{i=1}^{nm} \gamma_{ij}^* K_i}{\sum_{i=1}^{nm} \gamma_{ij} K_i^*} - 1$$

where K_i and K_i^* are the i^{th} modal stiffness of the arbitrary structure before and after damage;$\gamma_{ij} = \emptyset_i^T C_{jo} \emptyset_i$; $\gamma_{ij}^* = \emptyset_i^{*T} C_{jo} \emptyset_i^*$;$\emptyset_i$ and $\emptyset_i^*$ are the i^{th} modal vector before and after damage, respectively. Damage is indicated at j^{th} member if $\beta_j > 1$ and damage severity is indicated as the reduction in stiffness in the j^{th} member if$\alpha_j < 0$.

For Damage Index B:

$$\beta_j = \frac{E_j}{E_j^*} = \frac{\sum_{i=1}^{nm} (\gamma_{ij}^* + \sum_{k=1}^{n^e} \gamma_{ik}^*) K_i}{\sum_{i=1}^{nm} (\gamma_{ij} + \sum_{k=1}^{n^e} \gamma_{ik})\, K_i^*}$$

$$\alpha_j = \frac{\sum_{i=1}^{nm} (\gamma_{ij}^* + \sum_{k=1}^{ne} \gamma_{ik}^*)\, K_i}{\sum_{i=1}^{nm} (\gamma_{ij} + \sum_{k=1}^{ne} \gamma_{ik})\, K_i^*} - 1$$

For Damage Index B based damage detection method, damage is indicated at the j^{th} location if $\beta_j > 1$ and damage severity is indicated as the reduction in stiffness in the j^{th} member if$\alpha_j < 0$.

For Damage Index C:

$$\beta_{ji} = \frac{E_j}{E_j^*} = \frac{\gamma_{ij}^*}{\gamma_i g_i(\mu, \emptyset) + \gamma_{ij}} = \frac{Num}{Den}$$

$$\beta_j = \frac{\sum_{i=1}^{nm} Num}{\sum_{i=1}^{nm} Den}$$

$$\alpha_j = \frac{dE_j}{E_j} = \frac{1}{\beta_j} - 1$$

where $\gamma_{ij} = \emptyset_i^T C_{jo} \emptyset_i$ and $\gamma_{ij}^* = \emptyset_i^{*T} C_{jo} \emptyset_i^*$; $\frac{dE_j}{E_j}$ is the fractional changes in the stiffness of the j^{th} member; $g_i(\mu, \emptyset)$ is the dimensionless factor representing the systematic change in modal parameters of the i^{th} mode due to the damage. The same as before, damage is indicated at the j^{th} location if $\beta_j > 1$ and damage severity is indicated as the reduction in stiffness in the j^{th} member if $\alpha_j < 0$.

Then a two span continuous beam was constructed numerically and ten different damaged beams, with different locations and severities of damage, were simulated. After that, pre and post damage modal parameters of the results showed that the newly formulated method was able to locate damage and estimate severity of damage with reasonable accuracy.

A new damage detection algorithm based on modal strain energy is proposed by Wang (2010). The new proposed algorithm is capable not only of identifying the location of damage, but also of quantifying the severity of damage.

$$\beta_{ji} = \frac{E_j}{E_j^*} = \frac{\frac{\varphi_i \emptyset_{ij}^T \emptyset_{ij}}{\overline{MSE_{IJ}}}}{\frac{\varphi_I^* \emptyset_{IJ}^{*T} \emptyset_{IJ}^*}{\overline{MSE_{IJ}}^*}}$$

$$\beta_j = \frac{\sum_{i=1}^{nm} Num}{\sum_{i=1}^{nm} Den}$$

$$Z_j = \frac{\beta_j - \mu_{\beta j}}{\sigma_{\beta j}}$$

$$\alpha_j = 1 - \frac{1}{\beta_j}$$

where $\mu_{\beta j}$= mean of β_j values for all j elements and $\sigma_{\beta j}$= standard deviation ofβ_j for all j elemnts. Z_j is proposed as a damage location index to indicate the location of damage for given modes, and α_j is proposed as a damage severity estimator to quantify the

severity of damage for given modes. The basic principle is that damage will alter the stiffness of the j^{th} element, E_j, due to the damage in the element.

2.2 FRP Application on Timber Structures

André (2006) provides a summary of the methods in which FRP composites have been applied to timber for flexural strengthening in past investigations

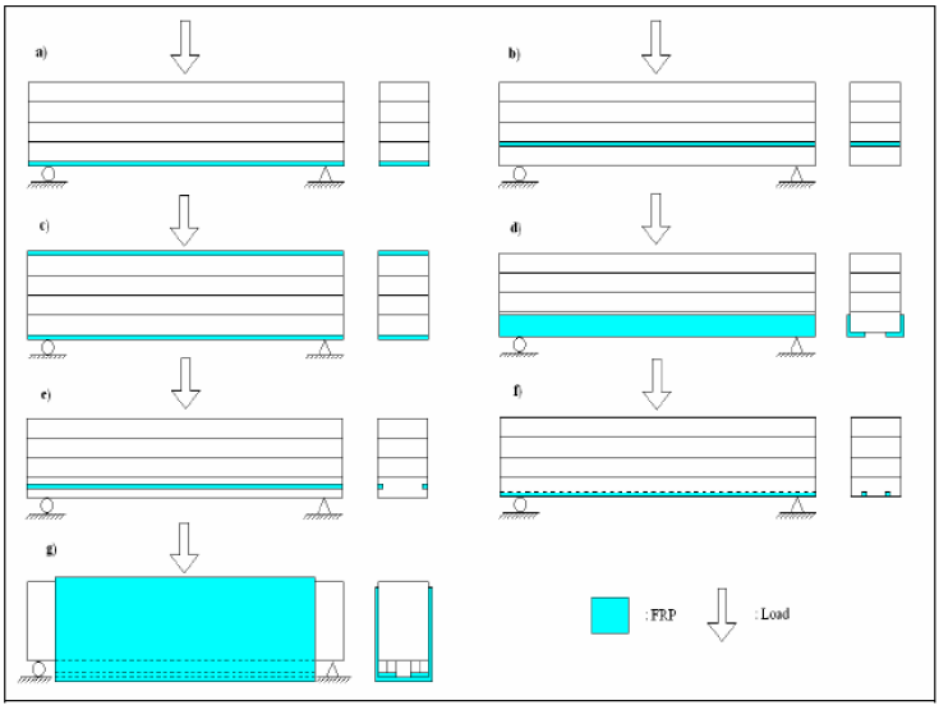

Figure 2.1 Different investigations to increase wood flexural properties (Andre 2006)

Method (a) involves external bonding of FRP layers onto the soffit (tension side) of the beam and is aimed primarily at increasing flexural strength. Method (b) incorporates FRP composites into the timber production process by hiding layers between lumbers typically for fire safety or aesthetic reasons. Method (c) provides FRP layers to both compression and tension sides of the beam and accordingly improves stiffness. While method (d) involves bounding FRP layers to the bottom tension lumber / laminate of the beam only. Methods (e) and (f) do not utilise sheets / strips but instead use near surface mounted (NSM) FRP bars which are inserted into grooves and bonded to the wood with an epoxy resin. Accordingly, this method decreases the risk of splitting caused by moisture movements, as it does not restrain large areas of timber. Lastly, method (g)

involves wrapping FRP sheets around the beam and is ideal for restoring partially deteriorated or cracked timber (Johnsson *et al*. 2006).

Plevris and Triantafillou (1992) examined the behaviour of timber beams strengthened with CFRP sheets bonded to the bottom tension face only. An analytical model was presented which considered the timber with linear-elastic behaviour under tension and an elastic-plastic behaviour under compression. The fibre was considered a linear elastic material. The behaviour of the FRP-wood beam was described with uniaxial stress-strain relationships in which the extreme tensile fibre strain could be associated with one of the following states: (a) Both wood and FRP are linear-elastic; (b) Wood is linear-elastic, FRP has ruptured; (c) Wood has yielded, FRP is linear-elastic; (d) Wood has yielded, FRP has ruptured. The experimental results showed that by increasing the area of external reinforcement, a transition from brittle to ductile failure is possible and were observed in beams which were reinforced with higher FRP ratios. The increases in strength would reach a peak before decreasing but tensile stresses would continue until rupture occurs below the peak moment. Plevris and Triantafillou (1992) justified the observations based on the formation of a plastic-hinge behaviour allowing extensive yielding before failing. *Figure 2.2* illustrates such behaviour where the control beams with no FRP reinforcement experienced brittle failure, while the beams with higher FRP fractions carried higher loads and exhibited more ductile failure.

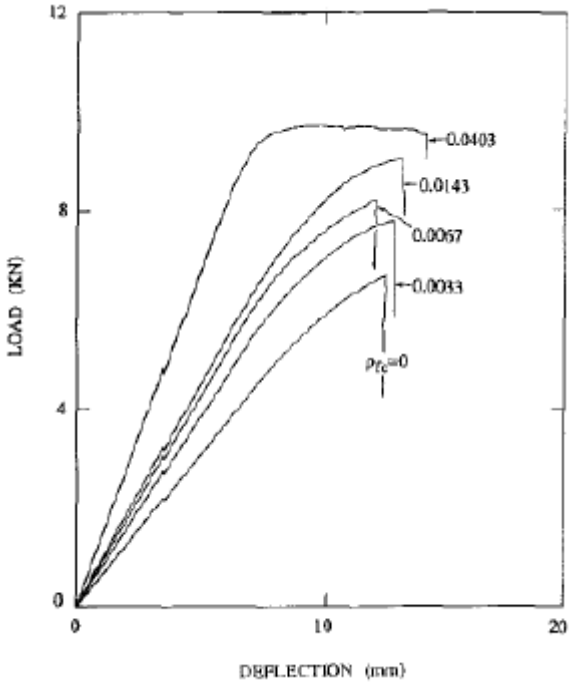

Figure 2.2 Load-deflection curves for CFRP-reinforced wood beams in three-point bending (Plevris and Triantafillou 1992)

The research by Plevris and Triantafillou demonstrated the potential of the FRP-wood composite member due to favourable increases in strength, stiffness and ductility. Generally, the failure of the reinforced specimens were governed by wood compressive yield producing a non-linear response, followed by rupture of the CFRP which resulted in a sudden drop of load and, in turn caused wood fracture in the tension face ending with collapse of the specimens.

The performance of Yellow-Poplar glulam reinforced with glass fibre reinforced polymer (GFRP) composites was investigated by Hernandez et al. (1997). The beams were reinforced in two ways: 1) with a single piece of GFRP to the outer compression and tension faces and2) two pieces of GFRP to the tension face only. The results did not agree well with a previous study conduct by Plevris and Triantafillou (1992), in which most beams failed catastrophically without warning before reaching ultimate load. Before ultimate load the authors observed two incidents, one of which was that the GFRP on the tension side delaminated completely and the other, after giving a closer inspection, revealed the failure happened through a finger joint in the outermost wood lamination on the tension side near mid-span. This could be due to the use of higher

fibre content GFRP with a richer resin matrix, insufficient surface preparation as well as improper curing time and temperature for the adhesive. Another study (Hernandez *et al*., 1997) evaluated numerous analytical techniques and indicated normal mechanic methods (e.g. transformed section analysis) can provide an accurate estimation of the stresses for a beam reinforced with GFRP on the top and bottom faces, since this beam behaves nearly linearly to failure. In contrary, a beam strengthened on the bottom tensile face was found to behave non-linearly and thus basic mechanic methods were not applicable in this case

The anchorage length effect of FRP applied on the tension side of commercial sawn timbers was presented by Johns and Lacroix (2000). There were three reinforced sample applied to weak and strong members from the timber population as depicted in *Figure 2.3*. The first two schemes involved applying CFRP to the area of constant moment only, while the only difference is the length of CFRP layer. The third sample was bonded with U-shape of GFRP.

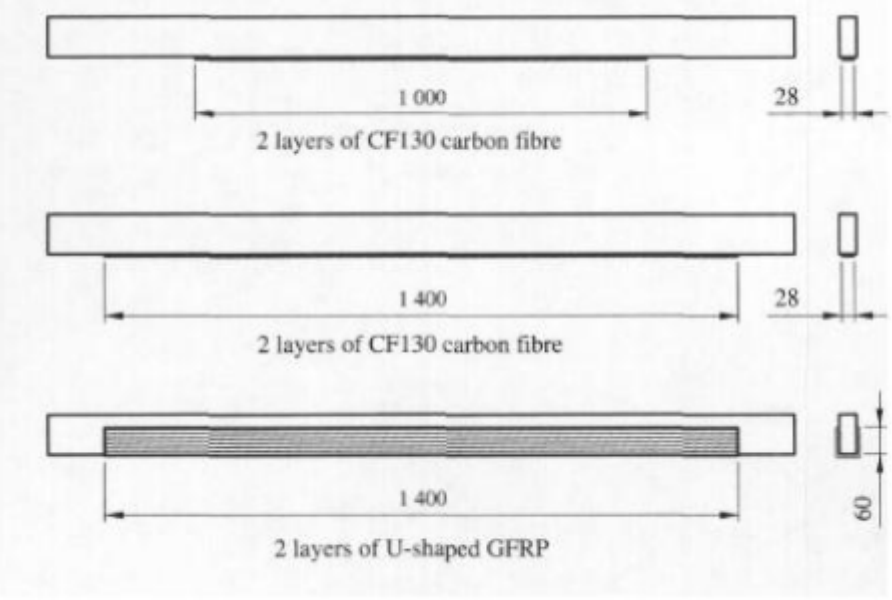

Figure 2.3 Reinforcing schemes for the three samples (Johns and Lacroix 2000)

Johns and Lacroix (2000) also indicate that failure in the wood occurred earlier than in composite. Some timbers failed beyond the composite zone because of the local defects. Compared with the effectiveness of the reinforcement configurations, Johns and Lacroix (2000) reported that the shorter carbon fibre case led to smaller improvement in strength, while the longer carbon fibre reinforcement and U-shaped glass fibre

reinforcement resulted in massive increases in strength. Johns and Lacroix (2000) showed a method for analysing composite-reinforced commercial timber beams and discussed the failure phenomena linked to reinforced beams. Greater increments in strength for almost all the 150 timber beams were observed in comparison with that estimated using simple transformed-section analysis and direct use of Code values for strength.

Buell and Saadatmanesh (2005) presented that FRP wraps and strips can be used to reinforce solid-sawn Douglas Fir timber beams which were part of a timber stringer bridge. The project investigated whether the load capacity of the beams were increased by bonding composites in the manner of either a fabric wrap or laminate strips to timber beams. There were six beams tested in flexure. Buell and Saadatmanesh (2005) found that applying CFRP to the timber beams provide significant improvement in bending and shear capacity and nominal increases in the stiffness of the beams. Buell and Saadatmanesh (2005) commented that a complete wrap was more effective than overlapping several strips of carbon fibre largely due to the fabric not adhering well to itself. This resulted in minor delamination and reduced the confinement of the wood fibres causing the beam to fail. The results also indicated that the addition of carbon laminate to the bottom of the beam followed by wrapping of the beam provided no improvement in strength in comparison to the wrapped specimens. Buell and Saadatmanesh (2005) also note that the beam failed in horizontal shear due to a shake that existed prior to the test. However, Buell and Saadatmanesh (2005) also commented that such failure could have been prevented if the member had been wrapped with carbon fabric.

Schober and Rautenstrauch (2005) carried out a similar investigation to Buell and Saadatmanesh (2005), which involved the repair and strengthening of existing timber floors under bending. Schober and Rautenstrauch (2005) compared two different reinforcement approaches – internal reinforcement and external reinforcement both using CFRP material. The beam specimens were preloaded spruce rafters and ceiling joists over 100 years old removed from an old residential house in Bavaria, Germany. As shown in figure 2.4, the first reinforcing scheme consisted of external bonding of CFRP to the tension zone (Vh), while the second and third reinforcing schemes consisted of internal bonding of CFRP either laterally on the sides (Vs) or vertically (Vv) to slots made in the beams,

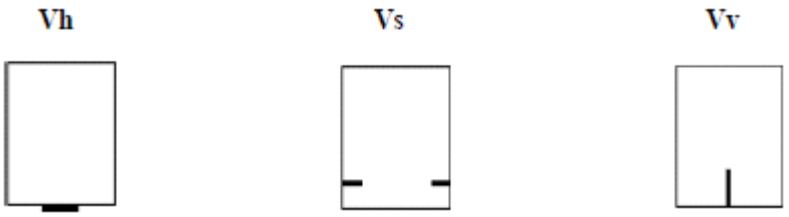

Figure 2.4 Reinforcement schemes (Schober and Rautenstrauch 2005)

The beams were subjected to a series of four point bending tests firstly without reinforcement to establish the initial stiffness and modulus of elasticity (MoE), then unloaded and reinforced with the schemes described above to determine the stiffness and MoE of the reinforced specimens. The reinforced beams were then loaded to failure to evaluate the ultimate load and fracture mode. Schober and Rautenstrauch (2005) note that each beam contained a number of defects, which varied across all specimens and consequently it was hard to say at what load the beams would fail. However, it was noticed that the reinforced specimens in general exhibited a more ductile behaviour. Quantitatively, the flexural strength increased on average about 25 % while the bending stiffness increased by about 6 %.

2.3 FE modelling on Timber and FRP

2.3.1 Modelling of Timber

There are quite a number of researchers that have used FE to model concrete and steel bridge structures. However, to the best of the author's knowledge, there are few publications found in literature on modelling of timber beams using finite element analysis for the purpose of structural dynamic system identification and damage detection.Kurian (2000) has used FE model to study the static behaviour of timber bridge structures. The connection between the deck and girder were of full composite, where deck and girder share the same connecting nodes. Duan (2003) utilised finite element analysis to characterise the dynamic behaviour of a laminated timber bridge. Several two-dimensional and three-dimensional models were developed using plastic analysis with different elements such as shell and beam as well as spring elements. The results showed that models with springs yield results closer to the experimental data compared to the ones without spring. Since the work done on FE modelling of timber

bridges is limited, the search extended to FE modelling of other timber structures such as work done byGerber and Crews (2005). They have utilised an arbitrarily element to model the connection between deck and joists, even then the connections were considered 100% composite. The results show that the FE model is capable to model, quite precisely, a timber structure validated with the static test.

2.3.2 Modelling of CFRP Rehabilitation

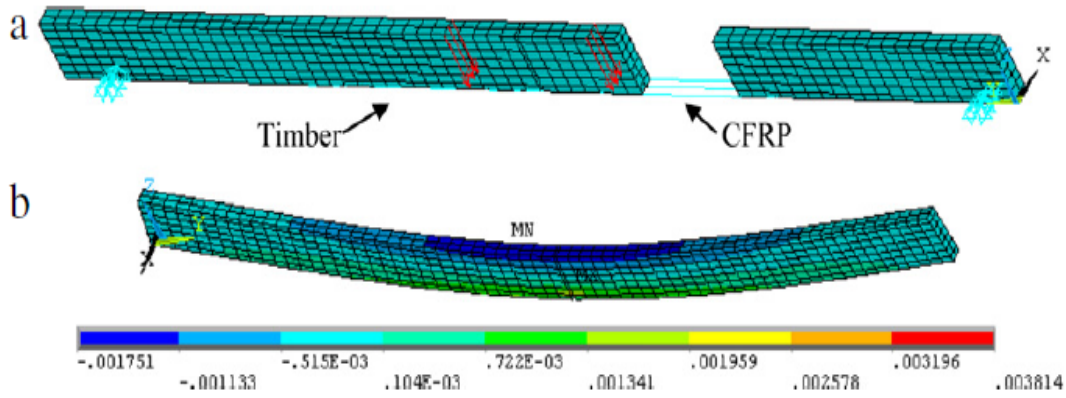

Figure 2.5 FEA model: (a) meshed beam with boundary condition (cut-away view of Beam DF5); (b) strain contour (Beam DF4).

A modelling approach was provided by Kim and Harries (2010) to estimate the fate of timber beams reinforced with carbon fibre reinforced polymer (CFRP) composites. The authors formulated a three-dimensional finite element analysis (FEA), according to the orthotropic constitutive characteristics of timber species. The model displayed the load displacement relationship, strain development, stress concentration, and failure modes of the CFRP-strengthened timber beams and those responses were compared to the experimental data. Figure 2.5 illustrates a developed FEA model applied by Kim & Harris (2010). In order to represent the timber species, three-dimensional solid elements (SOLID 45) were employed. The unidirectional CFRP composites were modelled with three-dimensional spar elements (LINK 8). This was in good agreement with the finding of Kim & Harris (2010) which demonstrated the element, comprising two nodes, included three translational degrees of freedom per nod and hence constraint equations were unnecessary so as to connect the timber elements and the CFRP elements (e.g. the

observation of compatibility of the degrees of freedom between the elements).Neither interface elements nor slip behaviour were taken into account for this analysis, as the strength of adhesives was higher than the cohesion-strength of timber grain and thus interfacial failure between the timber and the CFRP did not occur in the test specimens. In addition, the authors indicated that although the elastic modulus of the CFRP composites affected the failure mode of the reinforced beams, it may not have considerable impact on the strength-increase of the beams, given the fact that the properties of timber species, instead of the CFRP properties, are a major factor that affects the failure of the beams.

CHAPTER 3 EXPERIMENTAL INVESTIGATION

3.1 Introduction

This chapter presents the details of the experimental investigation carried out on undamaged, damaged and repaired laminated veneer lumber (LVL) beams. These tests were used to validate the finite element model (discussed in Chapter 4) and also to investigate the effectiveness of the damage detection technique.

3.2 Material Properties

3.2.1 LVL Beam

Laminated veneer lumber is an engineered wood product which uses multiple layers of thin wood veneers assembled with adhesives (Figure 3.1).There are several advantages of using LVL over sawn timber such as stronger, straighter and more uniform. The major elastic property of LVL timber beams is its modulus of elasticity. The Modulus of elasticity can be defined as the change of stress with respect to strain in the elastic range. For this research study, the modulus of elasticity of the test specimens is obtained from manufacture data which was 13 GPa.

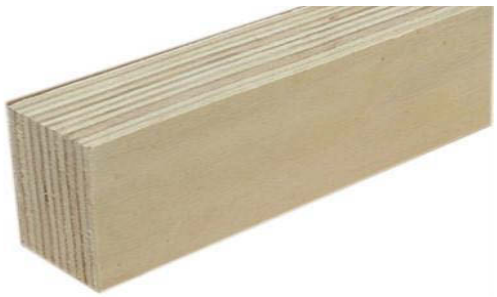

Figure 3.1 Laminated veneer lumber

3.2.2 Property of Carbon Fibre Reinforced Polymer

Carbon fibres reinforced polymer is composite material which consists of two parts: a matrix and reinforcement. In CFRP, the reinforcement is carbon fibre, which provides the strength. The matrix is usually a polymer resin, the material properties depend on these two elements. Unlike isotropic material like steel and aluminium, CFRP has

directional strength properties. The properties of CFRP depend on the layouts of the carbon fibre and the proportion of the carbon fibres relative to the polymer. Usually, there are two types of CFRP material used in civil engineering applications, which are carbon fibre and carbon fibre sheets. In this study, the carbon fibre sheets CF120 (figure 3.2) is utilized. Based on manufacturer's data, the CF120 has a thickness of 0.117mm and can attain a tensile strength higher than 3700 MPa, and an elasticity modulus of 240 GPa. As no adhesion is applied between individual fibres, the transmission of forces between the fibres is achieved using a polymer or resin matrix. Polymers, which contained the epoxy selected for this investigation, show a few strengths, such asreduced cost, ease of work-ability, and enhanced resistance to environmental impacts. The epoxy is applied to both sides of fabric. An ordinary point roller and hand pressure are used to ensure its effectiveness.

Figure 3.2 Carbon Fibre sheets

3.3 Design of Specimens

3.3.1 Dimensions of LVL Timber Beams

Five LVL beams were tested. Among the five beams, one beams was used as a control beam which is an intact beam without any damage while the other four beams were inflicted three levels of damage (light, medium and severe) at two locations (mid-span and quarter-span). Four point bending test and dynamic test were performed for each beam. Three of the beams were repaired with CFRP and were loaded under four-point bending load until failure to estimate remaining strength capacity. In addition to the control beam, the remaining four beams were used for experimental modal analysis followed by damage detection studies. The dimensions of the LVL timber beam are shown in Figure 3.3. The beam was 65 mm wide, 120mmdeep and 3240mm long.

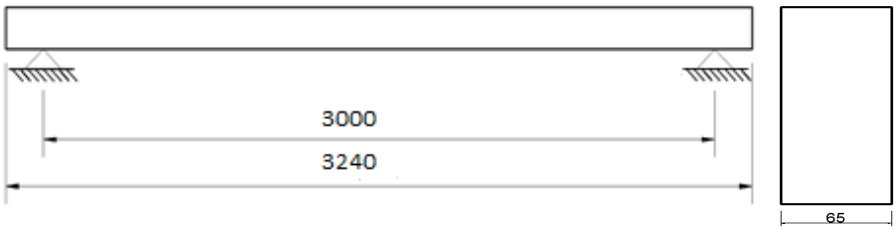

Figure 3.3 Dimension of Specimen

3.3.2 Inflicted Damage in Test Beams

Among the five LVL timber beams, one beam was used as a control beam whilst the remaining four beams were subjected to different damage scenarios as summarised in Table 3.1. In all damage scenarios, the damage consists of a rectangular notch on the soffit of the beam (Figure 3.4), located at quarter span and mid span of the span length to simulate damage. Regarding the damage scenarios, three levels of damage severity, namely light (L), medium (M) and severe (S) damage, were adopted in the experimental work. All damages were inflicted by a saw-cut. The width of the saw-cut was 30mm (or 1% of the clear span of the beam) and consisted of 25%, 50% and 75% of the beam depth, designated as damage cases L,M and S as shown in Table 3.1. For all three cases the cuts were made across the entire width of the beams, namely, 65mm.

Table 3.1 The size of different damage scenarios

Beam Number	Damage Case	Damage Scenario	Location of Span length	Length (mm)	Depth (mm)
Beam 1	1	4S	4	30	90
Beam 2	2	2S	2	30	90
Beam 3	3	4L	4	30	30
	4	4M	4	30	60
	5	4S	4	30	90
	6	4S2L	2, 4	30	30, 90
	7	4S2M	2, 4	30	60, 90
	8	4S2S	2, 4	30	90, 90
Beam 4	9	4L2S	2, 4	30	90, 30
	10	4M2S	2, 4	30	90, 60

Figure 3.4 Side view of a typical damage inflicted in test beams

3.3.3 Procedures of Using CFRP to Repair Damaged Timber Beams

The CFRP rehabilitation was carried out on Beams 1, 2 and 3 after all damage scenarios. The procedures of CFRP rehabilitation are described as follow. First of all, a small timber block pre-cut into the same size with damaged parts was glued on the damaged timber beam using a polyurethane glue so that the CFRP could be fully bonded to the soffit of the repaired beams. Figures 3.5 and 3.6 specifically illustrate the method of CFRP repairing. Secondly, using an air gun cleaned the dust at the soffit, and sikadur 330 epoxy was then applied on the soffit surface. The first carbon fibre sheet which was pre-cut into required width and length was then laid on top of the epoxy layer. The CFRP sheet was then rolled using a steel roller to ensure proper impregnation of the epoxy in between the CFRP fibres and to drive out any possible air voids. Finally, the second CFRP sheet applied on top of the first sheet using the same procedure.

Figure 3.5 LVL Timber beams repaired by CFRP

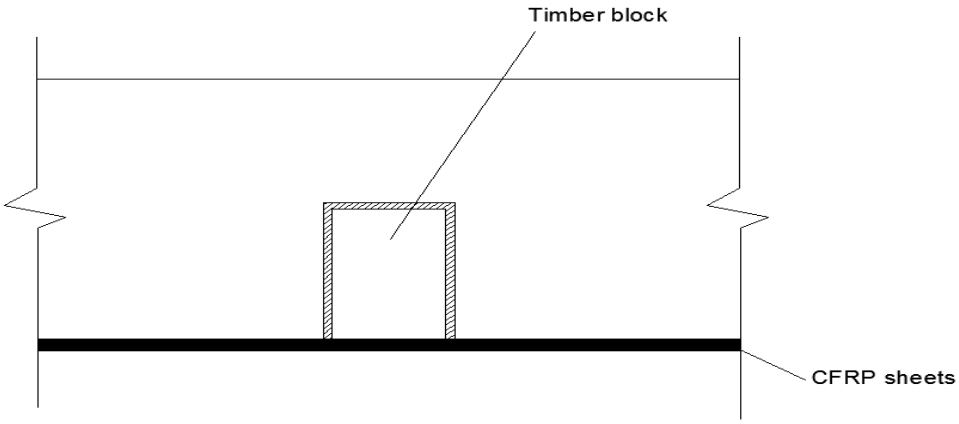

Figure 3.6 CFRP rehabilitation

3.4 Four-point Bending Test for the Specimens

Four point bending test was performed on each specimen to validate the modelling of LVL timber beams. Tests were conducted for each state of the beam, i.e. intact, damaged and repaired. Results of the test were used to compare with numerical results in Chapter 4.

3.4.1 Static Test Set up

Typical set up for the four-point bending test is shown in Figure 3.7. Two point loads were applied on the top of the beam at 900mm length from both end supports.

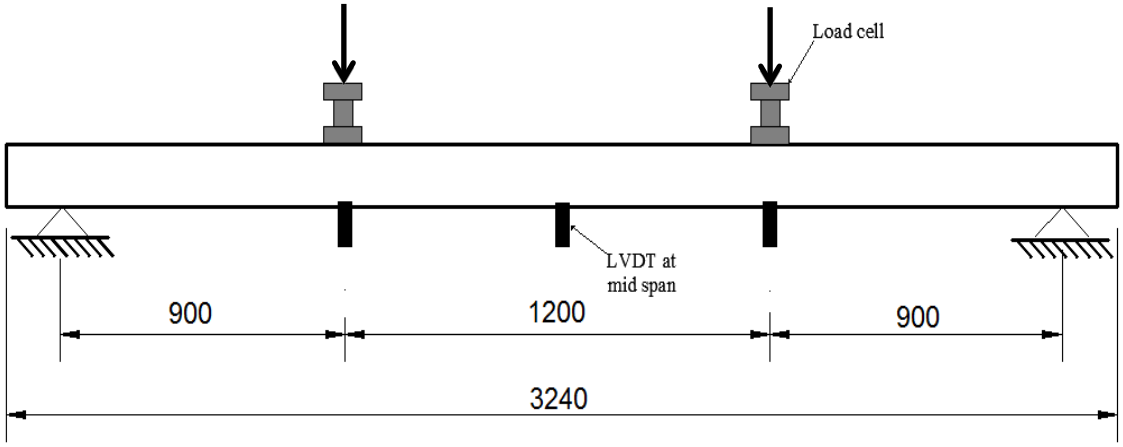

Figure 3.7 Four points bending test set up

In the static loading test three linear variable displacement transformers (LVDT), LVDTL, LVDTM and LVDTR were positioned on top of the beam to monitor the defections at mid-span and at the two loads points as shown in Figure 3.7

During the static load tests, the beams were loaded only to serviceability limit state load levels and were not loaded to failure. Load application was limited to mid-span deflection of 15 mm after which the load was released. The beams were loaded and unloaded for three times.

3.4.2 Static Test Results

Figure 3.9 shows the load-deflection curve comparison for beam 1 at three states intact, severe damage at mid-span and repaired severe damaged. The results illustrate significant drop in slope of load deflection curve which relates to loss of stiffness due to the severity of inflicted damage and an obvious recovery in stiffness after being repaired with CFRP. However, the slope of the load-deflection curve of repaired damaged beam is still less than the intact beam, which presents that the CFRP could not fully repair the severe damage. This result will be used to verify the capability of using modal strain energy method to evaluate the repair effectiveness for damaged timber beam after repairing with CFRP in Chapter 5. The static results of the other cases are shown in Appendix.

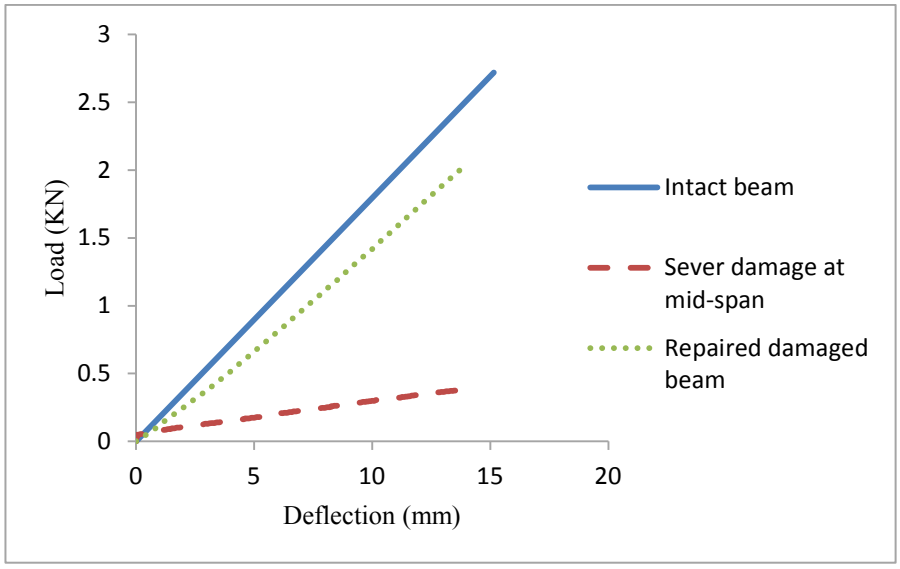

Figure 3.8 Load-deflection curve comparison for Beam 1

3.5 Modal Testing and Experimental Modal Analysis

Modal testing and experimental modal analysis (MT and EMA) is a process of determining the dynamic characteristics of a test structure by excitation of the structure artificially and identifying its modes of vibration (Ramsey, 1983).Vibration based damage detection method uses the output of MT and EMA such as natural frequencies, damping ratios and mode shapes to detect damage.

3.5.1 Modal Test Set Up

A schematic drawing of the modal test set up and the arrangement of instruments are shown in Figure 3.9. In this test system a special design pin-pin support system as depicted in Figure 3.9 was employed between the beam and the steel supports to provide a well-defined boundary condition.

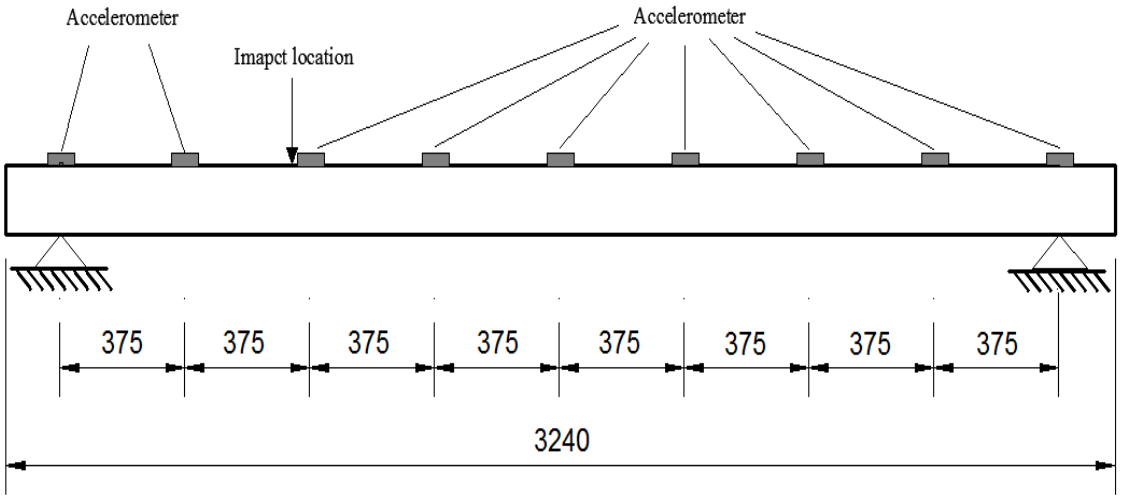

Figure 3.9 Modal test set up

Piezoelectric accelerometers as shown in Figure 3.10 were used in the modal tests to measure the acceleration responses due to an impact action. All accelerometers used in the model test were calibrated against one reference accelerometer selected amongst them in order to obtain a relatively synchronised mode shape data. Nine small steel plate glued on the top of beam and each accelerometer was attached to the plate using a magnetic based. The distance between each accelerometer was 1/8 of the span length stating from one end support of the beam to the other end. Nine measuring points were deemed sufficient for reconstructing mode shapes with the required accuracy using interpolation techniques.

Figure 3.10 Piezoelectric accelerometer

The test structure was then excited using a modal hammer. The test was repeated five to seven times for each beam. This test used impulse excitation to conduct structure

identification. An impact hammer (model HP 086C05) shown in Figure 3.11 was used to excite the test sample at the reference or driving point, i.e. point number 3. The impact location was set at quarter of the span length so that it could excite lower modes simultaneously. The impact hammer was used to generate input force and the data was measured by means of a force transducer in the hammer. The response signals of accelerometers and modal hammer were also amplified and conditioned using a multi-channel signal conditioner (Figure 3.12).

Figure 3.11Impact hammer

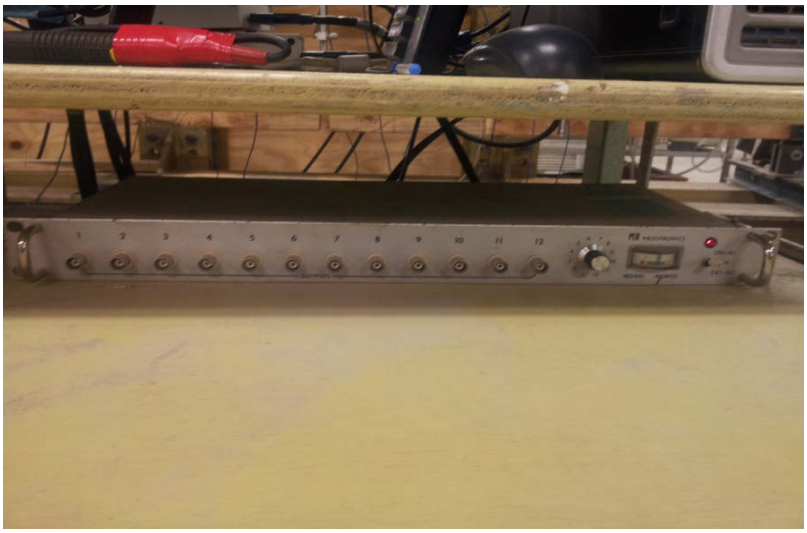

Figure 3.12 Multi-channel signal conditioner

3.5.2 Data Post-processing

After the input (impact force) and output (acceleration) data are acquired, these data went through a post-processing process. In the post-processing, the time domain data can be converted into frequency domain data using the fast Fourier transform (FFT) technique. Subsequently, the frequency data can be used to obtain the frequency response functions (FRFs) of the test beam using transfer function techniques. More details on frequency response function can be found in Craig and Kurdila (2006)

With frequency response function (FRF) being computed, modal parameter estimation technique was then performed to estimate the modal parameters. Modal parameter estimation is a key step in EMA. This technique is also known as a complex curve-fitting usually carried out using MATLAB Diamond program. Numerous modal parameter estimation methods have been developed and many different approaches have been published based on modal parameter estimation (Avitabile, 2006). Modal parameter estimation determines the three modal parameters, i.e. natural frequency damping ratio and mode shape. From the experimental time history of a test structure data,the obtained modal parameters describe the dynamic behaviour of the structure.

3.5.3 Results of Natural Frequency

In this research, as outlined above, five LVL beams were cast in the laboratory, four of which were used to carry out various damage scenarios. It is important to mention that for each damaged beam, a set of intact or undamaged modal data was collected before inflicting the damage. This intact/undamaged modal data modal data is used for comparison with the corresponding damage modal data in the following discussions.

Table 3.2 shows the results of natural frequency of Beam 3 at different modes under different damage scenarios. Table 3.3 depicts the percentage of shifts in natural frequency of Beam 3, whereby the percentage of reduction in natural frequency is defined as the percentage of difference between natural frequencies of the intact and damaged data. As can be seen from table 3.2, the frequencies of the damaged beams decrease after damage occurs. For inflicted single damage at mid-span, the frequencies drops for the second mode (less than 10%) are not obvious compared with other mode. The reason is that there is no deflection occurred at mid-span for second mode.

Furthermore, with the increase of damage size, the percentage of drop in frequencies is also increase. Therefore, natural frequency can be used as a good indicator to indicator to identify the existence of damage but there is no clear evidence that frequency change can be clearly correlated to damage severity, and the multi damage cases also cannot be identified. Furthermore, for the repaired cases shown in tables 3.2, 3.4 and 3.6, the natural frequencies have a significant recovery, but it still have a little drop compared with intact cases because the CFRP did not fully repairing the damage as discussed in section 3.5

Table 3.2 Comparison of natural frequencies of Beam 3 with different damage scenarios

Damage Cases	Natural Frequencies (Hz)		
	Mode 1	Mode 2	Mode 3
Undamaged	31.5	112.0	214.0
4L	30.0	110.0	204.0
4M	24.7	109.0	187.0
4S	17.4	106.0	166.0
4S2L	16.9	103.0	159.0
4S2M	14.8	88.4	151.0
4S2S	12.9	50.7	142.0
R4S2S	29.2	109.0	212.0

Table 3.3 Comparison of percentage of drop in natural frequencies of Beam 3

Damage Cases	Percentage of drop in natural frequencies (%)		
	Mode 1	Mode 2	Mode 3
4L	4.8	1.8	4.7
4M	21.6	2.8	12.6
4S	44.7	5.4	22.4
4S2L	46.3	8.0	25.7
4S2M	53.0	21.1	29.4
4S2S	42.9	54.7	33.6
R4S2S	7.3	2.7	1.0

The results from Beam 1, Beam 2 and Beam 4 follow the same pattern as that established in Beam 3, and the corresponding results are listed in Tables 3.4, 3.6 and

3.8, and Tables 3.5, 3.7 and 3.9, for shifts in frequency and their percentage, respectively. In general, the frequencies of damaged beams decrease with the increase of severity of damage.

In summary, the drop and recovery in natural frequencies corresponds to the severity of inflicted damage and CFRP rehabilitation. It can be used as one good indicator to identify the existence and rehabilitation of damage but not for assessing the extent of damage and evaluating the effectiveness of rehabilitation in LVL beams.

Table 3.4 Comparison of natural frequencies of Beam 2

Damage Cases	Natural Frequencies (Hz)		
	Mode 1	Mode 2	Mode 3
Undamaged	30.8	112.0	222.0
2S	21.6	81.4	205.0
R2S	30.6	107.0	214.0

Table 3.5 Comparison of percentage of drop in natural frequencies of Beam 2

Damage Cases	Percentage of drop in natural frequencies (%)		
	Mode 1	Mode 2	Mode 3
2S	29.9	27.3	7.7
R2S	0.7	4.5	3.6

Table 3.6 Comparison of natural frequencies of Beam 1

Damage Cases	Natural Frequencies (Hz)		
	Mode 1	Mode 2	Mode 3
Undamaged	32.5	117.0	228.0
4S	20.4	115.0	179.0
R4S	31.2	112.0	213.0

Table 3.7 Comparison of percentage of drop in natural frequencies of Beam 1

Damage Cases	Percentage of drop in natural frequencies (%)		
	Mode 1	Mode 2	Mode 3
4S	37.2	1.7	21.5
R4S	4.0	4.3	6.6

Table 3.8 Comparison of natural frequencies of Beam 4

Damage Cases	Natural Frequencies (Hz)		
	Mode 1	Mode 2	Mode 3
Undamaged	29.2	109.0	213.0
2S	20.2	75.6	195.0
2S4L	20.1	73.9	187.0
2S4M	16.8	67.6	165.0

Table 3.9 Comparison of percentage of drop in natural frequencies of Beam 4

Damage Cases	Percentage of drop in natural frequencies (%)		
	Mode 1	Mode 2	Mode 3
2S	30.8	30.6	8.5
2S4L	31.2	32.2	12.2
2S4M	42.5	38.0	22.5

Summary

At the beginning of this chapter, the details of the properties of LVL beam and CFRP were briefly introduced, and the dimension of the test specimen was described. The data of material utilized manufacturing characteristics. Then, the all inflicted damage scenarios were listed, and the procedure of CFRP reparation was presented. Furthermore, the set-up of the four-point bending test was outlined. It was indicated that the static tests were only conducted under service loads and the beams were not loaded to failure. The beams were loaded and unloaded for three times. Finally, the results of natural frequencies are listed, and the comparison of percentage drop in natural frequencies between the undamaged and damaged are evaluated. From the results, it can be concluded that the drop and recovery in natural frequencies corresponds to the severity of inflicted damage and CFRP rehabilitation. It can be used as one good indicator to identify the existence and rehabilitation of damage but not for assessing the extent of damage and evaluating the effectiveness of rehabilitation in LVL beams.

CHAPTER 4 FINITE ELEMENT MODELLING

4.1 Introduction

In this chapter, the procedure for establishing reasonable and reliable finite element (FE) models of intact and damaged timber beam and timber beam repaired with CFRP are presented. A linear elastic FE model for LVL beam was adopted to achieve a reasonably accurate result. Challenges in FE modelling of CFRP repair of damaged timber structure are due to the features of the CFRP materials, such as the thickness of CFRP and the modelling of boundary between CFRP and timber beam. In this study, the built FE timber beam model adopted manufacture data for timber as input of material properties. The geometry of the experimental test beam discussed in Chapter 3was used to develop FE model. Then, the simulation of notch damage is also introduced in this Chapter. Such inflicted damage features will be used for creating different type of damaged FE beams. After that, the method of simulation of using CFRP to repair damaged beam is described. Moreover, performing a mesh density discussion is necessary to determine a reasonable and optimal mesh size for a robust and accurate modal.

The FE model was firstly validated with the experimental data of static test results.The calibrated FE model was then used to perform a transient analysis to obtain dynamic characteristic to compare with experimental dynamic test data. The validated FE model was used for numerical study of the different damage detection methods proposed.

4.2 Finite Element Model for Intact Timber Beam

Using a finite element (FE) model, modal analysis was performed numerically on a LVL timber beam. All the FE analyses were carried out using ANSYS (2011) which is a commercially available finite element analysis (EMA) package. The modelling of a beam-like structure is straight forward.

For timber beam modelling, the solid elements (SOLID45) were utilised to model the beam, to which different damage scenarios can easily be introduced. The SOLID45 element was selected as recommended for the 3-D modelling of solid structures in ANSYS documentation. The element is defined by eight nodes having three degrees of

freedom at each node, i.e., translations in the nodal x, y, and z directions. The geometry, node locations, and the coordinate system for this element are shown in Figure 4.1.

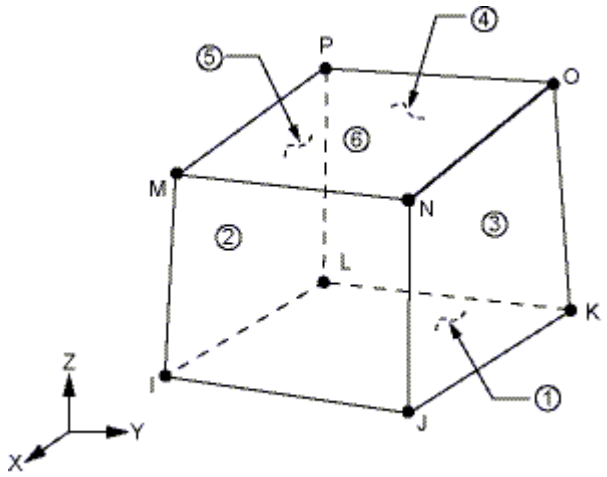

Figure 4.1 The geometrics properties of SOLID45

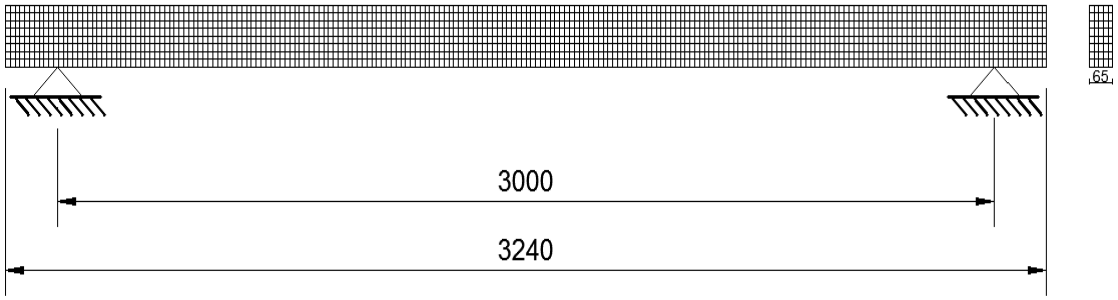

All dimensions are in mm

Figure 4.2 A typical FE model of a LVL timber beam

After the elements were selected, a finite element (FE) model of timber beam without any damage was created as shown in Figure 4.2. The width and depth of the beam was 65mm and 120mm, respectively with a span length of 3240mm. There are 217 nodes and 216 elements used in the longitudinal directions of the model. At the cross sectional area, the beam was divided into 8 elements across the height and 5 elements along the width. The FE model, in total, consists of 11718 nodes and 8640 elements. With this mesh configuration, the beam model had 35154 degrees of freedom. The boundary conditions for the model were set as pin-pin, which is close to the real boundary condition of girder timber beam structures. The material properties were simulatedas isotropic and linear elastic because it was deemed sufficient to represent the flexural

stiffness in longitudinal direction along the span length as this is the major contribution to the overall stiffness of timber beam. The material property data used in the FE modelling were provided from the manufacturer supplied data discussed in Chapter 3. The input value for the modulus of elasticity of timber beam was 13 GPa. The density of the test beam was 650 kg/m^3 and the Poisson's ratio was 0.3. Utilizing the modal analysis module to solve the eigenvalue problem in ANSYS, the first three flexural mode shapes were selected from the FE model as depicted in Figure 4.3

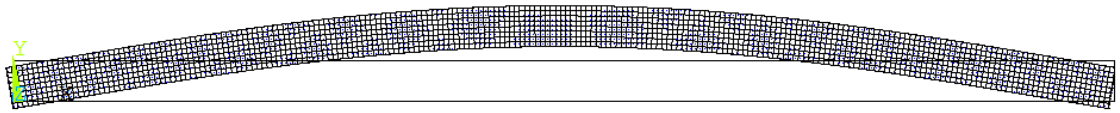

(a) First flexural mode

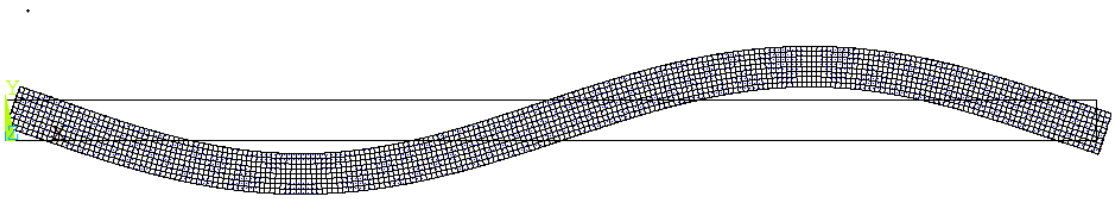

(b) Second flexural mode

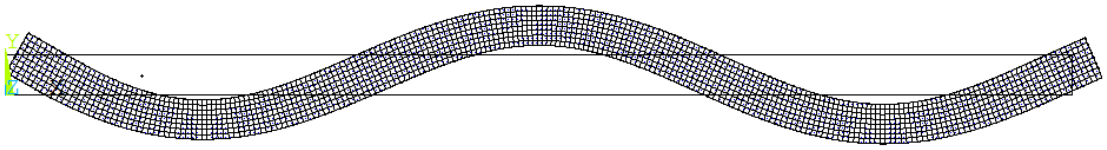

(c) Third flexural mode

Figure 4.3 First three flexural mode shapes for the FE beam model

4.3 Mesh Density

It is conceded that the quality of finite element analysis (FEA) relies on mesh, and the mesh size significant influence the analysis results (Dittmer et al., 2006) The standard of determining an optimum mesh size is often based on time and cost. Therefore, the mesh

size should be such that it gives reasonably accurate results with optimum number and size of elements.

4.3.1 Meshes Considered for Modelling

In FE modelling, the mesh size can be easily controlled for a simple structure. Hence, it is essential to be able to use a reasonable mesh size for the FE model to work efficiently. Two types of mesh size were created for comparison, i.e. coarse and fine.

For the coarse mesh density model illustrated in Figure 4.4 (a), there were 217 nodes along the length, 9 nodes along the height and 6 nodes along the width.

The fine meshed model of timber beam, as shown in Figure 4.4 (b), was divided into 325 nodes along the length, 13 nodes along the height and 8 nodes along the width.

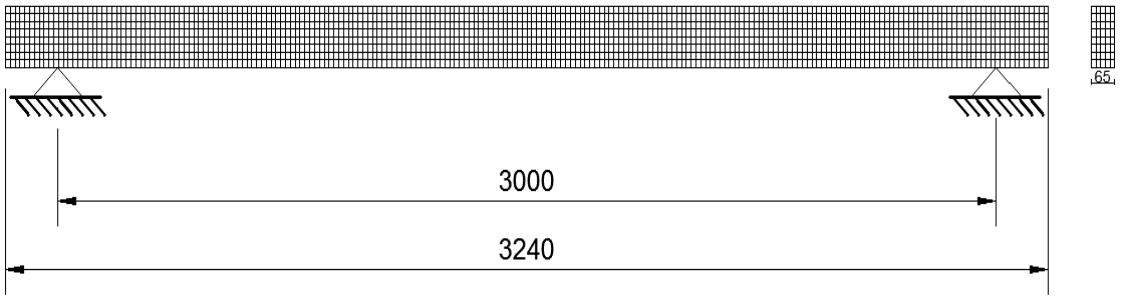

(a) Coarse

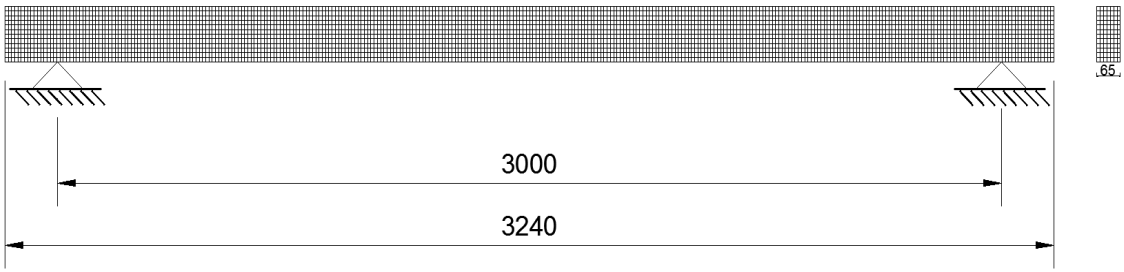

(b) Fine

Figure 4.4 Different mesh models of the timber beam

4.3.2 Comparison of Different Mesh Densities

Figures 4.5 show the results of the first three mode shapes obtained from two different meshed models of the LVL timber beam. In each figure, the legend of 217 Nodes and 325 Nodes denote number of nodes used along the length of the beam corresponding to

the coarse meshed model and fine meshed model, respectively. All mode shape data were collected evenly from all of nodes on the top of the beam with in the span length.

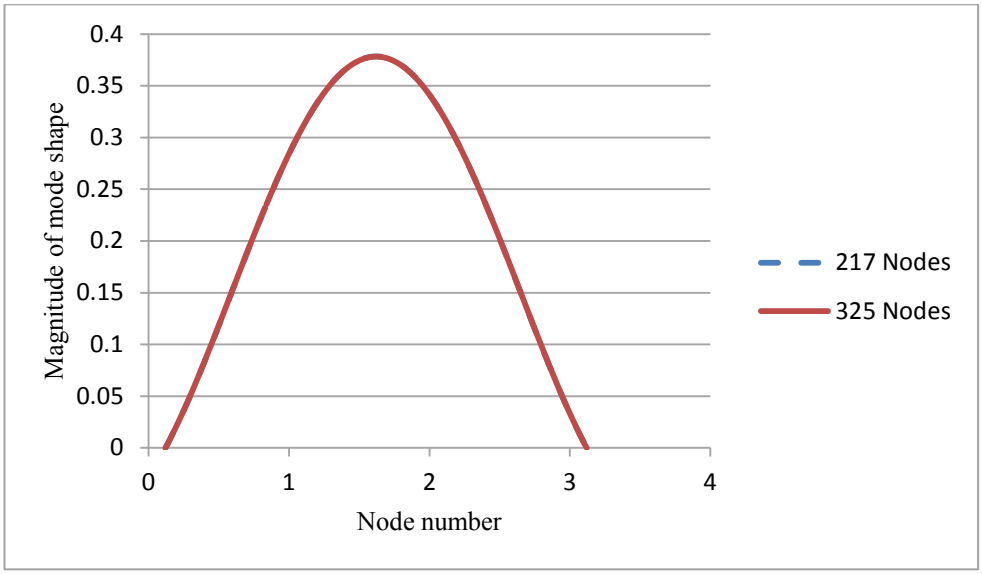

(a) The first mode

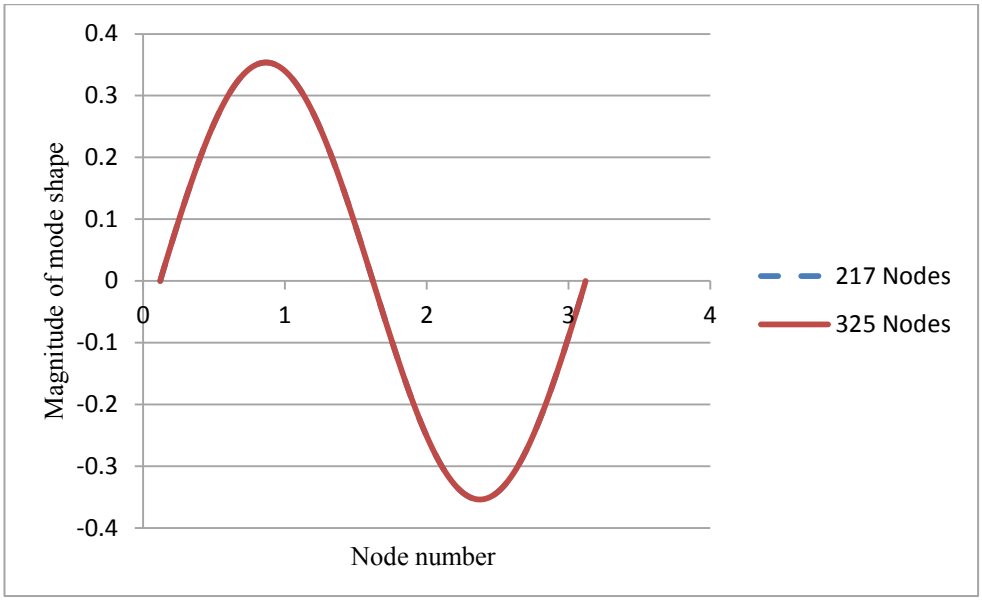

(b) The second mode

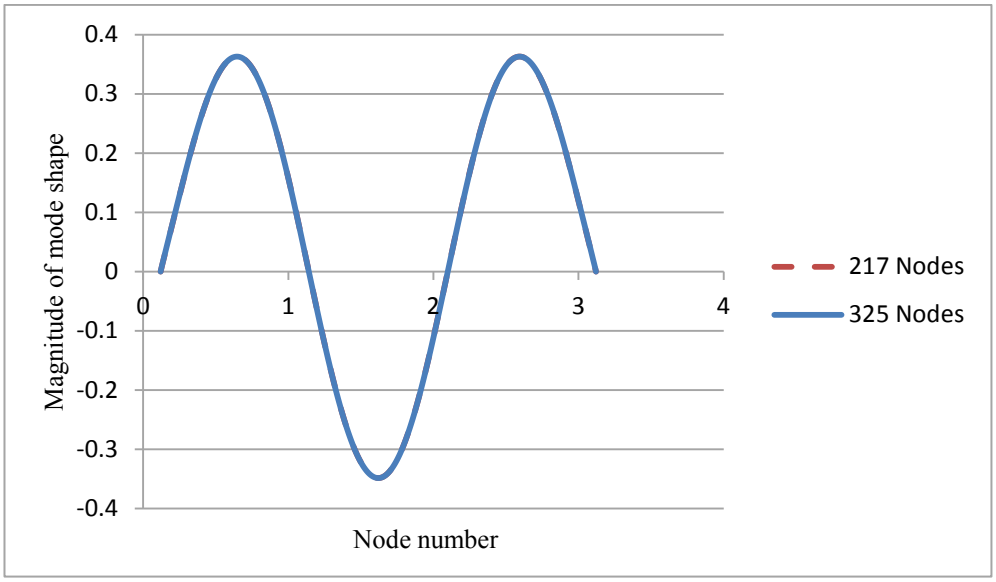

(a) The third mode

Figure 4.5 The mode shapes of intact FE beam with different mesh densities

Referring to Figure 4.5, the difference of mode shape results between different mesh densities is insignificant. Based on the comparison, it can be concluded that all meshed models are comparable and they are deemed good enough for the numerical work required in this study.

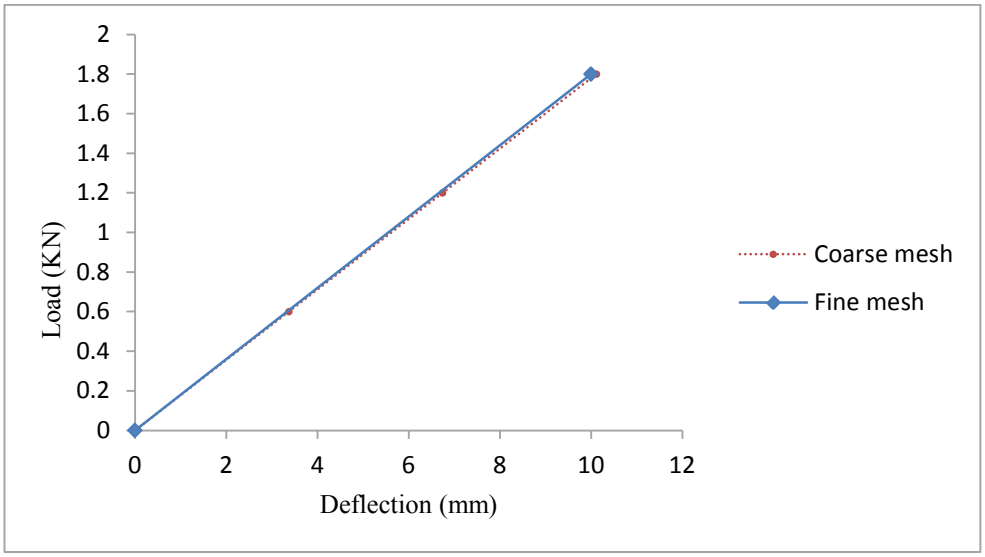

Figure 4.6 Numerical static test results comparison for different mesh size

Effect of the mesh density was also investigated in terms of mid-span deflection under static load. The Figure 4.6 illustrates the results of load deflection curve of numerical static test using coarse and fine mesh size. Slopes of both results have only minor difference. However, these differences are fairly small and significant influences on test results were not expected. From these two comparisons, considering the time and cost, the coarse mesh was adopted for all subsequent analysis and discussions due to the advantages of faster solution time.

4.4 Methods of Modelling Damage in LVL Beam.

The modelling of the inflicted damage, numerically, was used for developing finite element (FE) models of damaged LVL timber beams The inflicted damage in the damaged beam models is similar to that of actual experimental timber beams. Subsequently, the damaged beam FE models and the intact beam FE model will be employed for damage detection studies in Chapter 5.

The damage to be simulated in this investigation is pockets from rotten wood or termite attack, typically found in the girders of timber beam structures. Single and multiple damage scenarios were in traduced on a timber beam. The damage cases have described in Chapter 3 consists of a rectangular opening from the soffit of the beam along the span length. The method of equivalent stiffness reduction and changing the geometry is applied to the finite element models, but the elements were not deleted. This method locally reduces the stiffness to near 0 values and changes the damage geometry size to simulate light, medium and sever damage. This approach is easy to perform and does not introduce nonlinearities into the model. It is therefore sufficient to perform a linear analysis to ascertain the effects of the damage on the dynamic properties of the structure. The configuration of the damage case is shown in Figure 4.7

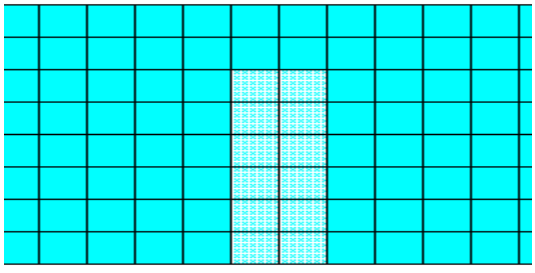

Figure 4.7 Configuration of a typical damage case

4.5 Methods of Modelling Damaged Beam Repaired with CFRP

ANSYS SHELL63 elements were used to model the CFRP in the FE model for beams repaired with CFRP. The SHELL63 element has both bending and membrane capabilities. Both in-plane and normal loads are permitted. The element has six degrees of freedom at each node. Stress stiffening and large deflection capabilities are included. The geometry, node locations, and the coordinate system for this element are shown in Figure 4.8

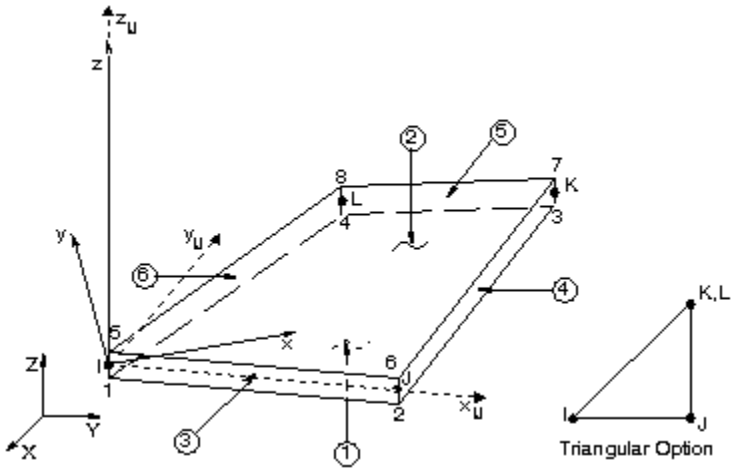

Figure 4.8 The geometrics properties of SHELL63 (ANSYS)

The element is defined by four nodes, four thicknesses, and elastic foundation stiffness, and the orthotropic material properties. During the FE modelling, the experimental thicknesses of the CFRP sheets are very small which is 2 × 0.117 mm. Furthermore, the model assumes full bond between timber and CFRP sheets, and this is so because the CFRP and timber share the interface nodes. Therefore, there was no volume built for the CFRP. The method of simulating CFRP is selecting the CFRP bonded areas and using SHELL63 element type to mesh these areas. The input value for the modulus of elasticity of timber beam was 200 GPa. The real constant of thickness is 0.234 mm.

4.7 The Results and Discussions on Load-deflection Relationship

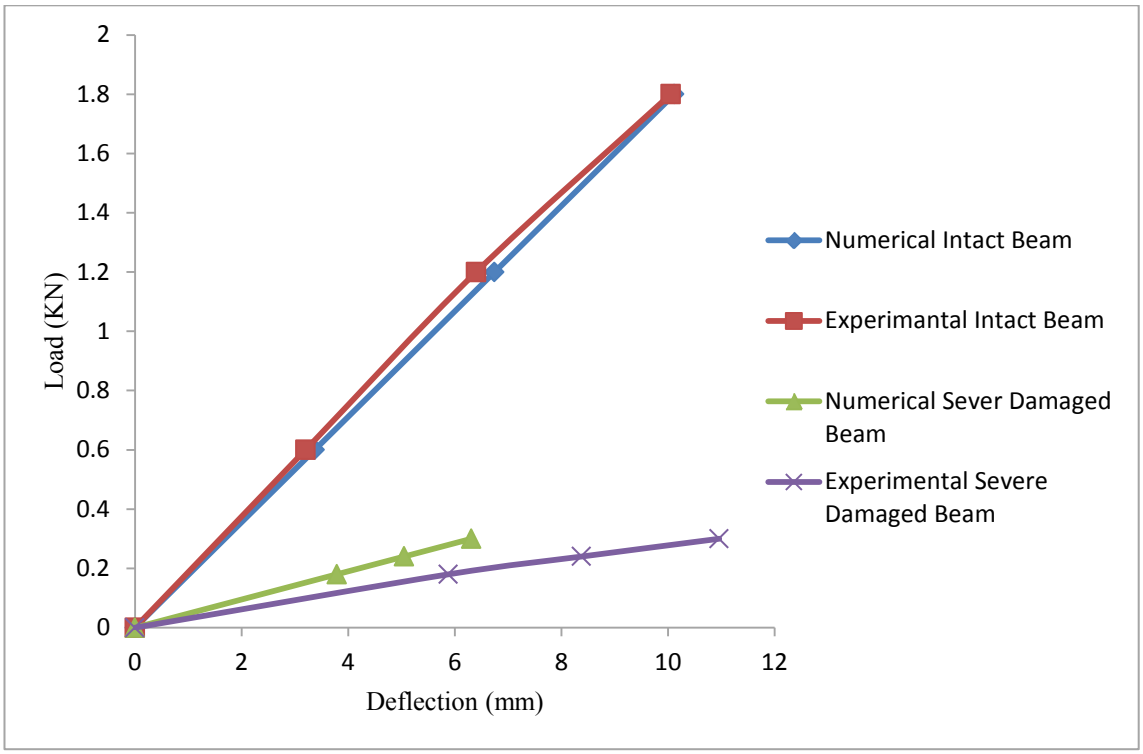

Figure 4.9 Load-Deflection comparison between numerical and experimental results

The numerical LVL beam model was subjected to static load test. The location of loading and the boundary condition which was simply supported were made the same as experimental LVL beam specimens. The intact beam result from the numerical study was validated by the experimental results. The modulus of elastic was calibrated using updating technique that minimises the error between the load-deflection result of intact FE model and that of experimental intact beam. Figure 4.9 shows the load versus mid-span deflection curve of the intact and severely damaged timber beam between numerical and experimental results. As shown in the Figure 4.9, slope of load-deflection curve for the intact beam between the numerical and experimental results is very similar. This comparison indicates that the simulation of intact beam FE modal is close to the experimental specimens. Therefore, this FE modal can be employed to the further analysis and this FE modal can be used as the reference for introducing different damage scenarios. However, there is an obvious difference between the numerical and experimental results of damaged beam. The slope of experimental severe damaged beam has a significant decrease compared with intact beam, while the slope difference

between numerical damaged beam results and intact beam results is smaller than experimental results. This comparison presents that the damage inflicted in numerical FE modal is not as severe asin experimental case. The reason of leading this situation is described as follow. Firstly, the damage introducing is produced by saw-cut which is performed by hand. Unlike using machine, the boundary of damaged part is not as perfect as the numerical FE model. There is a small over cutting along the longitudinal direction and horizontal direction as shown in Figure 4.10. These small cuts results in the stiffness decrease in the around area. Secondly, timber can have natural growth characteristics which mean that the properties may not be uniform throughout while the FE model assumes that the property is isotropic. Whilst this will be much less for LVL, compared to sawn timber, such characteristic in the LVL beams still exists. This difference will affect both the intact and damaged beam results. Lastly, timber fibres may not be perfectly oriented in the longitudinal direction and inter-winding of fibres is quite common. This means that cutting a notch of depth say 75% of the beam depth may actually results in cutting more than 75% fibres of vice versa, depending upon how straight the fibres are. With the FE, however, this effect of inter-winding fibres cannot be accurately modelled, and besides each piece of timber (or LVL) will be different. This effect would be more prominent when the damage is severe one. However, this property of severe damage cannot be reflected in the FE model. Therefore, to solve the difference between the numerical and experimental results, the material property of the elements in FE model located at the pointed out area shown in Figure 4.10 required to be changed

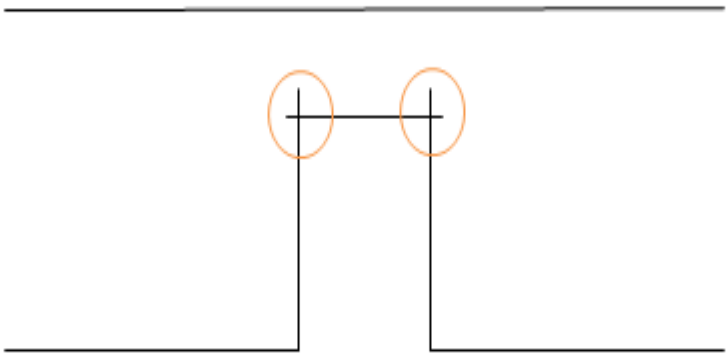

Figure 4.10 Over-cut damaged

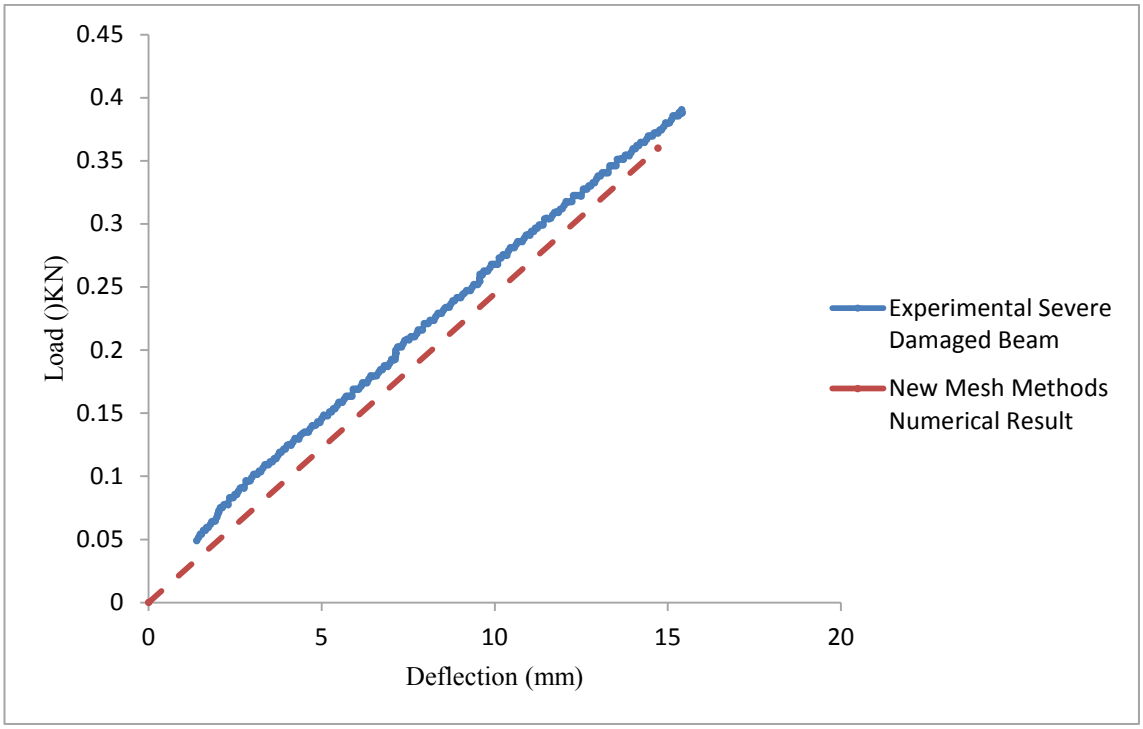

Figure 4.11Load-deflection curve comparison

Using the new method to introduce damage as discussed in previous paragraph, the results of load deflection curve is shown in Figure 4.11. It illustrates that the slope is become similar. Therefore the damaged modal can be permitted.

4.6 Correlation Analysis Using Dynamic Results

Correlation analysis is a technique to examine quantitatively and qualitatively the correspondence and difference between analytically and experimentally obtained modal parameters (Brownjohn and PINQI, 1999). This comparison forms a basis for selection of modal parameters pertaining to dynamic responses for model updating. In the beam analysis, a dynamic response, namely natural frequencies was used as the indices for the objective function (OF) for the correlation analysis. The goal of updating or calibration process of the finite element (FE) model was to minimise the objective function. The global objective function used is shown in equation 4.1.

OF = f(NFerror)

The dynamic responses (natural frequencies) of both numerical and experimental research are adopted in the correlation analysis. The numerical results are obtained from finite element modelling. The experimental results are obtained from experimental dynamic tests.

4.6.1 Natural Frequencies

For Natural Frequencies (NF), the relative error or difference between the analysis and experiments can be computed in order to check their correlation. In order to gauge the relative error in natural frequencies more clearly, and error index for the NF is suggested. The NFerror given in the OF is a function of natural frequency difference between FE and experimental models and is given as follows:

$$\text{NFerror}=\frac{|\omega_{Exp}-\omega_{FE}|}{\omega_{Exp}}\times 100 \qquad \text{Equation 4.1}$$

Where ω is the natural frequency. Its subscripts Exp and FE denote experimental and finite element results, respectively. The values of the natural frequency and NFerror are displayed in Table 4.1. The NFerror in general is less than 7%, except for mode 2. The reson for slightly larger NFerror value for mode 2 may be due to the fact that impact location falls on the anti-node point of this mode.

Table 4. 1Comparison of natural frequencies of the LVL beam

Mode	FE (Hz)	Experimental (Hz)	Absolute Difference (Hz)	NFerror (%)
1	35	32	3	9.37
2	100.57	110	20.43	9.43
3	235.83	228	7	3

Summary

This chapter presented the procedure of establishing reasonable and reliable Finite Element (FE) models of laboratory reinforced concrete beams. Firstly, Solid element 45 was selected in the FE model, simulating an actual LVL timber beam. After the elements were selected, an intact LVL beam FE model was developed. The approach used for simulating the damage in LVL beam was also introduced in this chapter. Mesh density comparison was also discussed in the chapter. The LVL beam FE model was subjected to dynamic test to investigate its validity in terms of dynamics. Furthermore, a comparison of static test results between numerical modal and experimental case is evaluate. The difference between these two results is due to the over cutting of damage, the natural growth characteristics and the features of timber fibre. Therefore, a calibration method of FE modal based on static test results are evaluated, which is changing the modulus of elastic value of elements located at nearing the damage area. Finally the correlation analysis results showed that the natural frequencies for the numerical model are larger than expect due to the impact location influence. Therefore, the LVL beam FE model can be used to represent the experimental test beams.

CHAPTER 5 Structural Damage Detection and Repair Evaluation of Timber Beams Using the Modal Strain Energy Method

5.1 Introduction

This Chapter presents details of a damage detection algorithm used in this study to identify damage locations, estimate the severity of damage and evaluate the effectiveness of CFRP rehabilitations. An algorithm for detection and severity estimation of damage namely Kim and Stubbs's method is introduced in Section 5.2, and the result of using this method to detect damage are discussed in Section 5.3. Furthermore, this Chapter presents a comprehensive numerical and experimental study of damage detection on damaged and repaired timber beams using proposed damaged detection method. The proposed damage detection method is used for detecting damage location, estimating damage severity and evaluating CFRP rehabilitation on a series of both numerical and experimental cases with single, multiple damage and repaired damage scenarios under various combinations of location and severity of damage. Finally, comparisons between the results obtained from the numerical studies and experimental studies are made.

5.2 Review of Proposed Damage Detection Methods

A non-destructive damage detection method to identify and assess damage from a few mode shapes of structures was presented by Kim and Stubbs (1995). This method was developed from an original conception that the fraction of modal strain energy is same for both damaged and undamaged structures. A damage index β_{ji} of i^{th} mode and j^{th} member was acquired:

$$\beta_{ji} = \frac{E_j}{E_j^*} = \frac{\emptyset_i^{*T} C_{jo} \emptyset_i^*}{\emptyset_i^T C_{jo} \emptyset_i} = \frac{NUM}{DEN}$$

E_j and E_j^* are parameters of the material stiffness properties associated with undamaged and damaged states, respectively; $\emptyset_i$ and $\emptyset_i^*$ are the i^{th} modal shapes associated with undamaged and damaged states, respectively; C_{jo} represented geometric quantities; and superscript 'T' denotes transpose of a vector.

For NM vibrational modes, a damage index β_i of j^{th} member was obtained:

$$\beta_j = \frac{\sum_{i=1}^{NM} NUM}{\sum_{i=1}^{NM} DEN}$$

Where $\beta_j \geq 0$ and damage is indicated at the j^{th} member if $\beta_j \geq 1$.

Moreover, the predicted location j was defined as follows:

$$Z_j = \frac{(\beta_j - \bar{\beta})}{\sigma_\beta}$$

β_j was the mean of the collection of β_j values and σ_β was the standard deviation of the collection of β_j values respectively.Finally, the severity of damage in the j^{th} member was estimated in the research work as follows:

$$\alpha_j = \frac{1}{\beta_j} - 1; \alpha_j \geq -1$$

5.3 Numerical Results Discussion

5.3.1 Obtaining Modal Parameters by Experimental Modal Analysis (EMA)

For given structural vibration responses, the vibration characteristics (natural frequencies, mode shapes and modal damping or stiffness and damping ratio) can be obtained from the modal analysis. These characteristics are important parameters in performing damage detection using modal based methods. In this study, mode shape was the main modal parameter used in the newly developed damage detection method. In this research work, experimental modal analysis (EMA) approach was used to obtain the modal parameters. The modal parameters were obtained from vibration response time histories (either numerically simulated or experimentally measured). The EMA is based on curve fitting techniques and consists of signal processing, frequency response function (FRF) calculation and modal parameter estimation.

When using experimental data, EMA can be costly and time consuming if it is required for parametric studies. Therefore EMA often uses numerical data first before costly experiments start. For numerical study, EMA includes modelling of a test structure,

simulation of excitation force acquisition output acceleration and modal parameters estimation.

A finite element model of a timber beam was developed and the details of the modelling are given in Chapter 4. Using the FE beam model, a transient dynamic analysis was performed. In the transient dynamic analysis, an impact loading, shown in Figure5.1, was applied on the top of the beam, at 2/8 of span length from the left support. The location of the impact loading was chosen to be the same as that in the experimental work.

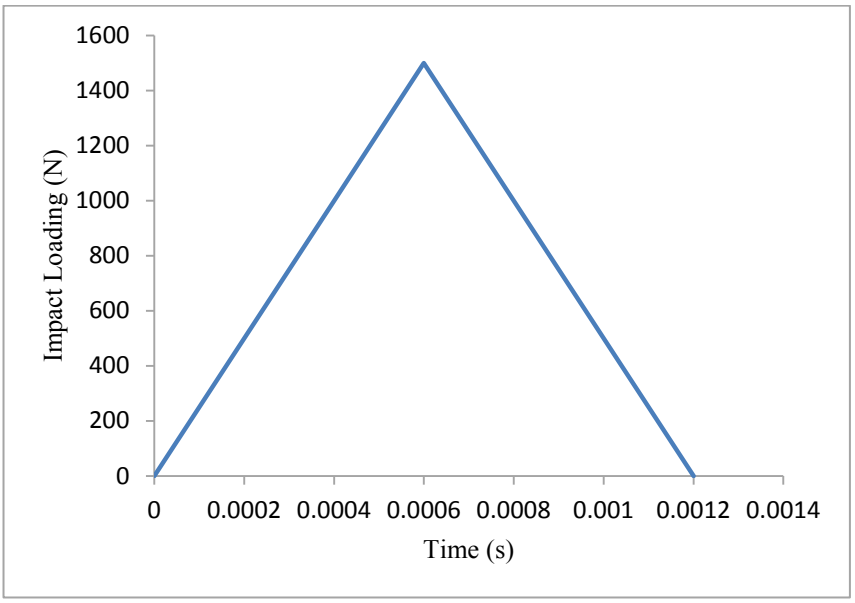

Figure 5.1 The applied impact loading in the transient dynamic analysis

To acquire more sensitive mode shapes from the transient dynamic analysis, the displacements at 21 measurement points, chosen evenly on the top of the beam, were obtained. These 21 measurement points also included the 9 measuring locations corresponding to the location of the accelerometers during the experimental investigation. Using in-house software written in MATLAB code, the accelerations of the 21-points were obtained by performing double differentiations on the displacements. At this stage all of the numerical results did not consider the influence of noise presence. From the acceleration data, the fast Fourier transform (FFT) and frequency response function (FRF) data of the timber beam were subsequently computed. Then, a modal analysis program-Diamond was used to identify the modal parameters from the

obtained FRF data. Finally, the modal parameters of the timber beam (natural frequencies and mode shapes) were obtained. Damping ratio was not acquired as it was not considered in the numerical work.

5.3.2 Identifying the Location of Single Notch Damage

First three modes on the proposed damage detection method were investigated for damage localisation. The choice of the first three flexural modes used in the damage detection method is mainly due to the constraint of the number of modes that can be reliably obtained from the experimental work.

In the numerical investigation presented in the following section, the damage location indexes are plotted against the span length of the timber beam. In principle, when the damage location index of a given location is greater than zero there exists a possibility that damage exists at that location. In the following figures, the actual damage locations are indicated with vertical black dashed lines.

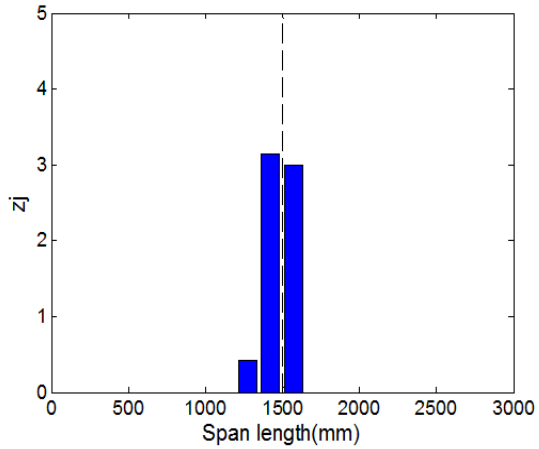

(a) Light

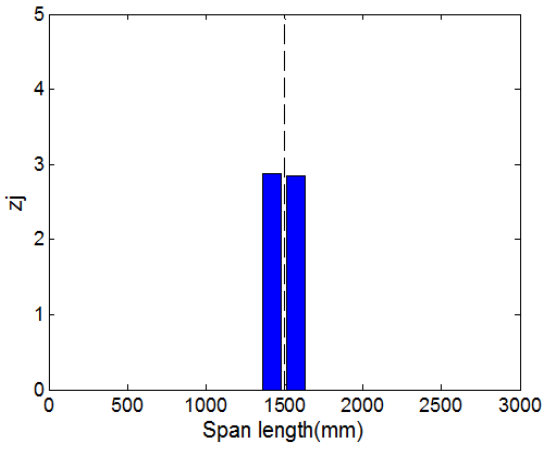

(b) Medium

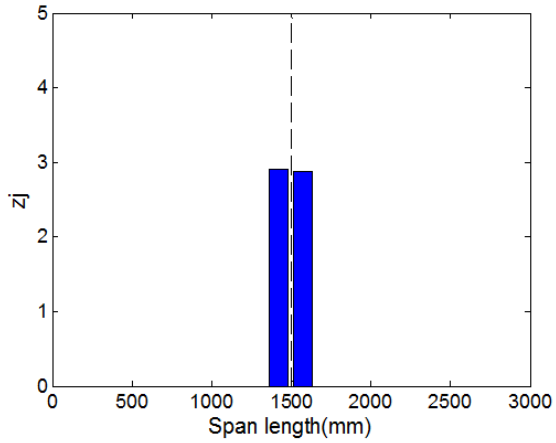

(c) Severe

Figure 5.2 Single Notch Damage Located at Mid-span

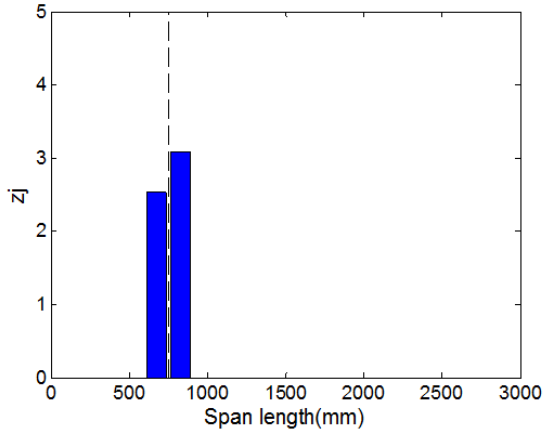

Figure 5.3 Single severe damage at quarter-span

Figure 5.2 and 5.3 show the results of the proposed damage detection algorithm applied to the timber beam models with single damage at different location. Figure 5.2 consists of three diagrams from (a) to (c), showing the different level of single damage detection results i.e. light, medium and severe damage ,respectively, located at mid span. The Figure 5.3 only depicts the severe damage at quarter-span.

From Figures 5.2 and 5.3, the single damage results are distinctly identified for all different level of damage and different locations. It is apparent that the proposed damage detection method performs effectively in locating damage for timber beam in the numerical studies. However, it can also be observed the magnitude of the damage location indexes (Z_j) for three different level of damage are the same which is close to 3.

Therefore, the index Z_j can only accurately detect the location of different level damage, but the index has less contribution on estimating the severity of single damage in numerical studies.

Figure 5.4 illustrate results from Kim and Stubbs (1995) method for multiple damage cases. There are 5 diagram included in Figure 5.4. Figure 5.4 (a) gives the result of light damage at quarter-span and severe damage at mid-span; Figure 5.4 (b) gives the result of medium damage quarter-span and severe damage at mid-span; Figure 5.4 (c)gives the result of severe damage at quarter-span and light damage at mid-span; Figure 5.4 (d) gives the result of severe damage at quarter-span and medium damage at mid-span; Figure 5.4 (e) gives the result of double severe damage at quarter-span and mid-span.

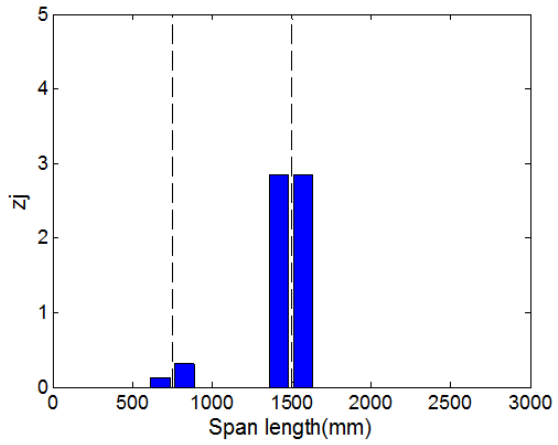

(a) 2L4S

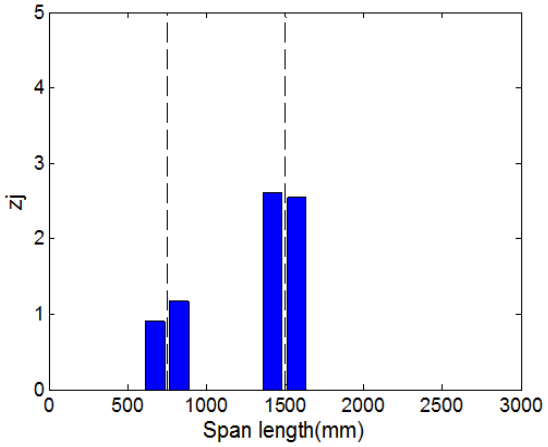

(b) 2M4S

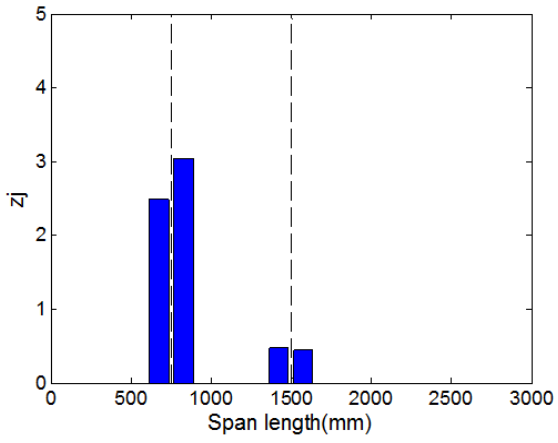

(c) 2S4L

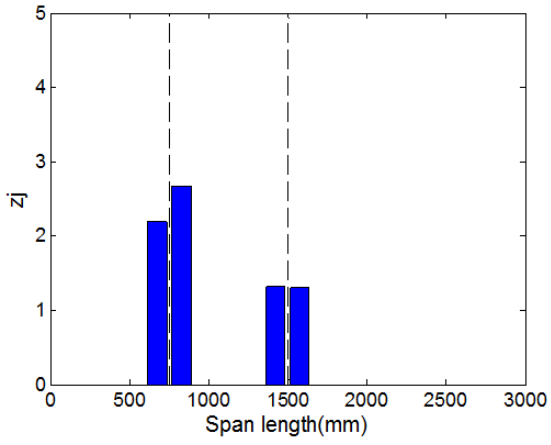

(d) 2S4M

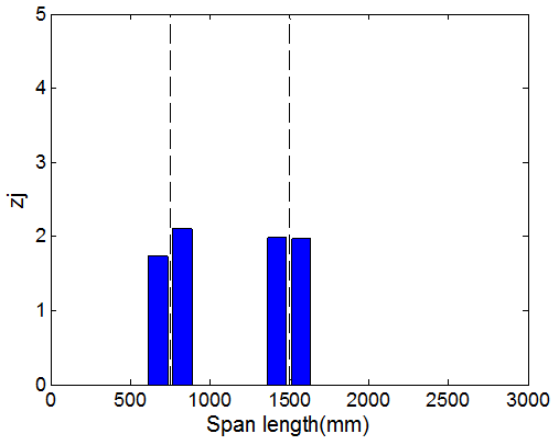

(e) 2S4S

Figure 5.4 Multi damage cases located at mid-span and quarter-span

From Figure 5.4, all damage locations were accurately identified. For example, the light damage at quarter span and severe damage at mid-span, respectively, were clearly located by the Kim and Stubbs (1995) method as shown in Figure 5.4. It can also observed that unlike the results of single damage cases, the magnitude of the damage location index Z_j in multi-damage cases increases with severity of damage indicating the increased probability of damage existence. It is possible to deduce that from the increases of the magnitude of the index Z_j, it can provide a preliminary forecasting for the severity of damage. It is concluded that the selected damage detecting algorithm is effective in identifying damage location of LVL timber beam for both single and multiple damage cases using all of first three modes in numerical studies.

5.3.4 Estimation of Severity of Damage

After determined the geometric location of damage, quantifying severity of damage is an important processing in damage detection. The proposed damage detection algorithm based on previous research which is Kim and Stubbs (1995) has been proved that it is capable of determining the location of damage effectively in various damage cases. This section will only focus on using the damage detection algorithm to estimate the severity of damage in single damaged cases. For damage severity estimation, the proposed damage detection algorithm uses all of the first three flexural modes and the formulations used in following discussions were presented in detail in previous section.

Three different damage sizes at mid-span were created to investigate the capability of the proposed damage detection method in estimation of severity of damage. The cases and results of simulation and estimation are presented in the follow Table 5.1.

Table 5.1Estimation of severity of damage

Cases	Damage Scenario	Actual severity 'Loss of I' (%)	Estimated Severity 'Loss of I' (%)
1	None	0	0
2	4L	57.8	40.5
3	4M	87.5	63.7
4	4S	98.4	73.1

In the numerical investigation presented in the following section, the damage severity estimators (α) are plotted against the span length of the timber beam. In all figures the actual damage locations are indicated by the vertical black lines and the simulated severity of damage is indicated with horizontal red dash line. The results of 4L, 4M and 4S are shown in Figure 5.5.

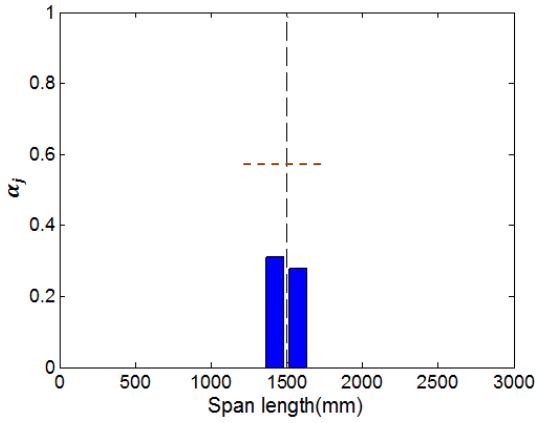

(a) Light

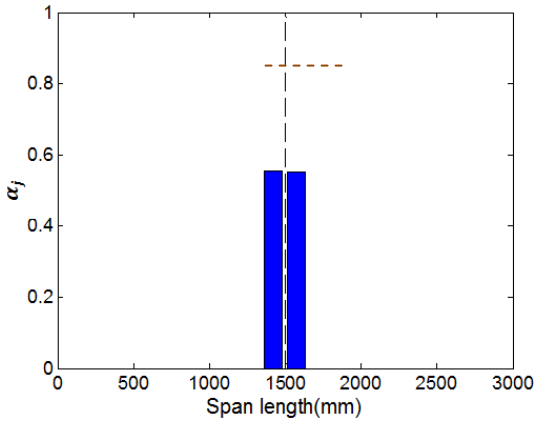

(b) Medium

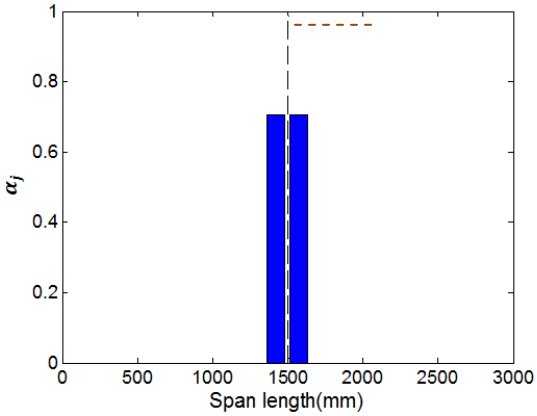

(c) Severe

Figure 5.5 Damage estimation index for single damage at mid-span

From Figure 5.5, it is obvious that the value of the damage severity estimators of three damage cases is different from the actual severity, and the error range is around 20% as shown in Table 5.1. However, the value of estimated severity does increase with the increase of damage sizes, and similar trend is observed between actual severity and estimated severity. Furthermore, from the further investigation, there is a correlation between the simulated severity and estimated severity. A comparison between these two results is presented in Figure 5.6 which shows that the trend between these two results is similar, and the differences between these two results become bigger with the increase in damage severity. Therefore, the actual damage and damage estimated can be related be a calibration relationship factorη. It seems that this calibration factor is merely a factor related to geometry and damage of a structure and therefore can be predetermined from the numerical. The calibrated severity estimator is presented as follow equation;

$\alpha_c = \eta\alpha_j$

α_c is the real estimated severity; η is calibration factor and α_j is the estimated severity before calibration.

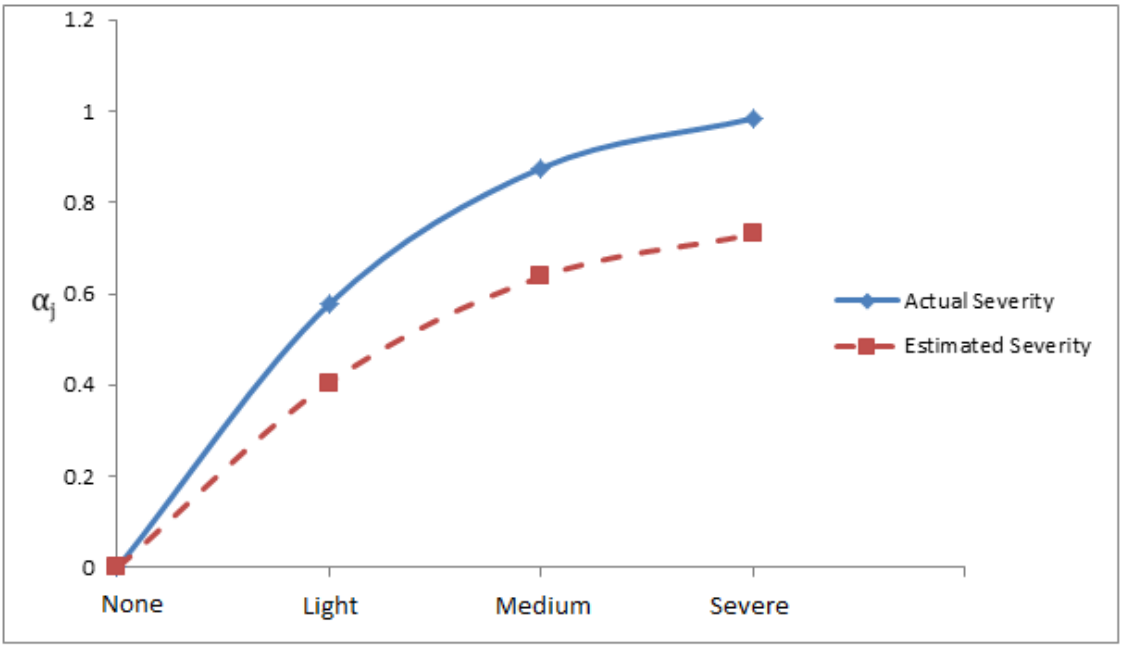

Figure 5.6Comparison of actual andestimated severity of damage

Table 5.2Calculation of calibration factor

Cases	Damage Scenario	Actual severity 'Loss of I' (%)	Estimated Severity 'Loss of I' (%)	η
1	None	0	0	0
2	4L	57.8	40.5	1.42
3	4M	87.5	63.7	1.37
4	4S	98.4	73.1	1.35

From Table 5.2, it is obvious that for three different size of damage, the calibration factorsfor three different type of damage are very closeranging from 1.35 to 1.45. The average of the calibration factor is 1.38. Therefore, using the factor to calibrate the estimated severity, and the results are shown in Figure 5.7 and Table 5.3. Both Figure 5.7 and Table 5.3 present that the results of after calibration are similar as the actual severity, and Table 5.3 indicate that the errors between calibrated severity of damage and actual severity of damage are fewer than 3%. Therefore, using the proposed damage

detection method to estimate the severity of single damage requires to be calibrated by a calibrated factor, and after the calibration the results are accurate and reliable.

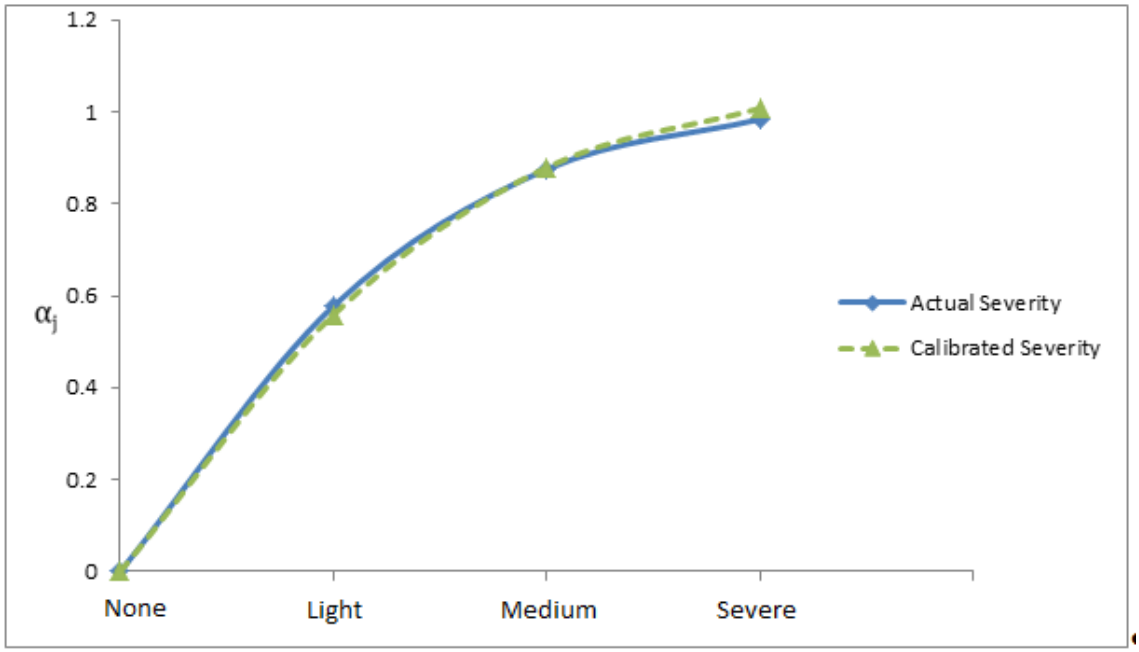

Figure 5.7 Comparison of actual and calibrated severity of damage

Table 5.3 Results of calibrated severity of damage

Cases	Damage Scenario	Actual severity 'Loss of I' (%)	Calibrated Severity 'Loss of I' (%)	Error (%)
1	None	0	0	0
2	4L	57.8	55.9	1.8
3	4M	87.5	87.9	0.4
4	4S	98.4	100.74	2.1

In summary, the propose damage severity estimator is able to quantify the severity of damage with reasonable accuracy, but the estimationresults required to be calibrated by a calibration factorηwhich can be obtain by numerical analysis.

5.3.5 Evaluating the Effectiveness of CFRP Rehabilitation

The location and severity of damage has been estimated by the proposed damage detection method. Three damaged cases, i.e. a single severe damage located at mid-span or quarter-span and a double severe damage located at both locations, were then

repaired by CFRP sheets. These three cases were used to evaluate the effectiveness of rehabilitation using the proposed damage detection method. The evaluation focuses on change in severity estimation before and after rehabilitation. The method is then verified by static test results. To represent the effectiveness of rehabilitation, a term effective factor of repair is introduced as follow:

$$\Delta\alpha_d = \frac{\alpha_s - \alpha_r}{\alpha_s} \quad \text{Equation 5.1}$$

Where α_s is the severity estimation of damage and α_r is the severity estimation of the repair, $\Delta\alpha_d$ is the indicator of effectiveness of the repair calculated from dynamic test results which can has a value ranging from 0 to 1. The effectiveness of the repair ($\Delta\alpha_d$) has a value close to 1 when the CFRP repair completely removes the damage effect i.e. restore the structure back to intact condition.

$$\alpha = 1 - \frac{1}{\beta} \quad \text{Equation 5.2}$$

Where α is the severity estimator;

$$\beta = \frac{E^* I^*}{EI} \quad \text{Equation 5.3}$$

β is the damage indicator; EI refer to the stiffness of structure and * means the damaged cases.

Substituting 5.2 and 5.3 into Equation 5.1 the Equation 5.1 can be rewritten as follow:

$$\frac{\alpha_s - \alpha_r}{\alpha_s} = \frac{E^r I^r - E^s I^s}{EI - E^s I^s} \quad \text{Equation 5.4}$$

Since EI of a beam proportional to P/δ which is the slope of load-deflection curve that can be determined by static test. The slope can be calculated from the excel slope function. Therefore the effectiveness of the repair estimator($\Delta\alpha_s$) can also be obtained from static test results from equation 5.5;

$$\Delta\alpha_s = \frac{Slope^r - Slope^s}{Slope - Slope^s} \quad \text{Equation 5.5}$$

Figure 5.8 to 5.10 depict the results of damage severity estimation for the case of damaged and repaired single and double severe damage located at mid-span and quarter-span. These results show that the severe estimators have the significant change before and after rehabilitation, and the results for repaired single damage are better than repaired double severe damage. It can also be observed that the severe damage was not completely repaired by CFRP sheets, and these observations are supported the static test results. Figure 5.11 illustrates the static results of single severe damage at mid-span. The stiffness of repaired damage case was not recovered to the intact cases, which means that the damage cannot be repaired completely. Furthermore, the below table lists the results of damage severity estimation of severe and repaired damage cases, and also shows the results of effectiveness of rehabilitation calculated by the method introduced at previous section using dynamic test and static test results.

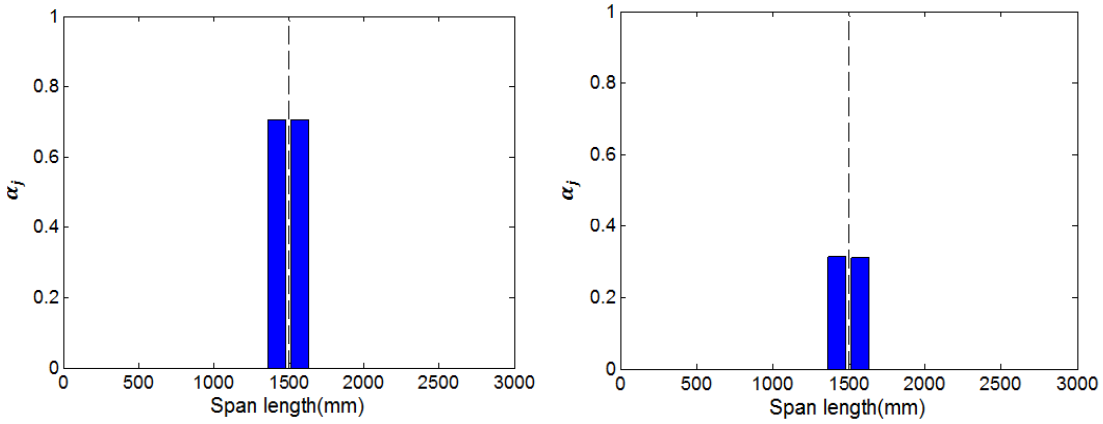

(a) 4S (b) R4S

Figure 5.8 Results of single severe damage at mid span before and after repairing

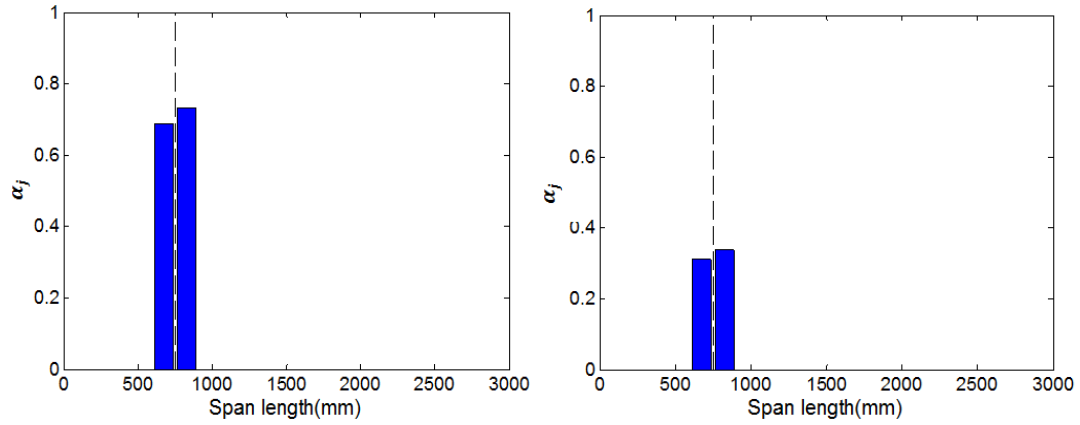

(a) 2S (b) R2S

Figure 5.9 Results of single severe damage at quarter span before and after repairing

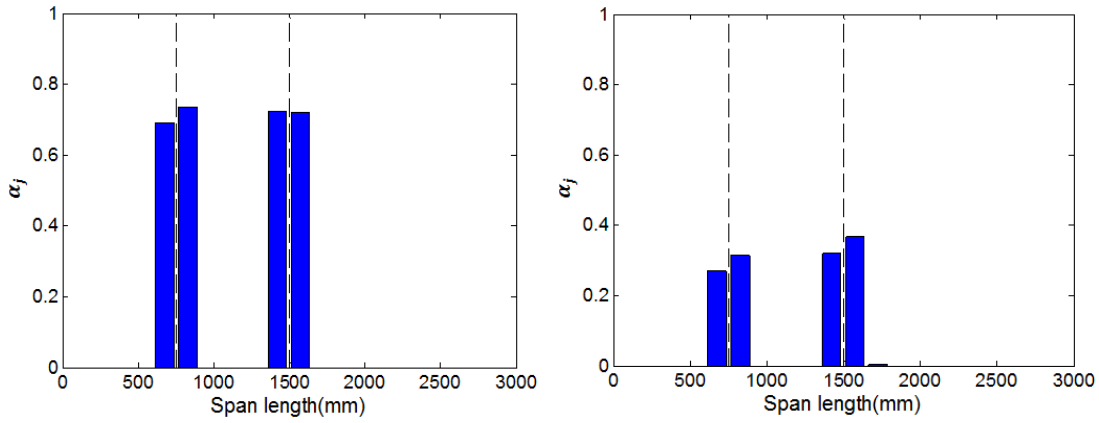

(a) 2S4S (b) R2S4S

Figure 5.10 Results of double severe damage before and after repairing

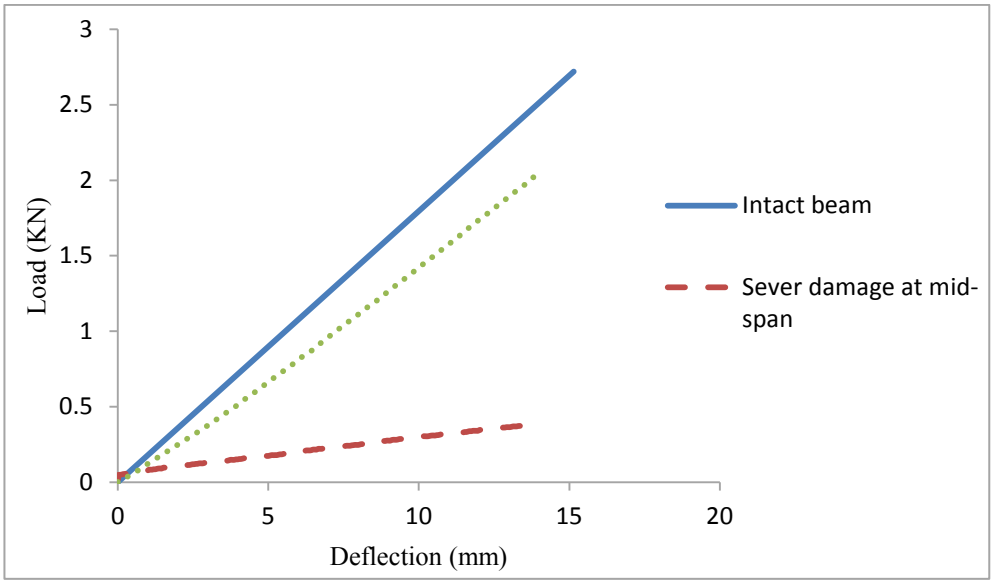

Figure 5.11 Load deflection curve for beam D1

The table 5.4 and 5.5 show that for single damage located at mid-span and quarter-span, the stiffness recovery by using CFRP repairing are 54.8% and 60.6% calculated using dynamic test results. Comparing with the results from static test data, the differences between dynamic and static results are 18.7% and 15.5% respectively. It can be seen that the results of stiffness recovery calculated from static test data is higher than the results calculated from dynamic data, and such difference is under 20%. The reason of the difference is that the impact load imparted to the structure for exciting the specimens during dynamic tests is small, which results in only linear elastic behaviour contrary to relative large loading in static where nonlinear behaviour CFRP and timber becomes prominent. Therefore, the stiffness repair effectiveness for dynamic test is not as obvious as the static test. However, the results of double severity damage case presents a large error between the results calculated using dynamic test data and static test data, which is more than 20%. It results from the fact most of modal based damage detection algorithms have encountered difficulties when detecting and evaluating multiple damage scenarios. It is merely due to the inherent nature of modal based approaches where contributions of damage to global modal behaviours affect by interaction between damage since modal parameters are global measures of the structural behaviour. Therefore, the proposed damage detection method to evaluate the effectiveness of CFRP rehabilitation on double damage cases is much less accurate than the single damage cases.

Table 5.4Comparison of effectiveness estimator for single damage at mid-span

Cases	α_S	Slope	$\Delta\alpha_d$ (%)	$\Delta\alpha_s$ (%)	Difference(%)
Intact		0.1779	54.8	73.5	18.7
4S	0.73	0.0307			
R4S	0.33	0.1487			

Table 5.5Comparison of effectiveness estimator for single damage at quarter-span

Cases	α_S	Slope	$\Delta\alpha_d$ (%)	$\Delta\alpha_s$(%)	Difference(%)
Intact		0.1779	60.6	76.1	15.5
2S	0.71	0.0245			
R2S	0.28	0.1421			

Table 5.6Comparison of effectiveness estimator for double damage case

Cases	α_S	Slope	$\Delta\alpha_d$ (%)	$\Delta\alpha_s$(%)	Difference(%)
Intact		0,1779	54.8, 56.9	79.1	24.3, 22.2
2S4S	0.73,0.72	0.0211			
R2S4S	0.33,0.31	0.1451			

In summary, the proposed approach of the repair effectiveness estimation repairing is able to evaluate the effectiveness of CFRP rehabilitation for single damage cases with reasonable accuracy. For the double damage cases, the error is escalated due to the nature of the method as aforementioned. This shortcoming can be compensated for by using other NDE techniques which work well on damage severity estimation for multi damage cases after damage locations are located.

5.4 Experimental results discussion

5.4.1 Identifying the Location of Single Notch damage

In order to locate damage, a large number of measurement points are desirable. However, considering practicality in real applications, the number of measurement

points is always limited. Due to limited number of sensors used in the test, the coarse mode shape and its derivatives used in the damage detection may not generate accurate results. In order to obtain better results cubic spline interpolation technique was used for reconstruction of finer mode shapes, expanding the initial 9 point mode shapes to the reconstructed 21 mode shapes. Further details of mode shape reconstruction techniques can be found inStubbs and Park (1996).

In the experimental studies, the Stubbs damage detection method employed the first three flexural modes for damage detection. The damage detection method was adopted because it can produce accurate damage detection results as concluded in the numerical work. All mode shapes considered in the experimental work have been mass normalised. In addition to the mass normalised mode shapes, mode shape curvatures are also normalise with respect to the maximum mode shape curvature value of each corresponding mode. In the following figures, the damage location index is plotted against the span length of the timber beam. In principle, when the damage location index value is larger than zero there is a possibility that damage occurs at that location. The actual damage locations are indicated with vertical dashed lines in all figures for LVL timber beams.

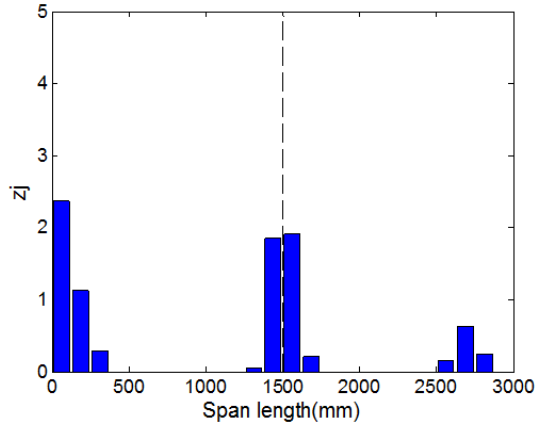

(a) Light

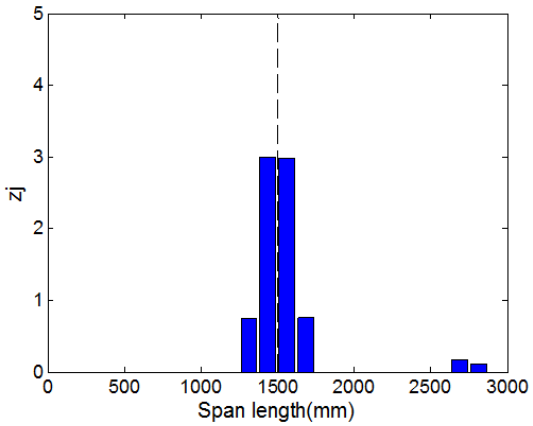

(b) Medium

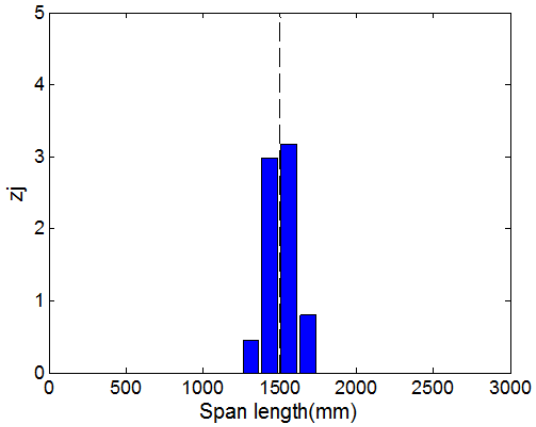

(c) Severe

Figure 5.12Single notch damage located at mid-span

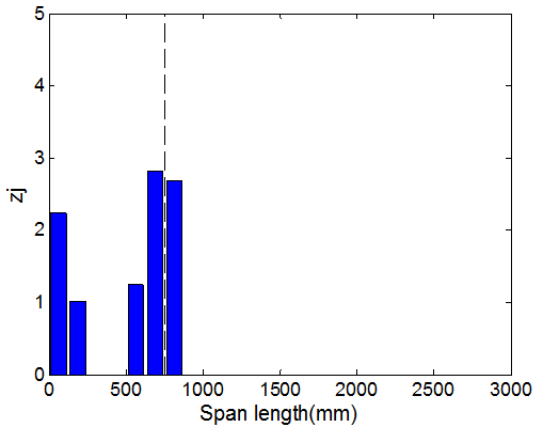

Figure 5.13 Single severe damage located at quarter span

Figure5.12 and Figure 5.13 illustrate the results of the single damage cases of 4L,4M, 4S and 2Susing the proposed damage detection method. It is observed that the method is capable of locating the damage for single damage cases in different location. However, in the case of single damage for 4L and 4M, the damage index has generated misleading

representation of the probability of existence of damage (false positive damage) when higher modes are used in the method. There are a number of reasons for the false positives. First of all, for node point of a mode shape where the displacement is approaching zero, the equation in the proposed damage detection method most probably generates singularity at that position. Therefore, false positive damage may result. Secondly, during the dynamic test, the accelerometers were attached to a small piece of steel plate, which was in turn glued on the top of the timber beam. There is a possibility that the acceleration response data acquired was actually from the steel plate and not from the test beam. This would affect the reconstruction of the mode shapes, and subsequently jeopardise the results of damage detection. Lastly, the inconsistency of materials in the timber beam and the noise in laboratory may be the reasons that false positives were generated. Furthermore, for the single damage case 4L and 2S, it is again seen that the false positive appears near one of the supports. As mentioned earlier, the false positive can be due to imperfections in the boundary conditions. In the experiment, the support system will never be an ideal pin-pin boundary condition as compared with the numerical ones. Instead of having zero displacement at the support, which occurs in the numerical simulation, the experimental support system is subjected to very small displacement under vibration. The magnitude of the displacement is close to the level of measured noise. Therefore, the measured modal displacement at the supports is strongly affected by measurement noise. Hence, the results of damage detection are affected by the noise polluted data. In practice, it is more important to have detected the damage, even though there may have been some spurious damage location, rather than not detecting the damage. This would help to reduce the risk of a catastrophic failure.

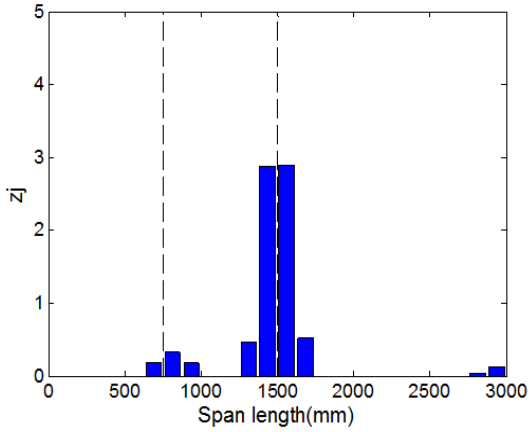

(a) 2L4S

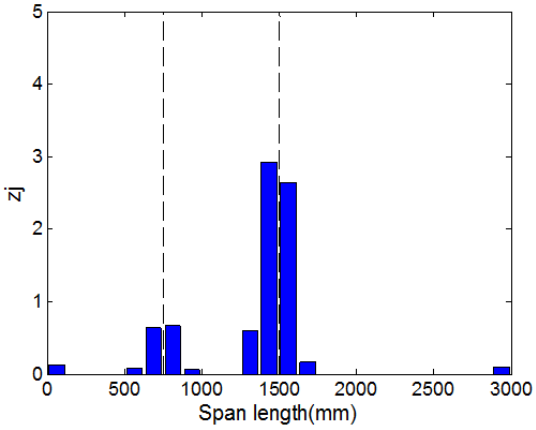

(b) 2M4S

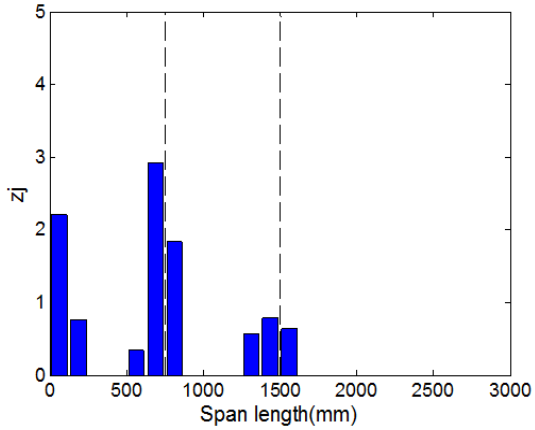

(c) 2S4L

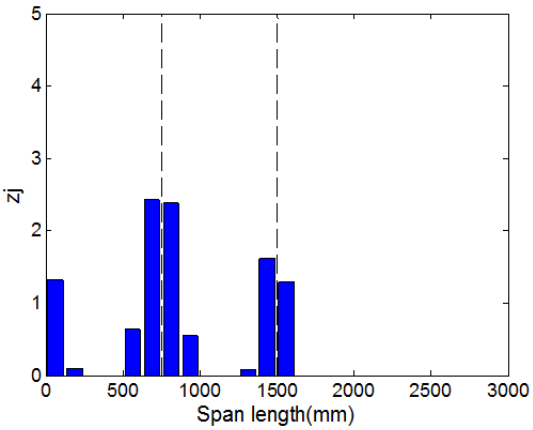

(d) 2S4M

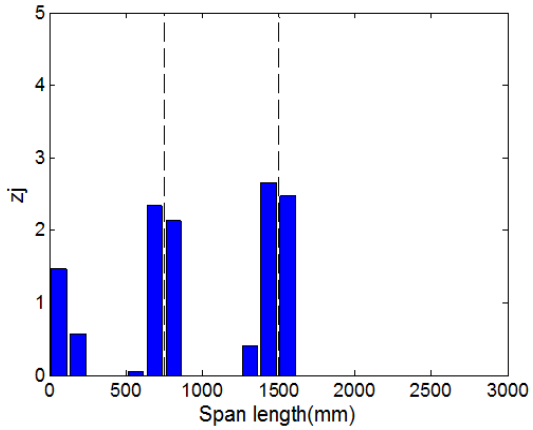

(e) 2S4S

Figure 5.14Double damage cases located at mid-span and quarter-span

Beams 4 and 5 were used to introduce multiple damage locations and they have five different scenarios of inflicted damage (2L4S, 2M4S, 2S4L, 2S4M and 2S4S). From Figure 5.14, it is again seen that the method is able to detect all locations of damage accurately at quarter-span and mid-span. False positive error also can be observed from these double damage results.

In summary, the proposed damage detection method shows promising capability of identifying the location of damage. However, due to uncertainties associated with measurement and processing errors, false positive or spurious damage location might be generated during performance of damage detection. They are explained as follows. First of all, as discussed above, in the experimental work, a pin-pin boundary system was used. However, the support system could never generate an ideal pin-pin boundary condition. Instead of having zero displacement, as occurs in the numerical simulation, the real supports are subjected to very small modal displacement under vibration, at which the magnitude of displacement is close to the level of measurement noise. Such small measured modal displacement at the supports is strongly affected by measurement noise. For any modal testing, in the case of both intact and damaged beams, the modal displacements obtained at the supports were mostly influenced by noise, rather than by the actual vibrations. The noise-polluted mode shape data at the supports was then employed in the reconstruction of the mode shape from coarse coordinates to a finer coordinates. This rendered distorted reconstructed results as compared to the ideal mode shape results. On the other hand, principle of the selected damage detection method identifies damage by using the mode shape curvatures between the undamaged and damaged cases. Therefore, the false positive of the difference in magnitude of modal displacement for the undamaged and damaged cases is due to noise. This accounts for the fact that some false positives were produced around the location of supports, and also for the phenomenon that the magnitudes of these false positives are sometimes larger than the magnitudes of real damage. However, even though some false positives were generated in the process of damage detection, the experimental results can still identify the location of inflicted damage. Secondly, during the modal test, some of the accelerations obtained may have contributions from the local vibration of the mounting steel plates rather than the test beam. This may attribute to generating false positives. Finally, in the modal test, nine accelerometers were used to obtain the acceleration data

of the reinforced concrete beams. After modal analysis, the measured nine-point mode shapes were then reconstructed into twenty-three point mode shapes, using cubic spline interpolation technique. The reconstructed mode shapes were used in the propose damage detection method to identify the location of damage, and to estimate its severity. However, the reconstructed mode shapes were not real mode shapes and there are always some differences between the real ones and reconstructed ones. Even though the difference between the real mode shapes and reconstructed mode shapes were small, the difference between the mode shape curvatures and modal strain energy were not ignorable after derivation. All these contributed to generating false positives.

5.4.2 Estimation of Severity of Damage

As discussed in section 5.3.4, the proposed damage detection method was shown to be able to detect locations of damage, and the method is capable of estimating the severity of damage with reasonable confidence by using numerically simulated data. However, the Kim and Stubbs (1995) method requires further development to calibrate the results, which introduced in previous section. Furthermore, it is challenging when the experimental data is to be used in estimation of damage severity in the proposed method, considering measurement noise, imperfect boundary conditions, uncertainties in materials and structures.

To evaluate the effectiveness of the proposed damage detection method in the damage severity estimation, the method is applied to data obtained experimentally from three single damage cases. As discussions have been presented in Section 5.3, since the locations of damage are already available, the processing of estimation of severity of damage only focuses attention on the damaged area. This approach is also adopted in the experimental results. The first three flexural modes are chosen for application in the damage severity estimation. The damage severity estimators are plotted against the span length of the beam. The actual damage locations are indicated with vertical dashed linesand the simulated severity of damage is indicated with horizontal red dash line.Table 5.7 presents the predicted and the estimated damage severities where each damage case corresponds to the percentage of loss of “I”.

Table 5.7 Estimation of severity of single damage case

Cases	Damage Scenario	Actual severity 'Loss of I' (%)	Estimated Severity 'Loss of I' (%)
1	None	0	0
2	4L	57.8	42.1
3	4M	87.5	68.5
4	4S	98.4	73.2

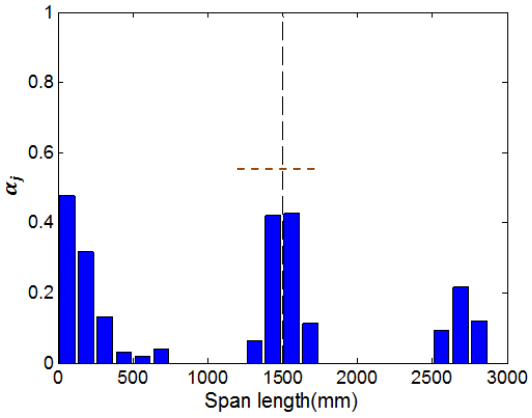

(a) Light

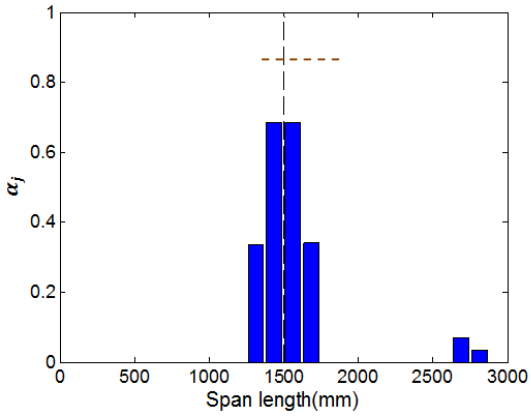

(b) Medium

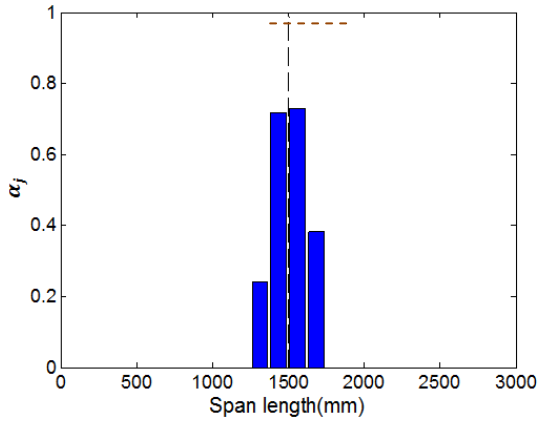

(c) Severe

Figure 5.15Damage estimation index for single damage at mid-span

Figure 5.15 illustrate the results of estimation of damage severity in three damage cases of 4L, 4M and 4S. Similar with the results of using numerical data to estimate the severity of damage, the method estimates the severity of damage with higher percentage of differences using the experimental data, but the Figure 5.16 shows that the predicted severity and estimated severity have the similar trend. Furthermore, there is also a correlation between the predicted severity and estimated severity. As discussed in

section 5.3, a calibration factor can be investigated to modify the estimated severity. Table 5.8 listed the calibration factor for these three cases, and the value ranging around 1.35. As discussed in section 5.3.4, the average value of calibration factor 1.33 was utilised to calibrate the results of estimated severity of damage. Both Figure 5.17 and Table 5.9 present that the results of after calibration are similar as the actual severity, and Table 5.3 indicate that the errors between calibrated severity of damage and actual severity of damage are fewer than 4.5%. The calibrated result of 4M case shown in figure of 4M is a bit larger than other two cases, which is due to the uncertainties in the experimental set up, imperfection in the modal analysis and presence of noise.

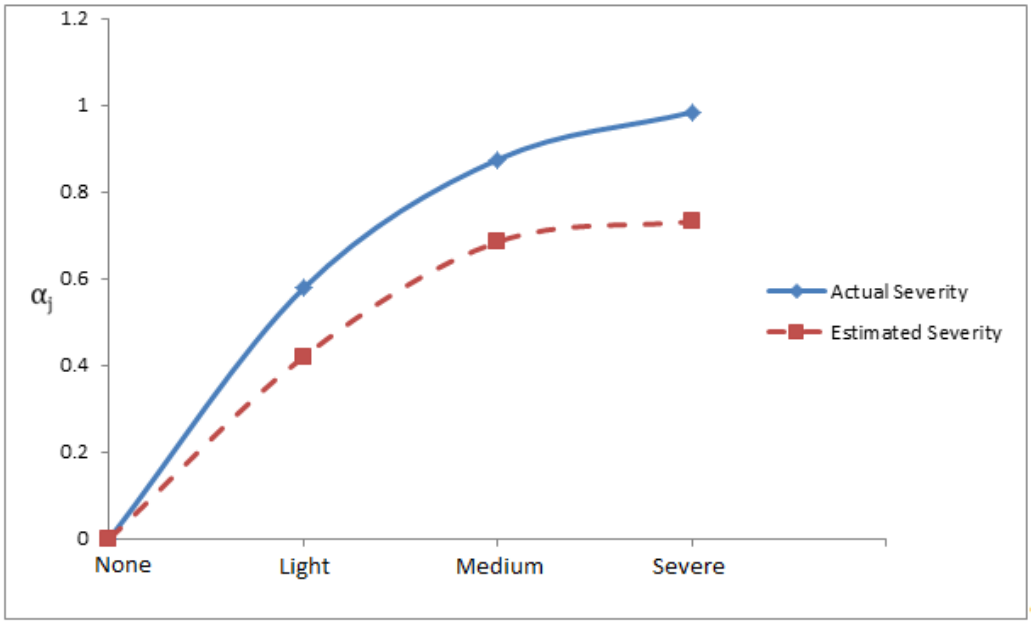

Figure 5.16 Comparison between actual and estimated results

Table 5.8Calculation of calibration factor

Cases	Damage Scenario	Actual severity 'Loss of I' (%)	Estimated Severity 'Loss of I' (%)	η
1	None	0	0	0
2	4L	57.8	42.1	1.37
3	4M	87.5	68.5	1.28
4	4S	98.4	73.2	1.35

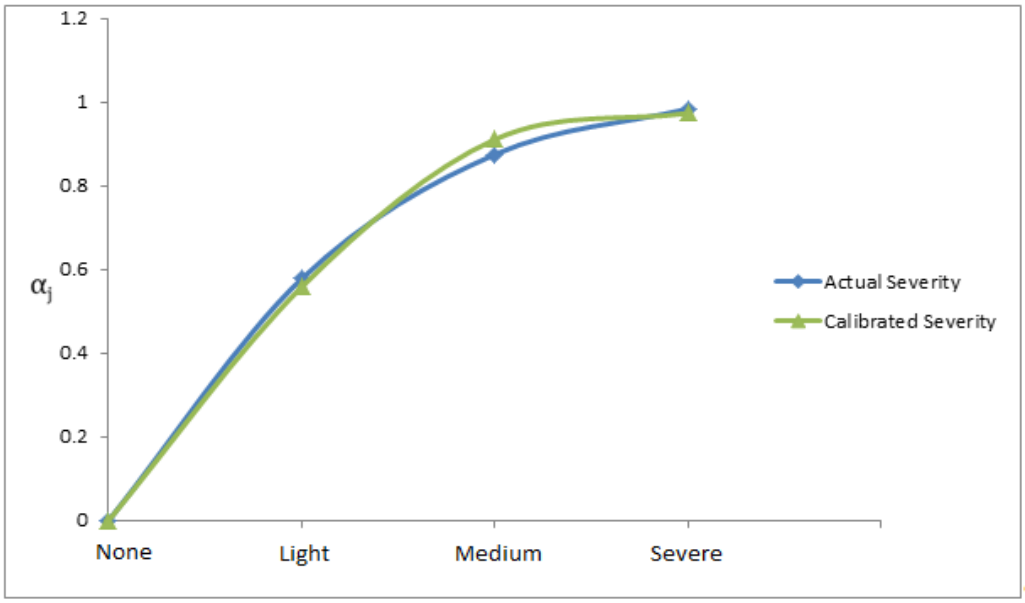

Figure 5.17 Comparison between actual and calibrated results

Table 5.9 Results of calibrated severity of damage

Cases	Damage Scenario	Actual severity 'Loss of I' (%)	Calibrated Severity 'Loss of I' (%)	Error (%)
1	None	0	0	0
2	4L	57.8	55.9	3.3
3	4M	87.5	91.1	4.1
4	4S	98.4	97.4	1.3

In summary, the propose damage severity estimator is able to accurately quantify the severity of damage with reasonable error (under 4.5%), but the estimation results required to be calibrated by a calibration factor ηwhich can be obtain by experimental data analysis. The small error occurred is because of the uncertainties in the experimental set up, imperfection in the modal analysis and presence of noise.

5.4.3 Evaluate the Effectiveness of CFRP Rehabilitation

The proposed damage detection approach has been proven that it is capable of detecting damage location and estimating damage severity in single damage cases with reasonable confidence as mentioned earlier. This section will focus on evaluating the effectiveness of CFRP rehabilitation for experimental work. The method to investigate the recovery in strength has been discussed in numerical study.

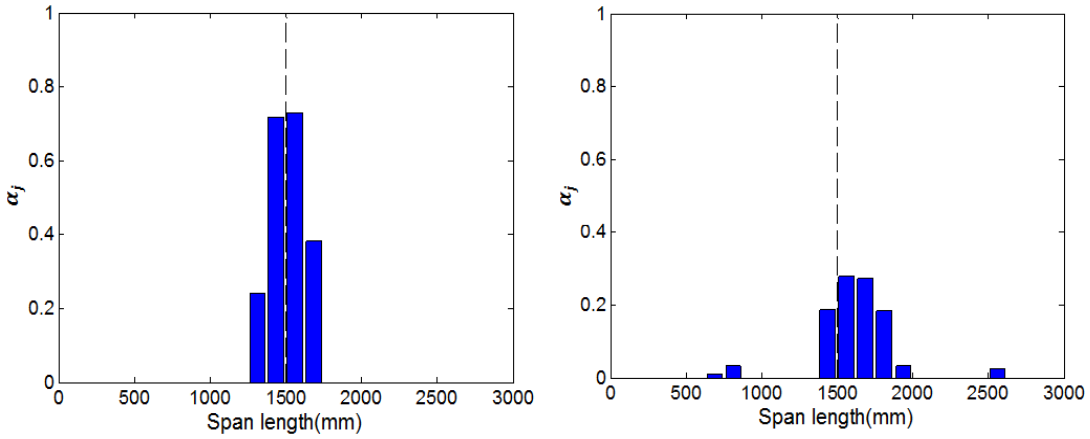

(a) 4S (b) R4S

Figure 5.18 Results of single severe damage at mid span before and after repairing

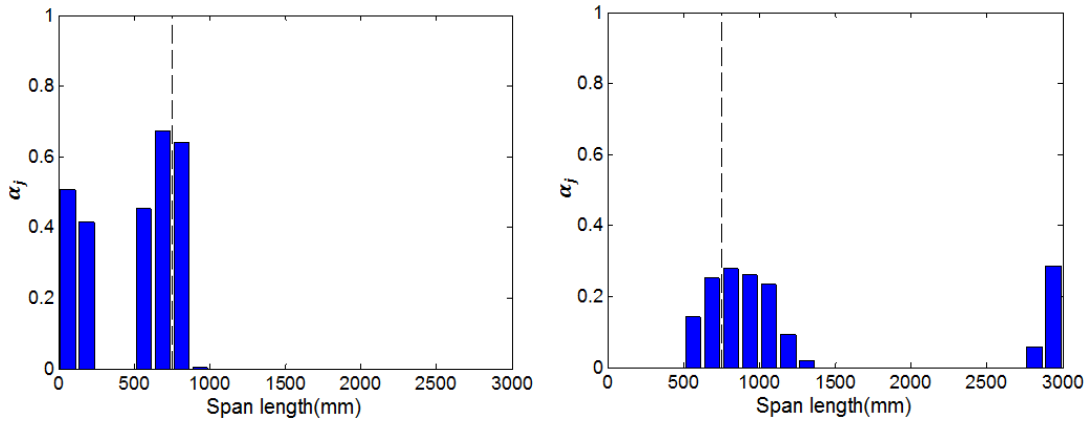

(a) 2S (b) R2S

Figure 5.19 Results of single severe damage at quarter span before and after repairing

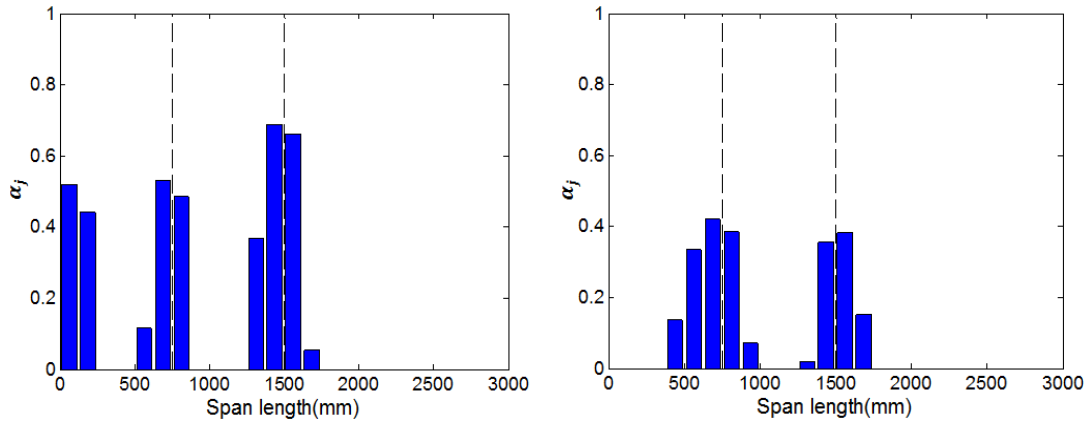

(a) 2S4S (b) R2S4S

Figure 5.20 Results of double severe damage before and after repairing

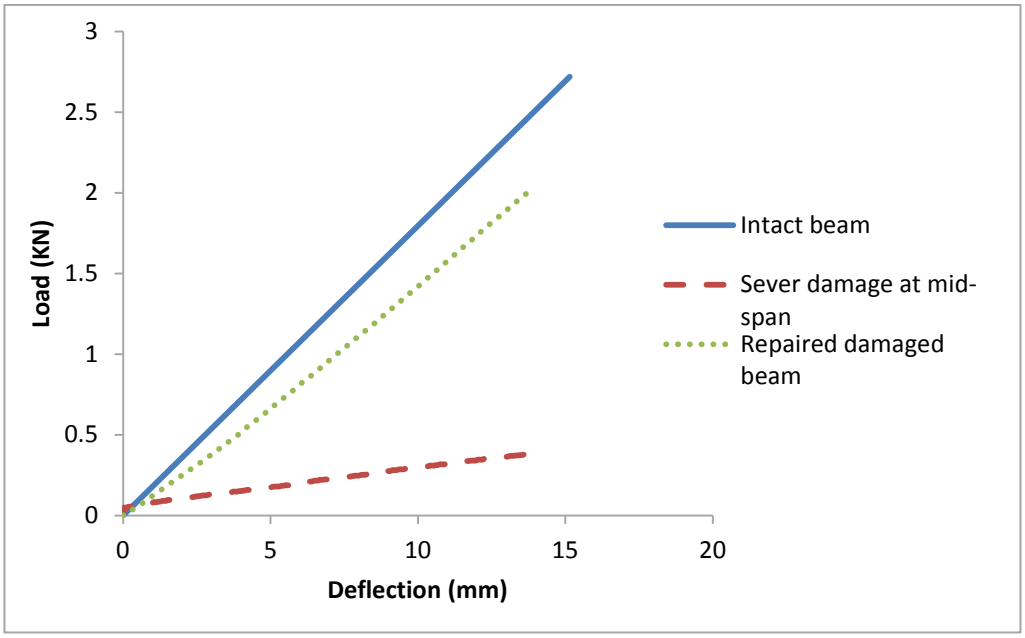

Figure 5.21 Load deflection curve for single damage located at mid-span

Figures 5.18 to 5.20 indicate that the results of damage severity estimation for the case of damaged and repaired single and double severe damage. Similar to results of numerical study, there is a significant change before and after rehabilitation, and the results for repaired single damage are better than repairing double severe damage. It can also be observed that the severity estimator occur in repaired damage cases, which means that the damage was not completely repaired. Furthermore, Figure 5.21 illustrates the static results of single severe damage at mid-span. The stiffness of repaired damage case is not recovered to the intact cases. Therefore, both dynamic test results and static test results report that the damage cannot be completely repaired. The Table 5.10 illustrate the results of damage severity estimation of severe and repaired damage cases, and also shows the results of effectiveness of rehabilitation calculated by the method introduced at section 5.3.5 using dynamic test and static test results.

Table 5.10 Comparison of effectiveness estimator for single damage at mid-span

Cases	α_S	Slope	$\Delta\alpha_d$ (%)	$\Delta\alpha_s$(%)	Difference(%)
Intact		0.2043	68.5	76.3	7.8
4S	0.73	0.0461			
R4S	0.23	0.1668			

Table 5.11 Comparison of effectiveness estimator for single damage at quarter-span

Cases	α_S	Slope	$\Delta\alpha_d$ (%)	$\Delta\alpha_s$(%)	Difference(%)
Intact		0.1761	71.6	80.6	9
2S	0.74	0.0257			
R2S	0.21	0.1475			

Table 5.12 Comparison of effectiveness estimator for double damage case

Cases	α_S	Slope	$\Delta\alpha_d$ (%)	$\Delta\alpha_s$(%)	Error (%)
Intact		0.1973	28.3,47.1	61.5	33.2,14.4
2S4S	0.53,0.68	0.0226			
R2S4S	0.38,0.36	0.1302			

Table 5.10 and 5.11 show the results of evaluating the effectiveness of CFRP rehabilitation using proposed evaluating method. For single damage cases 2S and 4S the recovery in stiffness are 68.5% and 71.6% for dynamic tests, while the repairing estimator of static test are 76% and 80.6%. The error of repairing estimator between dynamic test and static test is less than 10%. Therefore, in experimental study, the proposed method is able to accurately evaluate the effectiveness of CFRP rehabilitation with a reasonable error for single damage. As we discussed in Section 5.3.5, the reason of the difference is that the impact load imparted to the structure for exciting the specimens during dynamic tests is small, which results in only linear elastic behaviour contrary to relative large loading in static tests where nonlinear behaviour CFRP and timber becomes prominent. Therefore, the stiffness repair effectiveness for dynamic test is not as obvious as the static test. Furthermore, the results calculated from dynamic test in strength recovery is less than the results calculated from static test. The resulting underestimation of the capacity is more favourable than an overestimation, which would ultimately result in an over-designed structure should such method be utilised. The non-destructive method would hence be ideal for quick estimations of moment capacities prior to undertaking inelastic analysis which would be more time consuming. However, for the double damage cases results shown in Table 5.12, the recovery in strength for the quarter span only was 28.3%, and the error compared with single damage cases is quite large which is 33.2%. Therefore, the proposed method for evaluating the double damaged cases repaired by CFRP requires the further development.

In summary, the proposed method of evaluating the effectiveness of CFRP rehabilitation is capable of supporting the accurate results with the reasonable error for single damage cases. However, this method requires the further development to be adopted to evaluate the double damage cases repaired by CFRP.

5.5 Comparison between Numerical and Experimental Results

This section presents a comparison between the numerical and experimental results of damage detection on LVL timber beams, using the proposed damage detection approach. The discussions will be focused on comparing numerical and experimental results in terms of locating damage, estimating severity of damage and evaluating the effectiveness of CFRP rehabilitation.

5.5.1 Comparison in Locating Damage Results

To investigate the difference between numerical and experimental results, nine different cases, namely, 2S, 4L, 4M, 4S, 2L4S, 2M4S, 2S4L, 2S4M and 2S4S were used in the comparison. Figures 5.22 and 5.23 illustrate the results of the location of damage using both numerical experimental data for two damage cases of 4L and 2M4S, respectively. The results for all other cases are shown in Appendix.

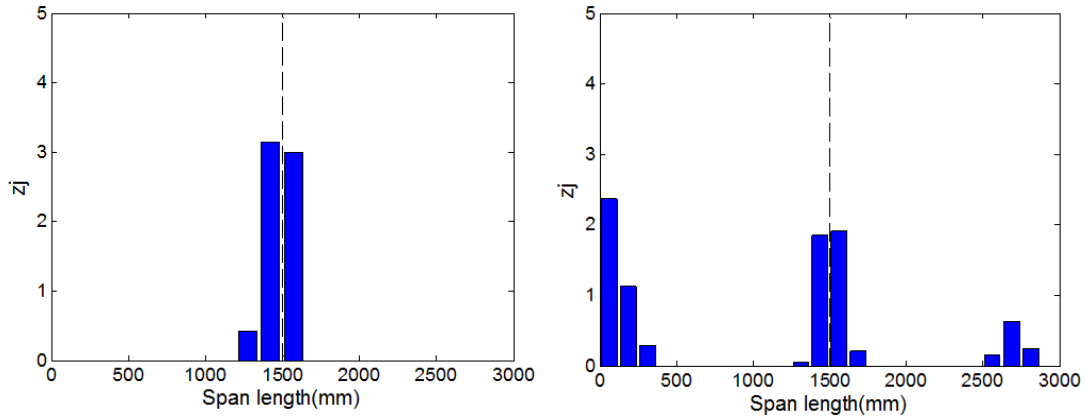

(a) Numerical (b) Experimental

Figure 5.22 Comparison between numerical and experimental results for 4L

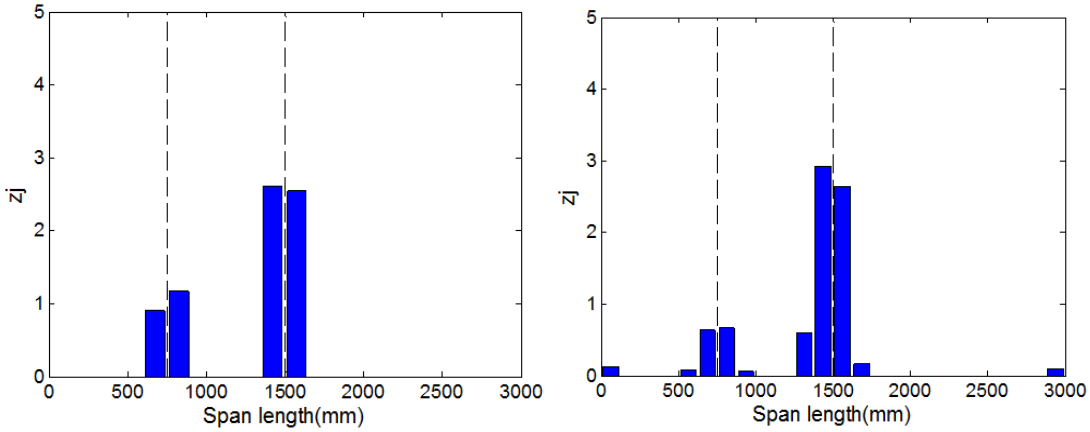

(a) Numerical (b) Experimental

Figure 5.23 Comparison between numerical and experimental results for 2M4S

The results show that the inflict damage in the timber beam can be identified from both numerical data and experimental data. The results of the numerical work are distinct and clear without any false identification. This is because the numerical data is ideal without noise pollution and free from errors of the imperfection of modal analysis. Some false positives were generated in the results of the experimental work due to noise pollution, environmental uncertainties and imperfection of modal analysis. Nevertheless, it is important to note that, in the experimental results, the damage was not missed and this would provide a safe and conservative assessment results and reduce any possibility of a catastrophic failure. It is possible to conclude that the proposed damage detection method is capable of detecting damage of notch types in LVL timber beams, numerically and experimentally.

5.5.2 Comparison in Damage Severity Estimation Results

In this section, three different cases, namely, 4L, 4M and 4S, are considered to illustrate the difference in estimation of severity of damage between the numerical and the experimental results. The numerical data without noise are adopted for the severity estimation. Both numerical and experimental results were obtained using the first three flexural vibration modes in the proposed damage severity estimation. Figure 5.24 depicts the difference of estimation of severities between numerical and experimental research in all single damage cases.

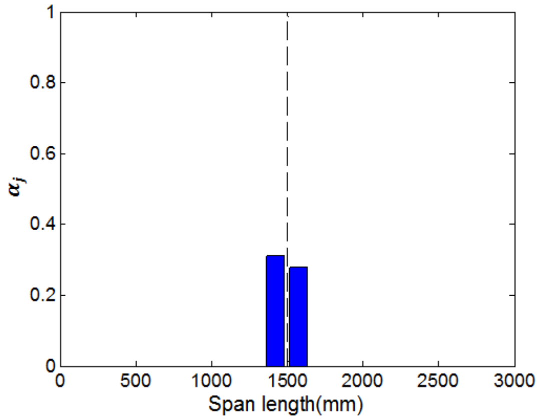

(a) Numerical

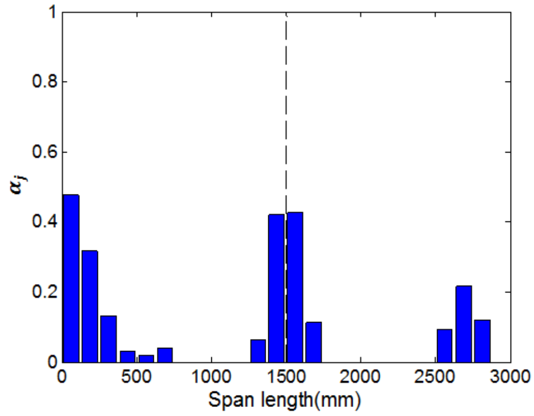

(b) Experimental

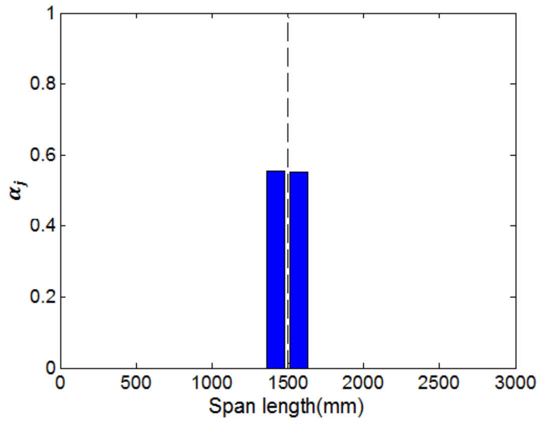

(a) Numerical

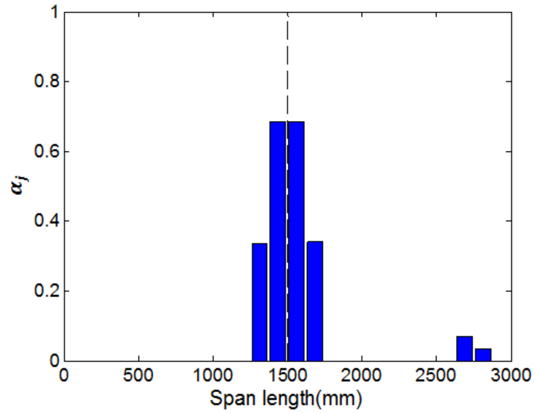

(b) Experimental

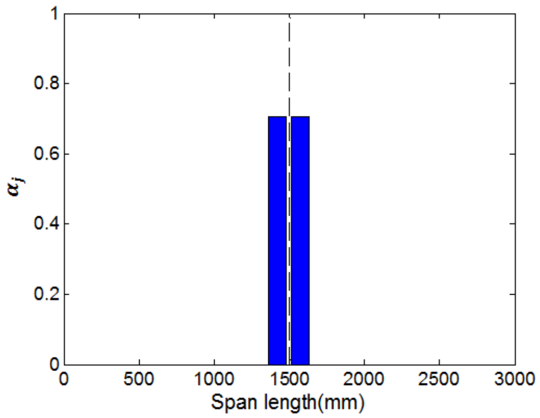

(a) Numerical

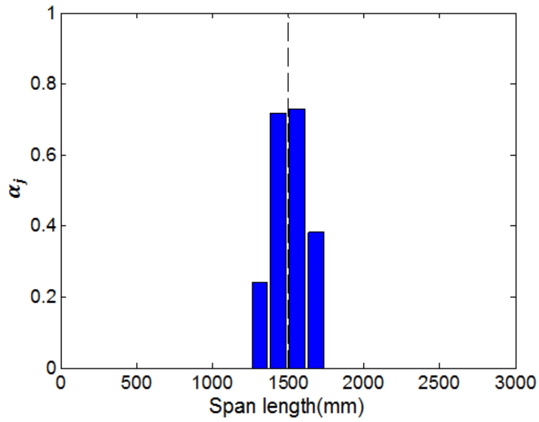

(b) Experimental

Figure 5.24 Comparison of severity estimation between numerical and experimental results

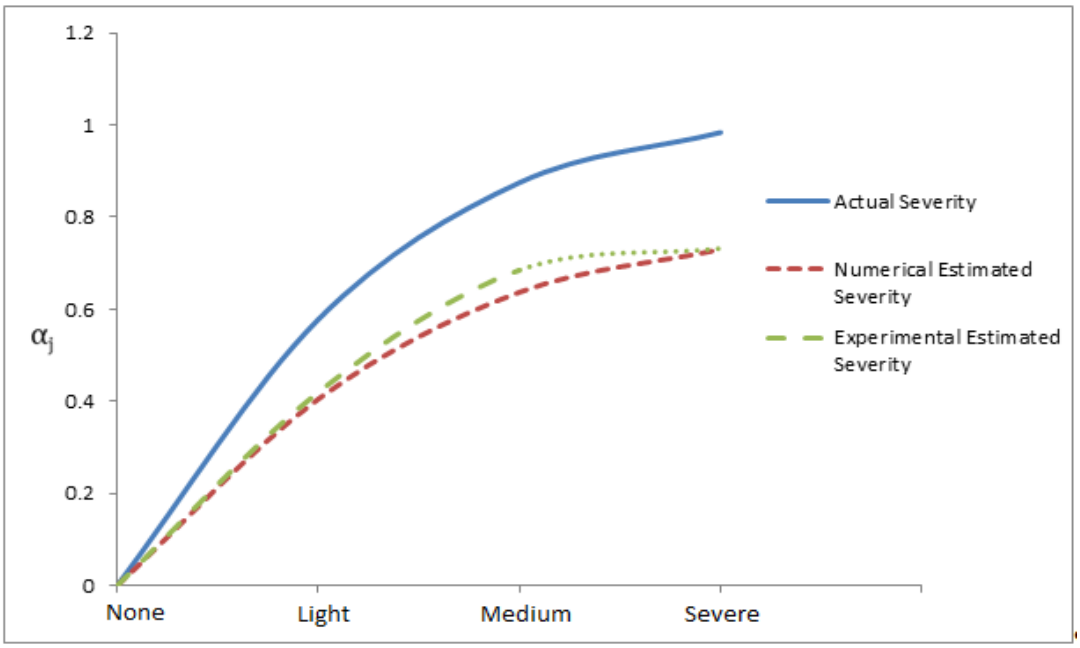

Figure 5.25 Comparison of estimated severity between numerical and experimental data

Table 5. 13 Comparison of estimated severity between numerical and experimental data

Damage Scenario	Actual severity 'Loss of I' (%)	Numerical Estimated Severity	Experimental Estimated Severity	Difference (%)
None	0	0	0	0
4L	57.8	40.5	42	1.5
4M	87.5	63.7	68.5	4.8
4S	98.4	73.1	73.2	0.1

Table 5.14 Comparison of calibration factor

Cases	Damage Scenario	η (Numerical)	η(Experimental)
1	None	0	0
2	4L	1.42	1.37
3	4M	1.37	1.28
4	4S	1.35	1.35

Figure 5.25 shows that both numerical and experimental provide similar results in terms of predicting damage severity. The percentage of differences between the numerical and

experimental results is less than 5% as shown in Table 5.13, but both predicted results have relatively large error in comparison with the actual damage severity. As discussed in section 5.3.4, therefore, the results of using the proposed damage detection method to estimate the severity of damage require a calibration by a calibration factor. Table 5.14 indicates that the calibration functions for both numerical results and experimental, ranging from around 1.35. The calibration factor for both numerical and experimental results are similar as expected Furthermore, Figure 5.25 also shows that the damage severity estimation results from numerical and experimental data are similar, with a trend that the increase of damage size elaborates the errors of damage estimation comparing to actual damage. Therefore, using the average value of calibration factor calculated by numerical and experimental data to calibrate the estimated severity and the results comparison are shown in Figure 5.26 and Table 5.15. Both Figure 5.26 and Table 5.15 show that the results of severity of damage after calibration are very close to actual damage severity. The percentage of differences between the numerical and experimental results is less than 4%. The calibrated result of 4M case shown in figure of 4M is slightly larger than other two cases, which is due to the uncertainties in the experimental set up, imperfection in the modal analysis and presence of noise.

Table 5.15 Comparison of calibrated severity between numerical and experimental data

Damage Scenario	Actual severity 'Loss of I' (%)	Numerical Estimated Severity	Experimental Estimated Severity	Difference (%)
None	0	0	0	0
4L	57.8	55.9	55.8	0.1
4M	87.5	87.9	91.1	3.2
4S	98.4	100.7	97.4	3.3

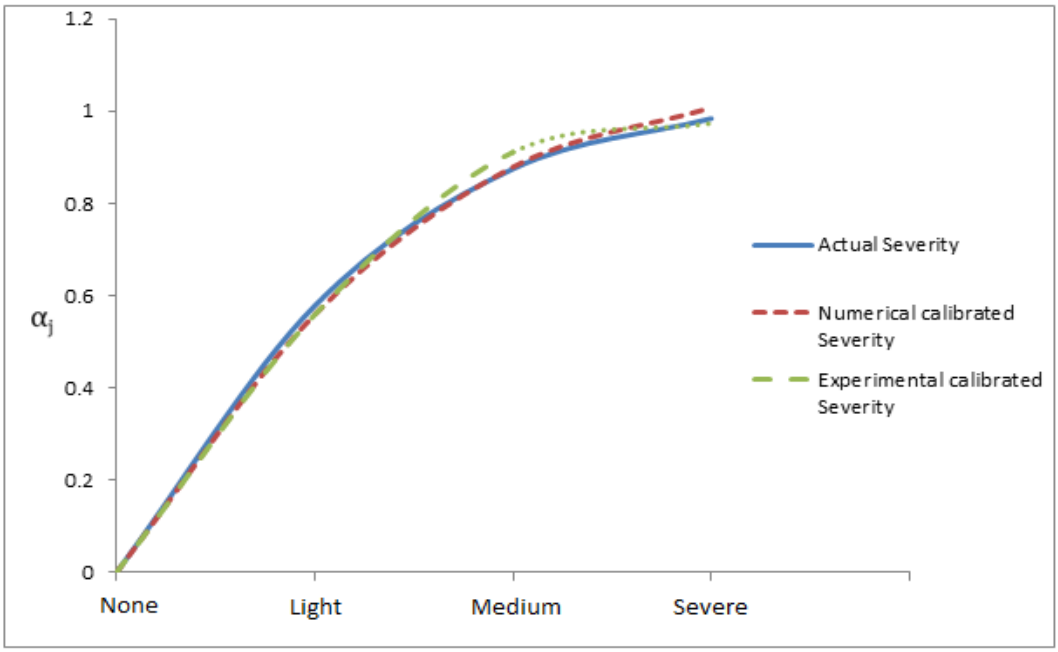

Figure 5.26 Comparison of calibrated severity between numerical and experimental data

5.5.3 Comparison in Evaluating the Effectiveness of CFRP Rehabilitation

Following the success on detecting damage location and estimating damage severity using proposed damage detection approach, in this section the method is to be used to evaluate the effectiveness of repair for damaged beams. Three different cases, R2S, R4S and R2S4S are used to investigate the difference in evaluation of effectiveness of CFRP rehabilitation between numerical and experimental results. The results comparison of effectiveness of CFRP rehabilitation calculated by proposed evaluating method introduced in section 5.3.5 are given in Table 5.6. Figure 5.27 depicts the difference of estimation of severities for repairing damaged cases (R2S, R4S and R2S4S) between numerical and experimental research.

Table 5.16 Comparison of effectiveness estimator between numerical and experimental results

Cases	Numerical Results		Experimental Results	
	$\Delta\alpha_d$ (%)	$\Delta\alpha_s$(%)	$\Delta\alpha_d$ (%)	$\Delta\alpha_s$ (%)
R2S	60.6	76.1	71.6	80.6
R4S	54.8	73.5	68.5	76.3
R2S4S	54.8,56.9	79.1	29.3,47.1	61.5

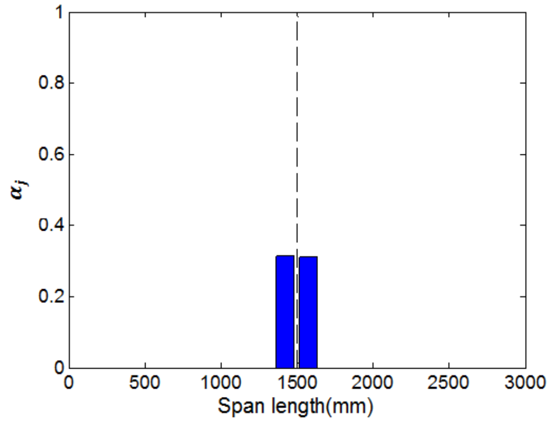

(a) Numerical

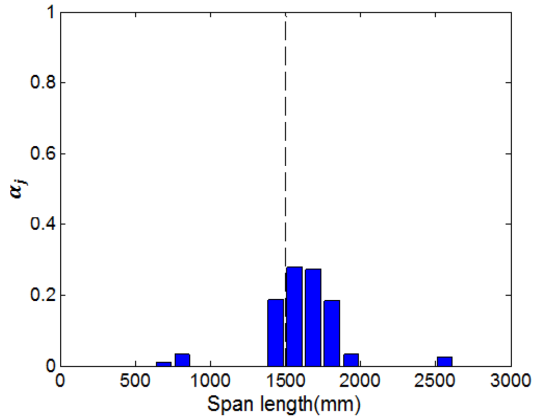

(b) Experimental

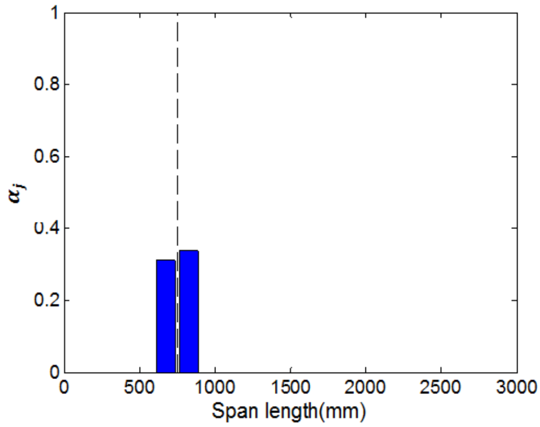

(a) Numerical

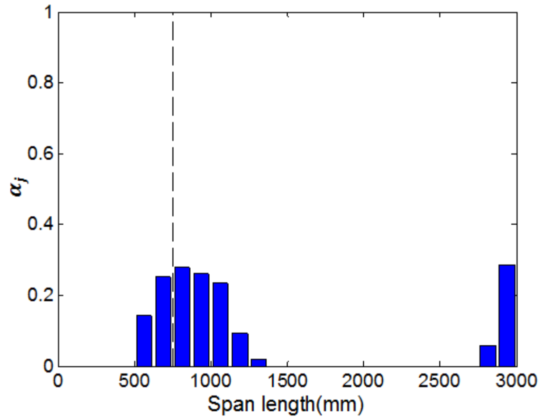

(b) Experimental

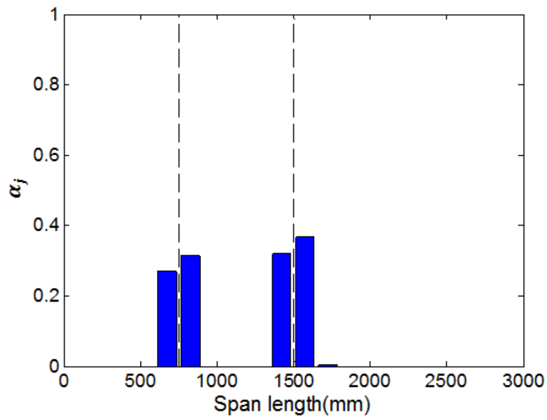

(a) Numerical

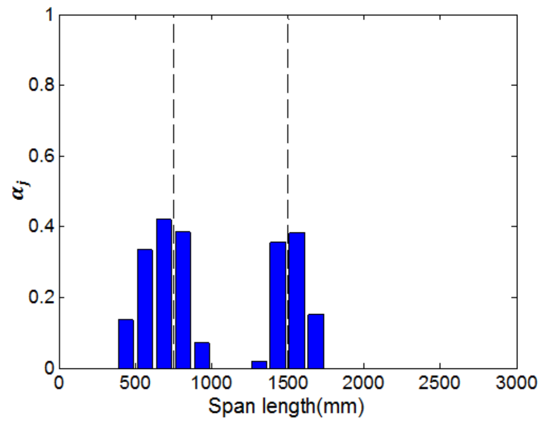

(b) Experimental

Figure 5.27 Comparison of repaired severity estimator between numerical and experimental results

Figure 5.27 illustrates that the results of experimental stiffness restoration from repair are larger than that of numerical results. For example, in the experimental results of stiffness recovery computed from dynamic test data and static test data are 68% and 71%, respectively while the numerical stiffness recovery results computed by from simulated dynamic and static are 54% and 60% respectively. The differences between experimental and numerical results calculated by dynamic data are more than 10%, but the results calculated by numerical and experimental static data are only around 4%. Furthermore, discrepancy between the dynamic estimation and static estimation of the repair effectiveness estimated from experimental data is much less than that from the numerical data. It seems that the experimental results produce better accuracy than the numerical results in terms of stiffness recovery estimation. The reason for this phenomenon may come from inaccuracy of FE modelling of beams with CFRP rehabilitation where assumption of the boundary condition between timber and CFRP after repair may not be able to capture some local effects due to damage whilethe experimental data truth fully reflected whatever was happened in the beams. To further investigation including modal updating of the FE model using the experimental data may be necessary but is out of the scope of this thesis.

Summary

This chapter presented the evaluation and verification of proposed damage detection method for damage detection and evaluation of CFRP rehabilitation on several experimental timber beams inflicted with different damaged scenarios and repaired scenarios.

Firstly, a method which is Kim and Stubbs (1995) method adopted in this Chapter to detect location and severity of damage and to evaluate the effectiveness of CFRP rehabilitation is reviewed. This method developed from an original conception that the fraction of modal strain energy is same for both damaged and undamaged structures.

The numerical results discussion was evaluated. The procedure of obtaining modal parameters from numerical transient analysis was discussed. Twelve damage cases, i.e. 2S, 4L, 4M, 4S, 2L4S, 2M4S, 2S4L, 2S4M, 2S4S, R2S, R4S and R2S4S, and corresponding intact cases were used for experimental evaluation of the proposed damage detection method.

The results of damage localisation showed that the selected damage detection method was capable of identifying the location of damage in all of damage cases both numerical and experimental results. The results confirmed that the results of numerical study is pure than the experimental results due to none noise polluted the numerical data. However, for the experimental results, false positive damage was generated. The reasons that caused false positives were discussed. For example, most of the experimental results have false positive error occurred at support point, which is due to the imperfect boundary conditions. The other false positive error occurred only for the light damage cases. The results also confirmed that the more severe the damage the higher is the confidence in locating the damage. Both numerical and experimental study proved that the proposed method was reliable and robust in identifying the location of damage.

Regarding the severity of damage, the results of estimating the severity of damage in experimental work is similar to the results from numerical model. However, predicted severity of damage from both numerical and experimental results had discrepancy with the simulated results, but a correlation between these two results exists. A calibration

factor was developed to update the predicted severity of damage. After the calibration, the results were able to estimating the severity of damage with reasonable accuracy. The shortcomings of the proposed method in estimation of severity of damage can be compensated for either by combination with other NDT methods that work well on the area, or by refinement of the estimation method as future research work.

Lastly, the chosen damage detection method was used to evaluate the effectiveness of CFRP rehabilitation from both numerical and experimental results. Two separate estimators to evaluate the recovery in strength calculated by dynamic test and static test, respectively, were developed. From the results, the developed effectiveness estimator was able to evaluating the effectiveness of CFRP repair with the reasonable differences. The reason of the differences is that the impact load imparted to the structure for exciting the specimens during dynamic tests is small, which results in only linear elastic behaviour contrary to relative large loading in static tests where nonlinear behaviour CFRP and timber becomes prominent. Therefore, the stiffness repair effectiveness for dynamic test is not as obvious as the static test. Furthermore, it was found that the estimator using experimental dynamic results were more accurate than the results from numerical model in single damage cases. The reason for this phenomenon may come from inaccuracy of FE modelling of beams with CFRP rehabilitation where assumption of the boundary condition between timber and CFRP after repair may not be able to capture some local effects due to damage while the experimental data truthfully reflected whatever was happened in the beams. To further investigation including modal updating of the FE model using the experimental data may be necessary. Furthermore, the results calculated from dynamic test underestimate the stiffness recovery when compared to static test results. The resulting underestimation of the capacity is more favourable than an overestimation, which would ultimately result in an over-designed structure should such method be utilised. The non-destructive method would hence be ideal for quick estimations of moment capacities prior to undertaking inelastic analysis which would be more time consuming.

CHAPTER 6 CONCLUSIONS AND RECOMMENDATIONS

6.1 Conclusions

This thesis investigated a novel concept of utilising vibration responses for evaluation of repair effectiveness of rehabilitated timber LVL beams after damage was repaired. The investigation started with to implementing a modal based damage detection approach (Kim & Stubbs, 1995) to detect the location and severity of damage in LVL beams and then innovatively utilising such method to evaluate the effectiveness of repaired LVL beams repaired by CFRP. The research consisted of numerical modelling using finite element method (FEM) and experimental testing and analysis of LVL beams, including static testing and dynamic modal testing. Finite element model was validated using experimental load-deflection curves from static tests and modal parameters obtained from dynamic tests. Three types of damage severity scenarios were introduced, namely Light, Medium and Severe damage for both FE model and experimental specimens, which located at either mid-span or/and quarter-span. The inflicted damage type introduced in FE model and experimental specimen was notch type of damage. For the single and double severe damage specimens repair also carried out by applying CFRP after initial tests. Four point bending test and dynamic test were performed on all damage cases (2S, 4L, 4M, 4S, 2S4L, 2S4M, 2L4S, 2M4S, 2S4S, R2S, R4S and R2S4S).

Based on the material properties obtained from the manufacturer's data, numerical modelling using finite element method (FEM) of LVL beams was carried out. Intact beams, damaged beams (damage at various locations and severities) and repaired beams (damage repaired by CFRP) were modelled with FEM. In the FE modelling, equivalent stiffness reduction method was employed to simulate notch damage. The intact beam FE model was verified using static experimental test results, and it has been observed that under static loading results of FE model are relatively stiffer than the experimental results. The reasons are that when the damage (i.e. notch) was experimentally introduced by saw cut it inevitably damaged the surrounding fibre at roots, while in FE model the timber material was simulated as isotropic and the notch (damage) was perfectly cut. Discontinuity of timber fibres due to cutting damage on surrounding area of experimental specimens weakened flexural stiffness of the timber beam specimens

and resulted in lower stiffness measurements. To discuss numerical and experimental results under a same benchmark, the numerical model was update to reflect the reality. Furthermore, for dynamic test results, the correlation analysis results also show that the natural frequencies obtained from the numerical model are close to the experimental ones, with error of less than 10% for *NFerror*.

A modal based damage detection method developed by Kim & Stubbs (1995) was proposed for damage detection of LVL beams. From the discussions of numerical and experimental results, the proposed method was capable of identifying the location of damage and quantifying the severity of damage with robustness and reliability. Furthermore, an approach for evaluating the effectiveness of damaged LVL beam repaired by CFRP was also developed from the method, and the estimator combined both static results and dynamic results.

Numerical studies of damage detection using a finite element model of LVL beams with the proposed methods were performed. Results of the numerical investigation show that the proposed damage detection method using different combination of first three flexural modes is reliable and robust in locating damage for LVL beams, for both single and multiple damage scenarios. For experimental studies, the proposed damage detection method shows promising capability of identifying the location of damage while some false positive errors occurred in the results. First of all, as discussed above, in the experimental work, a pin-pin boundary system was used. However, the support system could never generate an ideal pin-pin boundary condition. Instead of having zero displacement, as occurs in the numerical simulation, the real supports are subjected to very small modal displacement under vibration, at which the magnitude of displacement is close to the level of measurement noise. Such small measured modal displacement at the supports is strongly affected by measurement noise. This accounts for the fact that some false positives were produced around the location of supports, and also for the phenomenon that the magnitudes of these false positives are sometimes larger than the magnitudes of real damage. Secondly, during the modal test, some of the accelerations obtained may have contributions from the local vibration of the mounting steel plates rather than the test beam. This may attribute to generating false positives. Finally, in the modal test, nine accelerometers were used to obtain the acceleration data of the reinforced concrete beams. After modal analysis, the measured nine-point mode shapes

were then reconstructed into twenty-three point mode shapes, using cubic spline interpolation technique. The reconstructed mode shapes were used in the propose damage detection method to identify the location of damage, and to estimate its severity.

For estimating the severity, the proposed damage severity estimator is able to quantify the severity of single damage with reasonable accuracy, but the severity estimator need to be calibrated by a calibration factorη. After the calibration, the results were able to estimating the severity of damage with reasonable accuracy (error less than 5%). The calibration factor for both numerical and experimental results are similar (around 1.35) as expected Small error occurred for the calibrated result of 4M due to the uncertainties in the experimental set up, imperfection in the modal analysis and presence of noise.

Lastly, the estimator developed from the proposed method to evaluate the effectiveness of CFRP rehabilitation from both numerical and experimental results is capable of supporting the accurate results for single damage cases. However, this method requires further development to be adopted to evaluate the double damage cases repaired by CFRP. From the results, it was found that the estimator using experimental dynamic results was more accurate than the results from numerical model in single damage cases. The reason could be due to inaccuracy of FE modelling of beams with CFRP rehabilitation where assumption of the boundary condition between timber and CFRP after repair may not be able to capture some local effects due to damage while the experimental data truthfully reflected whatever was happened in the beams. To solve the problems, numerical model requires performing the modal updating. Furthermore, the results calculated from dynamic test underestimate the stiffness recovery when compared to static test results. The resulting underestimation of the capacity is more favourable than an overestimation, which would ultimately result in an over-designed structure should such method be utilised. Hence, the non-destructive method would be ideal for quick estimations of moment capacities prior to undertaking inelastic analysis which would be more time consuming.

In summary, the proposed damage detection method was proven to be capable of identifying the location of damage and quantifying the severity of damage with robustness and reliability. Significantly, an estimator for evaluating the repair

effectiveness of damaged LVL beam repaired by CFRP was also developed. Extensive numerical and experimental investigations have found that the estimator can produce the accurate results in single damage cases for evaluating repair effectiveness of damage beams.

6.2 Recommendations and Future Work

Further work and some refinements are recommended to make this research work more practical for application. Hence, the purpose of this section is to focus on the issues that should be addressed by future researchers to make use of the proposed method and the developed estimator as a practical tool for damage detection and evaluating the effectiveness of CFRP rehabilitation in timber structures, as well as the reinforced/repaired applications.

First of all, since the number and spacing of sensors are critical to the damage detection results, it is recommended that using a beam system, parametric studies on sensitivity of number of sensors and spacing be carried out. Besides, it is also recommended to study the threshold of damage that can be detected using different combination of number of sensors and spacing.

Secondly, mode shape plays an important role in damage detection. In this research mode shape was reconstructed using Cubic Spline interpolation technique. Since there are still differences between the reconstructed and the real mode shapes, it is recommended that research should be carried out on how to reconstruct mode shape in order to further minimise the difference between the reconstructed mode shape and the real mode shape.

Thirdly, evaluation of repair effectiveness on various damage types such as loss of section externally, or internally, termite damage, irregular damage pattern (due to rotten) etc.

Fourthly more in-depth and extensive numerical modelling should be considered, e.g. orthotropic material modelling for timber, advanced model updating etc.

Finally, from the study of modal parameter investigation, the results of natural frequency of FE model were slight different to the experimental cases (error around 10%). Perfect pin-pin boundary conditions were simulated for the support in the FE model is a perfect boundary condition while the support system in experimental test could never generate an ideal pin-pin boundary condition. Therefore, the simulation of support system in FE model requires to be modified. For example, one end of support boundary can be modified to a spring system, and the coefficient of stiffness of the spring can be changed to obtain the same boundary condition with the support system in experimental test.

REFERENCES

ABDO, M. A. B. & HORI, M. 2002. 'A numerical study of structral damage detection using changes in the rotation of mode shapes'. *Journal of Sound and Vibration,* 251**,** 227-239.

ALLEMANG, R. & BROWN, D. 1983. 'A correlation coefficient for modal testing'. *Proceedings of the 1st International Modal Analysis Conference*.

ANDRE , A. 2006. 'Fibres for strengthening of timber structures'.*Luleå tekniska universitet/Civil and Environmental Engineering/Structural Engineering.*

AVITABILE, P. 2006. 'Modal Space in Our Little World'. *Sound and Vibration Magazine*.

BERNAL, D. & GUNES, B. 2002. 'Damage localization in output-only systems: A flexibility based approach'.*Proc. of the International Modal Analysis Conference (IMAC) XX, Los Angeles, California*. 1185-1191.

BROWNJOHN, J. M. & PINQI, X. 1999. 'Finite element model updating of a damaged structure'. SPIE proceedings series. *Society of Photo-Optical Instrumentation Engineers*, 457-462.

BUELL, T. W. & SAADATMANESH, H. 2005. 'Strengthening Timber Bridge Beams Using Carbon Fiber'. *Journal of Structural Engineering,* 131**,** 173-187.

CAWLEY, P. & ADAMS, R. D. 1979. 'The location of defects in structures from measurements of natural frequencies'. *The Journal of Strain Analysis for Engineering Design,* 14**,** 49-57.

CHOI, F., LI, J., SAMALI, B. & CREWS, K. 2008. 'Application of the modified damage index method to timber beams'. *Engineering Structures,* 30**,** 1124-1145.

CORNWELL, P., DOEBLING, S. W. & FARRAR, C. R. 1999. 'Application of the strain energy damage detection method to plate-like structures'. *Journal of Sound and Vibration,* 224**,** 359-374.

CRAIG, R. R. & KURDILA, A. J. 2006. 'Fundamentals of structural dynamics', *John Wiley & Sons.*

DEPARTMENT OF TRANSPORT AND REGIONAL SERVICES 2003, *2002-2003 Report on the operation of the Local Government (Financial Assistance) Act 1995*, Commonwealth of Australia, Canberra.

DITTMER, J. P., JENSEN, C. G., GOTTSCHALK, M. & ALMY, T. 2006. 'Mesh optimization using a genetic algorithm to control mesh creation parameters'. *Computer-Aided Design and Applications,* 3**,** 731-740.

DOEBLING, S. W., FARRAR, C. R., PRIME, M. B. & SHEVITZ, D. W. 1996. 'Damage identification and health monitoring of structural and mechanical systems from changes in their vibration characteristics: a literature review'. *Los Alamos National Lab., NM (United States).*

DUAN, M. 2003. 'Finite element analysis of a laminated timber bridge'. *10th Asia-Pacific Vibration Conference* Gold Coast, Queensland, Australia, pp. 104-108.

GERBER, C. & CREWS, K. 2005. 'Investigation of the ultimate behaviours and FEA of wood stressed-skin panels'. *Collaboration and Harmonization in Creative Systems,* 1**,** 397.

HERNANDEZ, R., DAVALOS, J. F., SONTI, S. S., KIM, Y. & MOODY, R. C. 1997. 'Strength and stiffness of reinforced yellow-poplar glued-laminated beams'.

JOHNS, K. C. & LACROIX, S. 2000. 'Composite reinforcement of timber in bending'. *Canadian Journal of Civil Engineering,* 27**,** 899-906.

KIM, B., STUBBS, N. & SIKORSKY, C. 2002. 'Local damage detection using incomplete modal data'.*20th IMAC*. 435-441.

KIM, J.-T., RYU, Y.-S., CHO, H.-M. & STUBBS, N. 2003. 'Damage identification in beam-type structures: frequency-based method vs mode-shape-based method'. *Engineering Structures,* 25**,** 57-67.

KIM, J.-T. & STUBBS, N. 1995. 'Model-Uncertainty Impact and Damage-Detection Accuracy in Plate Girder'. *Journal of Structural Engineering,* 121**,** 1409.

KIM, J. T. & STUBBS, N. 2002. 'Improved damage identification mehtod based on modal'. *Journal of Sound and Vibration,* 252**,** 223-238.

KIM, Y. J. & HARRIES, K. A. 2010. ‚Modeling of timber beams strengthened with various CFRP composites,. *Engineering Structures,* 32**,** 3225-3234.

KURIAN, A. 2000. 'Analytical modeling of glued laminated girder bridges using Ansys'. *Transportation Scholars Conference*. 54-64.

LIEVEN, N. & EWINS, D. 1988. 'Spatial correlation of mode shapes, the coordinate modal assurance criterion (COMAC)'. *Proceedings of the 6th international modal analysis conference*. 690-695.

NANNI, A. 2000. 'FRP reinforcement for bridge structures'.*Proceedings, Structural Engineering Conference*, The University of Kansas, Lawrence, KS.

PANDEY, A. K. & BISWAS, M. 1994. 'Damage Detection in Structures Using Changes in Flexibility'. *Journal of Sound and Vibration,* 169**,** 3-17.

PANDEY, A. K., BISWAS, M. & SAMMAN, M. M. 1991. 'Damage detection from changes in curvature mode shapes'. *Journal of Sound and Vibration,* 145**,** 321-332.

PLEVRIS, N. & TRIANTAFILLOU, T. C. 1992. 'FRP-reinforced wood as structural material'. *Journal of Materials in Civil Engineering,* 4**,** 300-317.

RAMSEY, K. 1983. 'Experimental modal analysis, structural modifications and FEM analysis on a desktop computer'. *SOUND AND VIBRAT.,* 17**,** 19-27.

SCHOBER, K. & RAUTENSTRAUCH, K. 2005. 'Experimental investigation on flexural strengthening of timber structures with CFRP'.*Proceedings of the International Symposium on Bond Behavior of FRP in Structures*, Weimar, Germany. 457-463.

SMITH, S. T. & TENG, J. G. 2002. 'FRP-strengthened RC beams. I: review of debonding strength models'. *Engineering Structures,* 24**,** 385-395.

STUBBS, N., KIM, J.-T. & FARRAR, C. 1995.'Field verification of a nondestructive damage localization and severity estimation algorithm'.*Proceeding-spie the international society for optical engineering*, 210-210.

STUBBS, N. & PARK, S. 1996. 'Optimal sensor placement for mode shapes via Shannon's sampling theorem'. *Computer-Aided Civil and Infrastructure Engineering,* 11**,** 411-419.

ZHU, H. P. & XU, Y. L. 2005. 'Damage detection of mono-coupled periodic structures based on sensitivity analysis of modal parameters'. *Journal of Sound and Vibration,* 285**,** 365-390.

APPENDIX A: Static Test Results

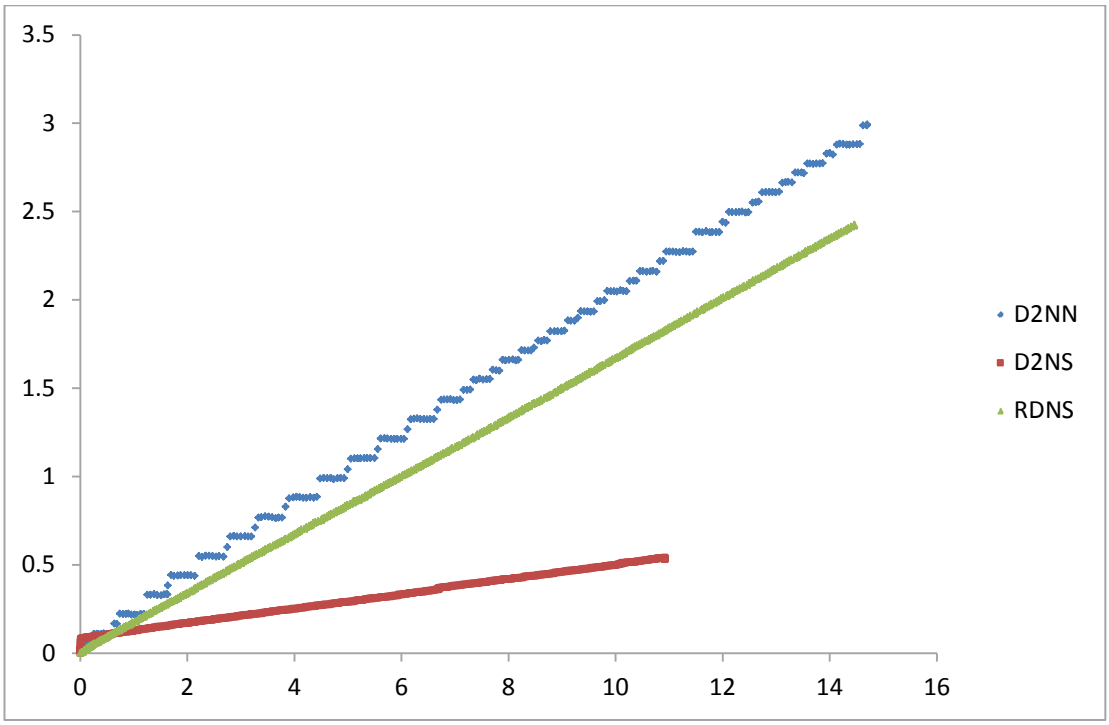

Load-deflection Curve for Beam 3 with different damage cases

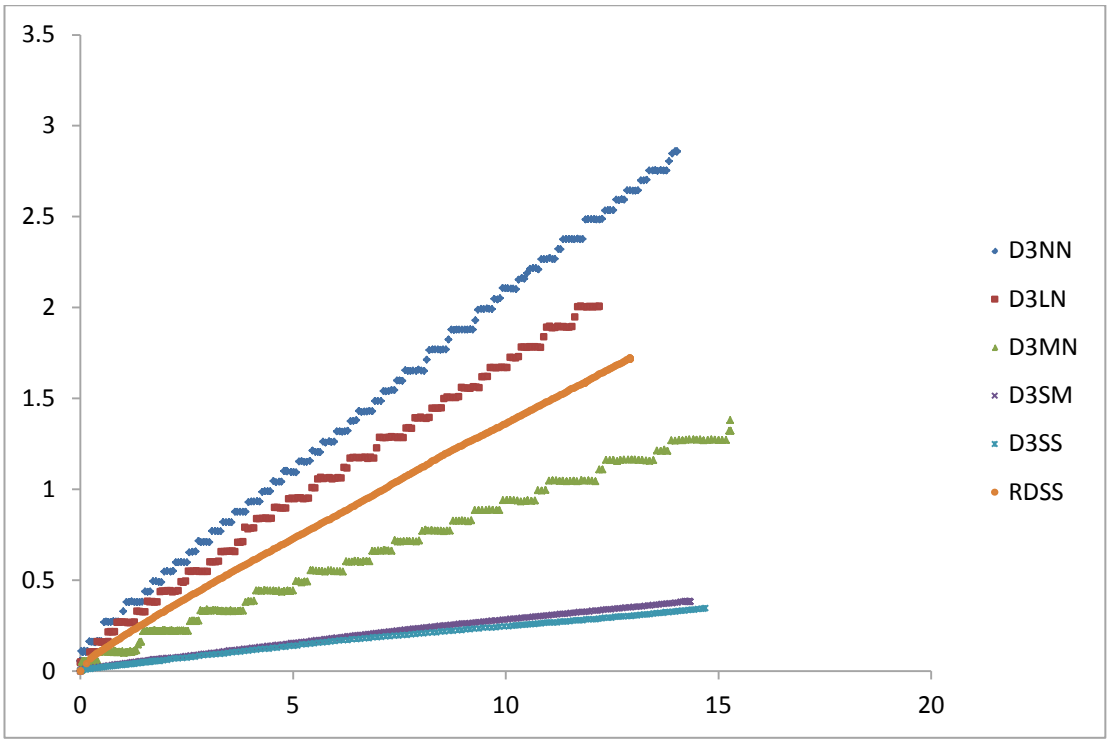

Load-deflection Curve for Beam 4 with different damage cases

APPENDIX B: Comparison in Locating Damage Results

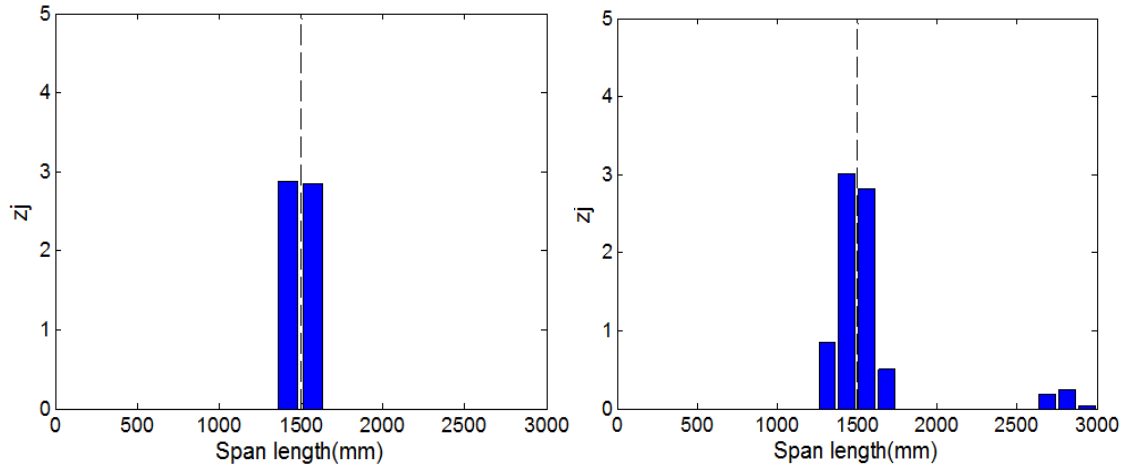

(a) Numerical (b) Experimental

Comparison between numerical and experimental results for 4M

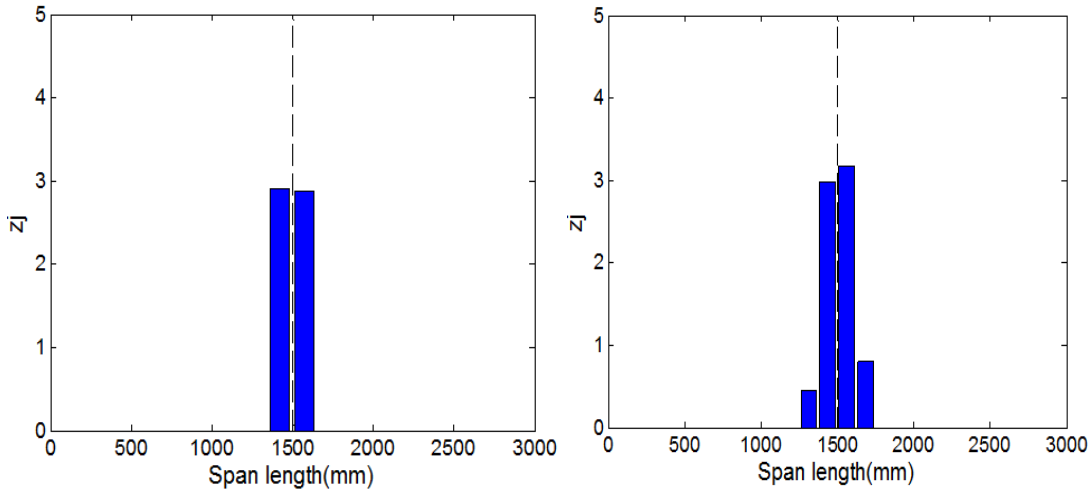

(a) Numerical (b) Experimental

Comparison between numerical and experimental results for 4S

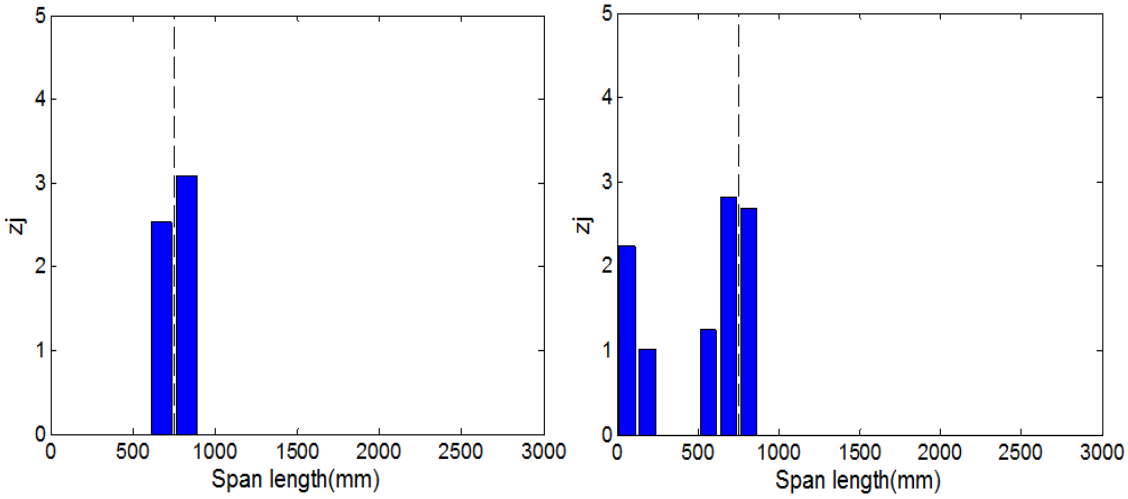

(a) Numerical (b) Experimental

Comparison between numerical and experimental results for 2S

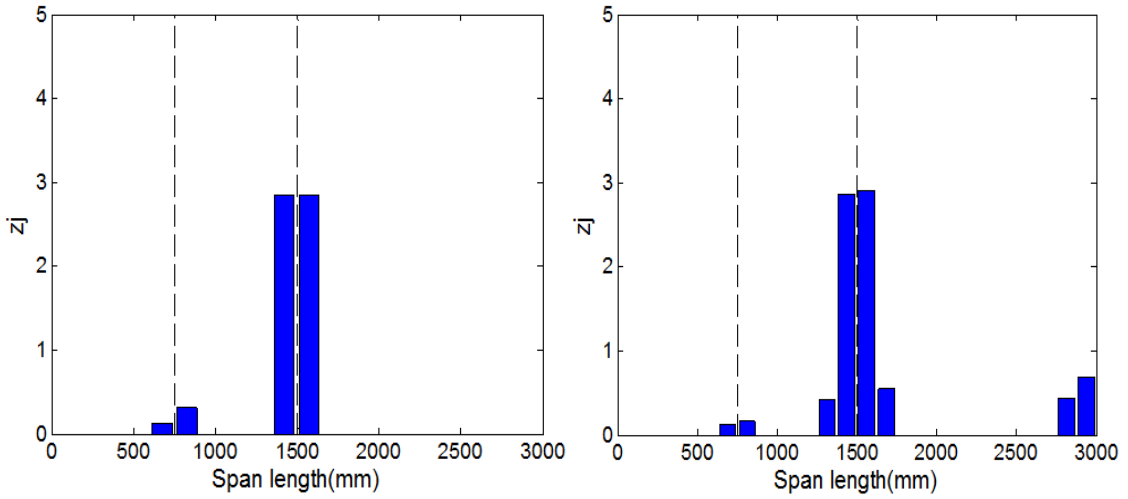

(a) Numerical (b) Experimental

Comparison between numerical and experimental results for 2L4S

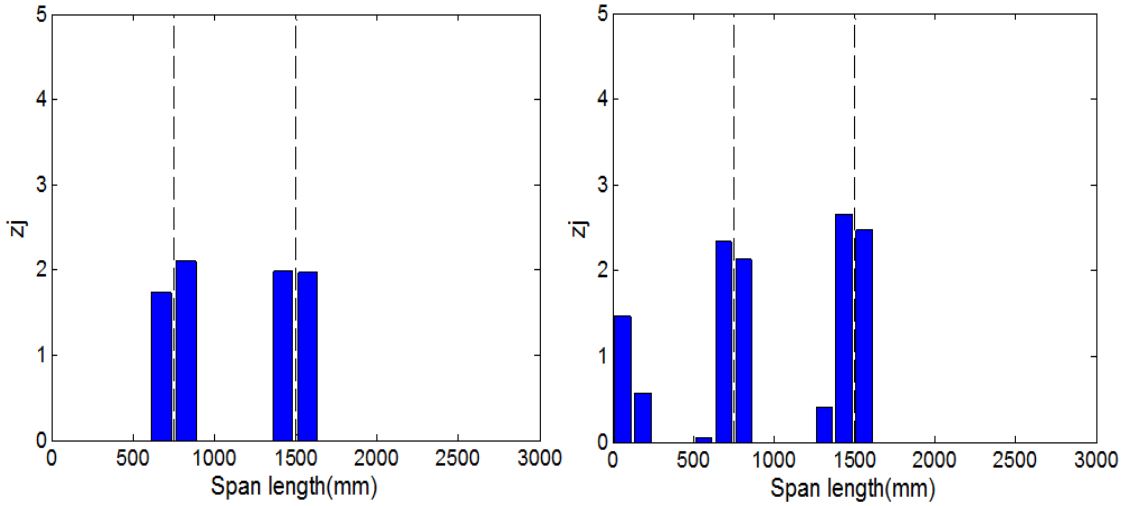

(a) Numerical (b) Experimental

Comparison between numerical and experimental results for 2S4S

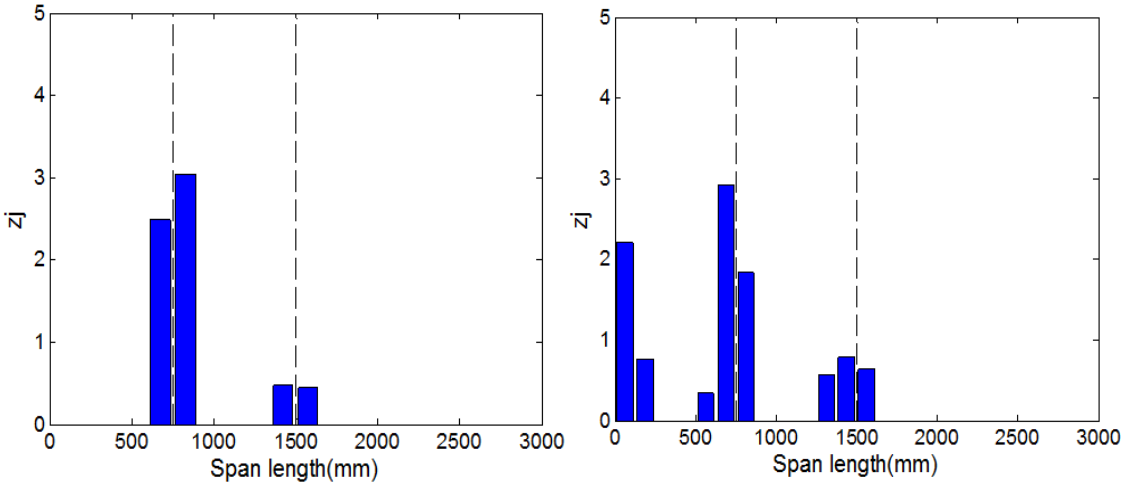

(a) Numerical (b) Experimental

Comparison between numerical and experimental results for 2S4L

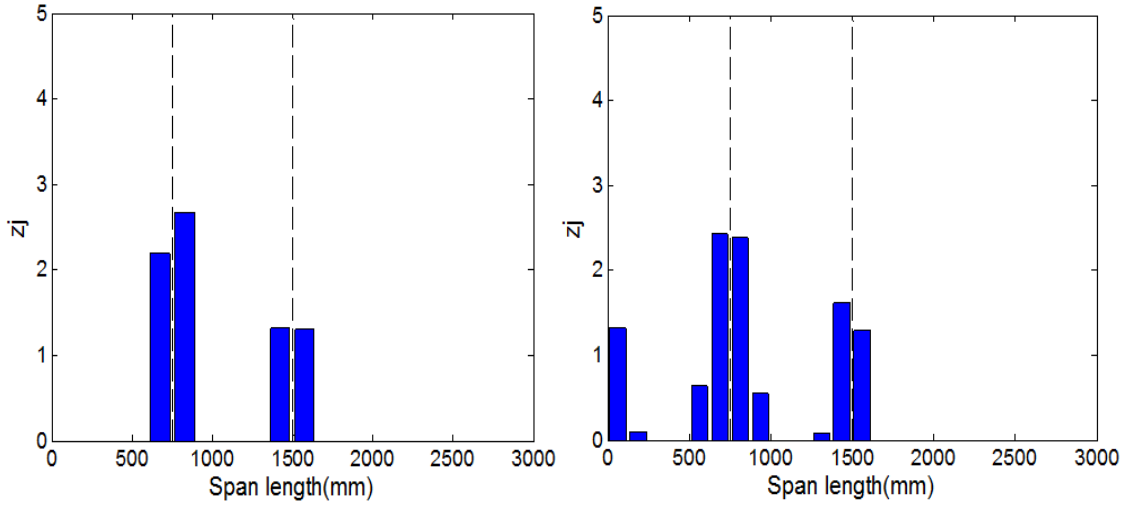

(a) Numerical (b) Experimental

Comparison between numerical and experimental results for 2S4L